AWARD NUMBER: W81XWH-15-1-0396

TITLE: An Herbal Derivative as the Basis for a New Approach to Treating Post-Traumatic Osteoarthritis

PRINCIPAL INVESTIGATOR: Malcolm Whitman.

CONTRACTING ORGANIZATION: Harvard University, Boston
Boston, MA 02115-5819

REPORT DATE: JUNE 2019

TYPE OF REPORT: Final

PREPARED FOR: U.S. Army Medical Research and Materiel Command Fort Detrick, Maryland 21702-5012

REPORT DOCUMENTATION PAGE

Form Approved
OMB No. 0704-0188

1. REPORT DATE	2. REPORT TYPE	3. DATES COVERED
JUNE 2019	Final	01-SEP-2015 - 28-FEB-2019

4. TITLE AND SUBTITLE

An Herbal Derivative as the Basis for a New Approach to Treating Post-Traumatic Osteoarthritis

5a. CONTRACT NUMBER

5b. GRANT NUMBER
W81XWH-15-1-0396

5c. PROGRAM ELEMENT NUMBER

6. AUTHOR(S)
Malcolm Whitman Ph.D.

5d. PROJECT NUMBER

5e. TASK NUMBER

5f. WORK UNIT NUMBER

7. PERFORMING ORGANIZATION NAME(S) AND ADDRESS(ES)
Harvard College, President & Fellows of
Sponsored Programs Admin.
22 Shattuck St.
Boston, Ma.02115-6027

8. PERFORMING ORGANIZATION REPORT

9. SPONSORING / MONITORING AGENCY NAME(S) AND ADDRESS(ES)

U.S. Army Medical Research and Materiel Command
Fort Detrick, Maryland 21702-5012

10. SPONSOR/MONITOR'S ACRONYM(S)

11. SPONSOR/MONITOR'S REPORT NUMBER(S)

12. DISTRIBUTION / AVAILABILITY STATEMENT

Approved for Public Release; Distribution Unlimited

13. SUPPLEMENTARY NOTEs

14. ABSTRACT Osteoarthritis (OA) is a painful disease that causes the progressive destruction of joint structures, and is the most common cause of disability among military service members who are removed from active duty for medical reasons. In preliminary work with a small number of animals, we have found that the natural product derivative halofuginone (HF) shows promise with respect to reducing cartilage damage in the destabilized medial meniscus (DMM) mouse model of PTOA. HF inhibits glutamyl- prolyl-tRNA synthetase (EPRS), the enzyme responsible for charging tRNAs with the amino acid proline. The goal of this grant is to test the hypothesis that EPRS inhibitors will provide the basis for a new therapeutic strategy for PTOA. We report here: 1) Data demonstrating that the EPRS inhibitors HF and its less toxic derivative HFol, are effective as therapeutics for PTOA in mice, using the DMM model; 2) Detailed immunohistochemical data examining the effect of HF/Hfol on effectors of OA 3) A new ex vivo assay using intact joint cartilage to test ex vivo efficacy of EPRS inhibitors as therapeutics for OA.

15. SUBJECT TERMS
Post Traumatic Osteoarthitis (PTOA), Halofuginone (HF), tRNA synthetase inhibitor, chondrocyte, MMP, GCN2, Destabilized Medial Meniscus (DMM) model.

16. SECURITY CLASSIFICATION OF:			17. LIMITATION OF ABSTRACT	18. NUMBER OF PAGES	19a. NAME OF RESPONSIBLE PERSON USAMRMC
a. REPORT	b. ABSTRACT	c. THIS PAGE			19b. TELEPHONE NUMBER *(include area code)*
U	Unclassified	Unclassified	Unclassified	61	

Table of Contents

Page

INTRODUCTION. Osteoarthritis (OA) is a painful disease that causes the progressive destruction of joint structures, and is the most common cause of disability among military service members who are removed from active duty for medical reasons. The progressive period in PTOA provides a target for therapeutic intervention. In preliminary work with a small number of animals, we have found that the natural product derivative halofuginone (HF) shows promise with respect to reducing cartilage damage in the destabilized medial meniscus (DMM) mouse model of PTOA. HF inhibits glutamyl- prolyl-tRNA synthetase (EPRS), the enzyme responsible for charging tRNAs with the amino acid proline. Low-level inhibition of EPRS triggers a metabolic sensor, a stress signal that initiates a sustained adaptive response across affected tissues. The goal of this grant is to test the hypothesis that EPRS inhibitors, acting to suppress a multi-cellular cytokine-driven tissue destructive program, will provide the basis for a new therapeutic strategy for PTOA. The Aims of this grant are to: 1) *Characterize the therapeutic timing and functional effects of HF, or novel related EPRS inhibitors, on PTOA in mice, using the DMM model*; 2) *Examine the early time course of cellular and molecular responses to EPRS inhibitor treatment in the DMM mouse model, as well as in ex vivo in chondrocytes and synoviocytes.* We believe that these studies both will establish the molecular and cellular basis for the benefit of a new drug class for PTOA treatment, and provide tools to evaluate different therapeutic strategies (e.g. novel compounds, delivery methods) prior to the appearance of joint pain or dysfunction.; 3) *Develop and apply tools for testing the efficacy of* EPRS inhibitors *following drug delivery to the joint in DMM mice.*

KEYWORDS: Post Traumatic Osteoarthitis (PTOA), Halofuginone (HF), tRNA synthetase inhibitor, chondrocyte, MMP, GCN2, Destabilized Medial Meniscus (DMM) model.

ACCOMPLISHMENTS Over the grant funding period**,** we have examined and compared the action of HF and the novel HF derivative HFol on osteoarthritis in vivo and the catabolic responses of joint structural cells in vitro as outlined in the original Aims. We have completed two sets of in vivo experiments to establish the efficacy of HF and Hfol in the DMM model of PTOA, and a third set of in vivo studies in which we harvested joints from treated or control animals at early time points during the development of PTOA to allow examination of the molecular effects of Hfol during early stages of post damage response. In addition, we have identified a novel mechanism by which HF/HFol act to inhibit transcription of a catabolic program induced by inflammatory cytokines in synovial fibroblasts, and shown that a similar program exists in chondrocytes as well. These observations provide a fundamentally novel link between local amino acid levels in tissues and the activation of catabolic effectors by cytokines in the joint. This work points to a new set of approaches to thinking about how nutrients and metabolism are linked to chronic tissue remodeling in PTOA and other chronic degenerative diseases. The work in synoviocytes has been submitted to the journal eLife (Kim et al submitted, included as appendix); the manuscript on chondrocyte gene expression, efficacy of HF vs HFol in vivo, and effects of HFol treatment on early gene expression in the joint following traumatic damage is currently in the final stages of data analysis and manuscript preparation. .

A) Major activities: i. Completion of a new DMM study with HFol treatment, in this case harvesting samples at early time points to allow us to identify the earliest molecular changes underlying the therapeutic effects of EPRS inhibitors. All surgeries and treatment courses are completed, joints have been harvested and analysis is in progress. **ii.** Analysis of effects of HF/Hfol on expression of key arthritis effectors in joints; **iii.** Analysis of mechanism of HF/Hfol action on arthritis effectors in joint cells in vitro.

B) Specific objectives: i. to identify and quantify molecular changes in joints from DMM animals following treatment with HFol at time points before the development of frank arthritis. We are using immunohistochemistry and Q-RT-PCR to assess early changes in arthritis effectors. **ii**: to develop and test HF/HFol responsive markers and effectors of arthritic damage as tools for assessing treatment efficacy in vivo, and to test role of signaling molecules mediating HF/HFol action in articular cells. **iii**.to test HFol effects on DMM in vivo at early time points (2-4 weeks). **iv.** to develop and apply ex vivo tools for the study of arthritogenic responses to cytokines and the effects of HF/HFol on these responses, enabling correlation of early effects of HF/HFol in vivo to mechanistic understanding gained from studies of joint cells in culture.

C) Significant results: Major activity i; (Principal effort, Li and Whitman Labs) :

Objective 1: To determine whether HF and HFOL can prevent/delay the progression of articular cartilage degeneration resulting from DMM surgery.

Rationale: In our previous studies, we found that it took about 16 weeks for mice to develop a typical OA knee joint after DMM surgery. Therefore, we planned to use 16 weeks after DMM surgery as the end point to characterize mouse knee joints for evidence of articular cartilage degeneration.

***Methods and results*:**

Experiment 1. Treatment of mice with HF or HFOL

There are four groups of mice: sham surgery treated with PBS, DMM surgery treated with PBS, DMM surgery treated with HF and DMM surgery treated with HFOL. There are 8 mice in each group. Mice (C57BL/6j) at the age of 10 weeks old were subjected to the surgery. Two weeks after surgery, mice were treated either with PBS or HF (0.2 mg/kg body weight) or HFOL (1 mg/kg body weight) every other day. At 8 weeks after the surgery, one set of four groups of mice was euthanized for the collection of knee joints. Another set of four groups of mice was kept alive to the age of 16 weeks after the surgery and then the mice were euthanized for the collection of knee joints.

Experiment 2. Measurement of mouse body weights

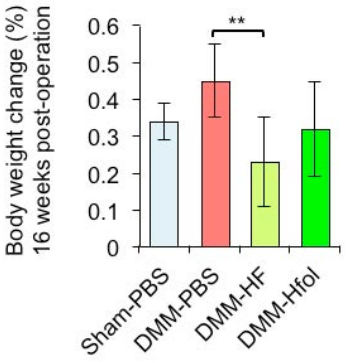

We measured the body weight of the mice during the drug treatment. Body weight changes (%) were calculated. There was no difference in body weight gain among the groups at 8 weeks following the surgery. However, the DMM/HF group showed a significantly less body weight gain compared with that of the DMM/PBS group, *p<0.01*, at 16 weeks after the surgery. There was no difference between DMM/HFol and DMM/PBS, *p>0.05.*

Experiment 3. Measurement of bone volume in epiphysis of tibia in mice by micro-computed tomography (μCT)

A high-resolution desktop micro-tomographic imaging system (μCT40, Scanco Medical AG, Brüttisellen, Switzerland) was used to assess trabecular bone microarchitecture, total and bone volumes, and mineral densities of the tibial epiphysis. Scans were acquired using a 10 μm^3 isotropic voxel size, 70 kVP, 114 mAs, 200 ms integration time, and were subjected to Gaussian filtration and segmentation. Images and results were shown below.

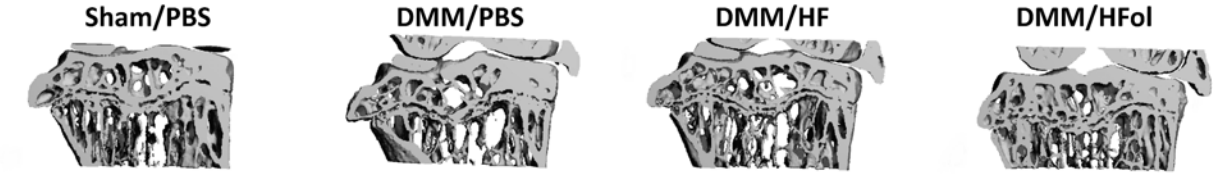

As indicated in the image and the figure, the bone volume is reduced in DMM/HF group, compared with that in the sham (p=0.0040) and DMM (p=0.0056).

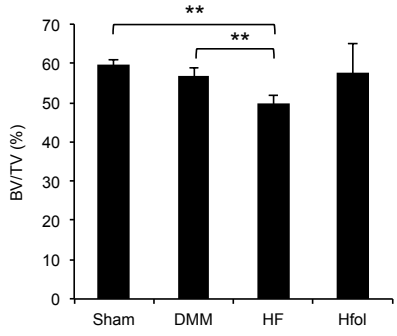

		p-value	
	BV/TV (%)	vs Sham	vs DMM
Sham	59.67	-	-
DMM	56.67	0.0840	-
HF	49.96	0.0040	0.0056
Hfol	57.52	0.6167	0.8443

Experiment 4. Morphological analysis of knee joints

We have completed the histological analyses of mouse knee joints. In the experiment, there were four groups of mice: sham surgery treated with PBS, DMM surgery treated with PBS, DMM surgery treated with HF and DMM surgery treated with HFOL. There are 7-8 mice in each group. Mice (C57BL/6j) at the age of 10 weeks old were subject to the surgery. Two weeks after the surgery, mice were treated either with PBS or HF (0.2 mg/kg body weight) or HFOL (1 mg/kg body weight) every other day. At 8 weeks after the surgery, one set of four groups of mice was euthanized for the collection of knee joints. Another set of four groups of mice was kept alive to the age of 16 weeks after the surgery and then the mice were euthanized for the collection of knee joints. All of the samples were embedded in paraffin and 10 of them were sectioned and stained by Safranine O/Fast green. For histology analysis, Knee joints were decalcified in Morse's solution. For each knee joint, 6 μm thick serial sagittal sections were cut. Every tenth section was collected for Safranin O/Fast green staining.

Figure 1. Articular cartilage of mouse knee joints at 8 weeks after DMM

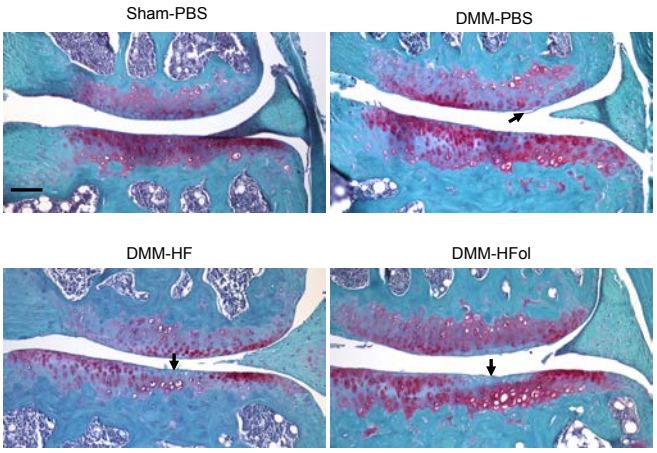

No overt morphological changes were observed in mice with sham surgery (A) Small fibrillations were seen in mice with DMM (see arrow in B). However, there were only slight proteoglycan degradations observed in DMM/HF (see arrow in C) and DMM/HFol (see arrow in D) treatment groups. This indicates that HF and HFol treatments delay the progressive process of articular cartilage degeneration induced by DMM. Bar = 100 mm

Figure 2. Articular cartilage of mouse knee joints at 16 weeks after DMM

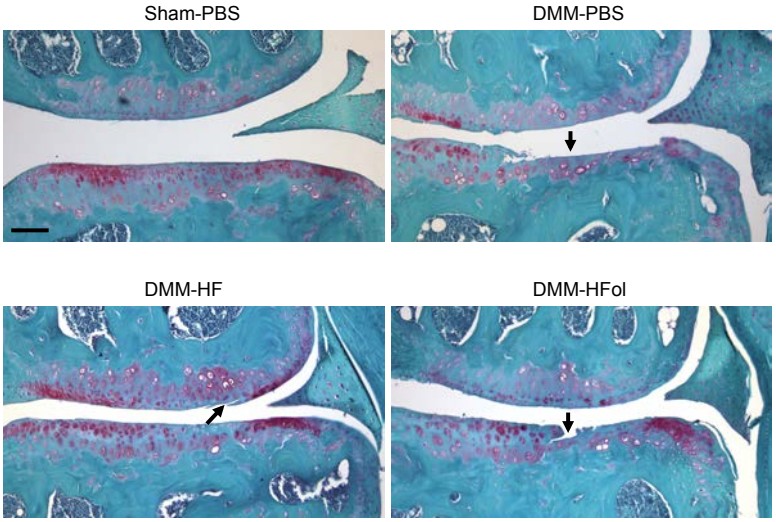

Slightly localized proteoglycan degradations were seen in mice with sham surgery (A). Loss of articular cartilages were observed in mice after DMM (see arrow in B). However, only fibrillations were seen in DMM/HF (see arrow in C) and DMM/HFol (see arrow in D) treatment groups. This indicates that HF and HFol treatments delay the progressive process of articular cartilage degeneration induced by DMM. Bar = 100 mm

The condition of articular cartilages was also evaluated by a modified Mankin Score system for mouse articular cartilage, recommended by Osteoarthritis Research Society International (Glasson et. al., The OARSI histopathology initiative e recommendations for histological assessments of osteoarthritis in the mouse. Osteoarthritis and Cartilage, 2010, 18:S17-S23).

Table 1. Scores of articular cartilages of mouse knee joints after DMM

Time (weeks after the surgery)	Sham-PBS		DMM-PBS		DMM-HF		DMM-HFol	
	n	Means ± SD	n	Means ± SD	n	Means ± SD	n	Means ± SD
8	7	0.14 ± 0.23	7	2.00 ± 0.53	7	0.57 ± 0.17	7	0.71 ± 0.52
16	8	0.94 ± 0.30	7	4.14 ± 0.83	8	2.13 ± 0.78	7	2.14 ± 0.99

Figure 3. Evaluation of articular cartilage of mouse knee joints at 8 weeks after surgery

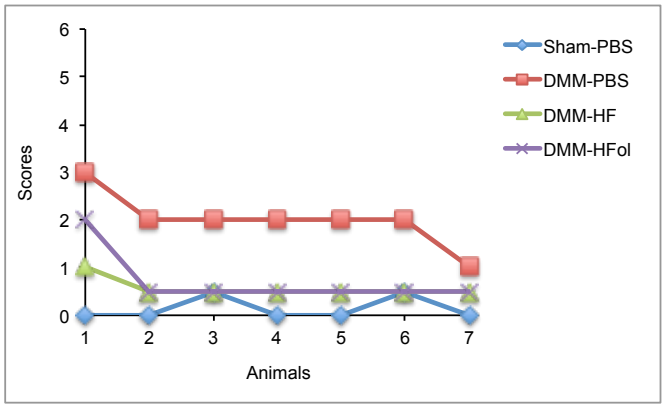

Figure 4. Evaluation of articular cartilage of mouse knee joints at 16 weeks after surgery

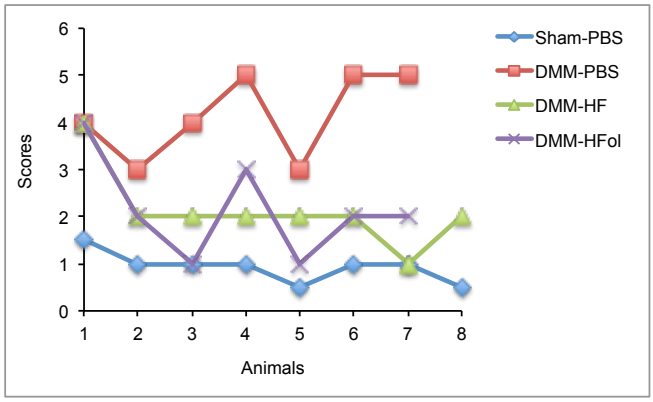

Figure 5. Comparison of scores between the experimental groups at 8 weeks after surgery

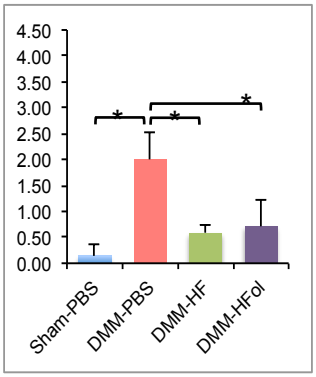

**: p<0.001

***: p<0.0001

Figure 6. Comparison of scores between the experimental groups at 16 weeks after surgery

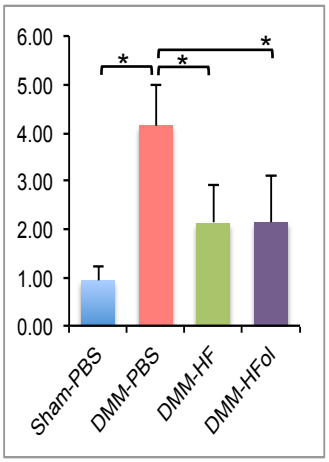

**: p<0.001

***: p<0.0001

Conclusion: HF and HFol can significantly delay the progressive process of articular cartilage degeneration induced by DMM.

Objective 2: To analyze gene expression associated with cartilage damage in articular cartilage of knee joints by the treatment of HF/Hfol

Rationale: A number of genes have been shown to involve in articular cartilage degeneration, which eventually leads to OA, genes such as MMP-13, Zip8, TGF-β1, HTRA1 and DDR2. We analyzed whether or not the expression of these genes was affected by treatment with HF/Hfol in articular cartilage of mouse knee joints.

***Methods and results*:**

We performed immunohistostaining to examine the expressions of genes, including MMP-13), ZIP8, TGF-β1, HTRA1 and DDR2 in the articular cartilage of mouse knee joints. Four knee joints were randomly selected from each group of mice at 8 weeks after DMM. Eight to ten paraffin sections, distributed throughout each knee joint, of articular cartilage were selected for immunohistostaining. Paraffin sections were incubated with a polyclonal antibody against the genes. An appropriate concentration of each primary antibody for the experiment was determined by the examination of a serial dilution of the antibody on the sections. After overnight incubation with a primary antibody at 4°C, the sections were washed and incubated with a biotinylated secondary antibody. Color development was performed using a peroxidase substrate (VECTOR Laboratories, Burlingame, CA). Staining without primary antibody was performed as a negative control.

Figure 7. The expression of Mmp-13 in mouse knee articular cartilages

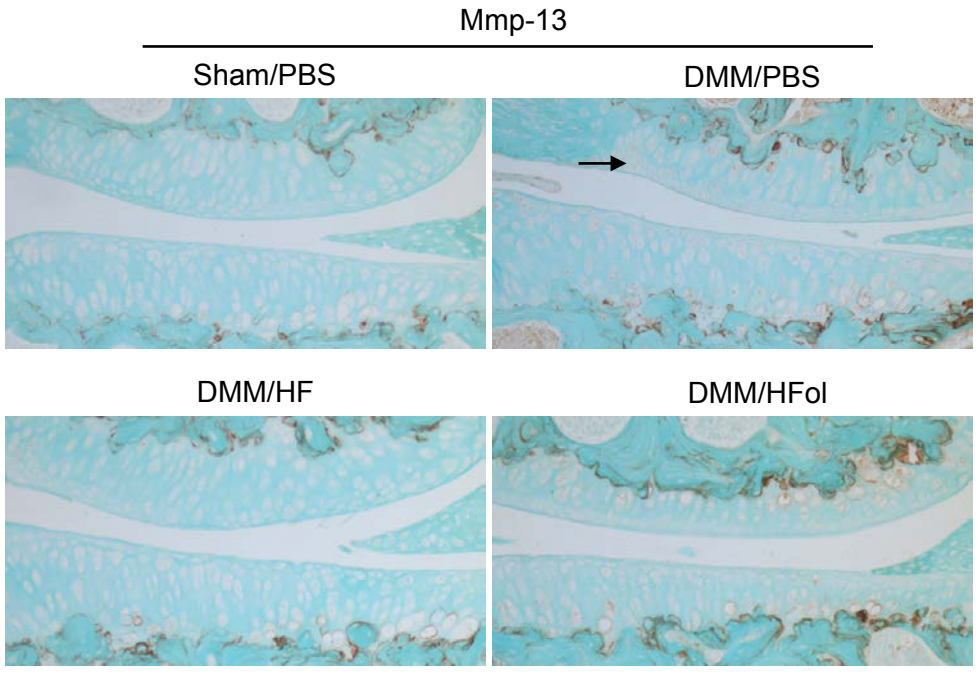

A rabbit polyclonal antibody (1μg/μl at the final concentration of 1:400 dilution) against Mmp-13 (Abcam, Cambridge, MA) was used in this experiment. The expression of Mmp-13 was increased in the DMM/PBS group (see the arrow in figure 7). There were no positive staining cells detected in other groups. This suggests that HF or HFol inhibits the induction of Mmp-13 in the articular cartilage of mouse knee joints induced by DMM.

To understand possible mechanisms responsible for the down-regulation expression of Mmp-13 by HF or HFol, we investigated whether or not two regulatory molecular pathways were involved in the induction of Mmp-13 in the articular chondrocytes of mouse knee joints. The result from a study indicates that the zinc-ZIP8-MTF1 (metal regulatory transcription factor-1) axis induces expression of MMP-13 in chondrocytes. Data from several independent research groups demonstrate that the TGF-β1-HTRA1-DDR2 forms a molecular pathway to induce the expression of MMP-13 in chondrocytes.

Figure 8. The expression of Zip 8 in mouse knee articular cartilage

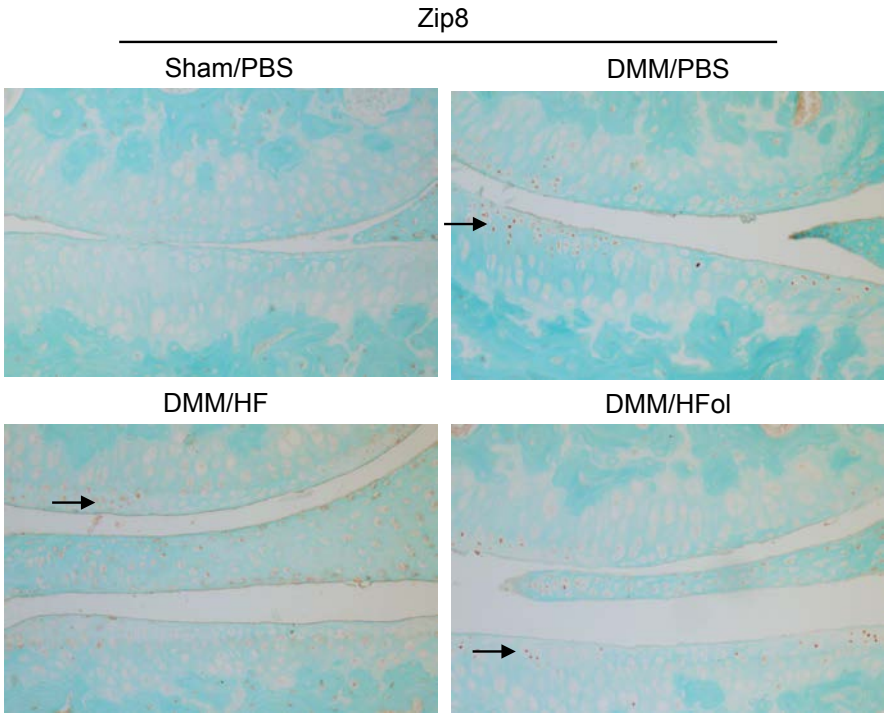

A rabbit polyclonal antibody (the final concentration of 1:150 dilution) against Zip 8 was used. The expression of Zip8 was increased in DMM/PBS group (see brown-color staining cells in figure 8). The expression of Zip8 was also detected in DMM/HF and DMM/HFol groups.

Figure 9. The expression of TGF-β1 in mouse knee articular cartilage

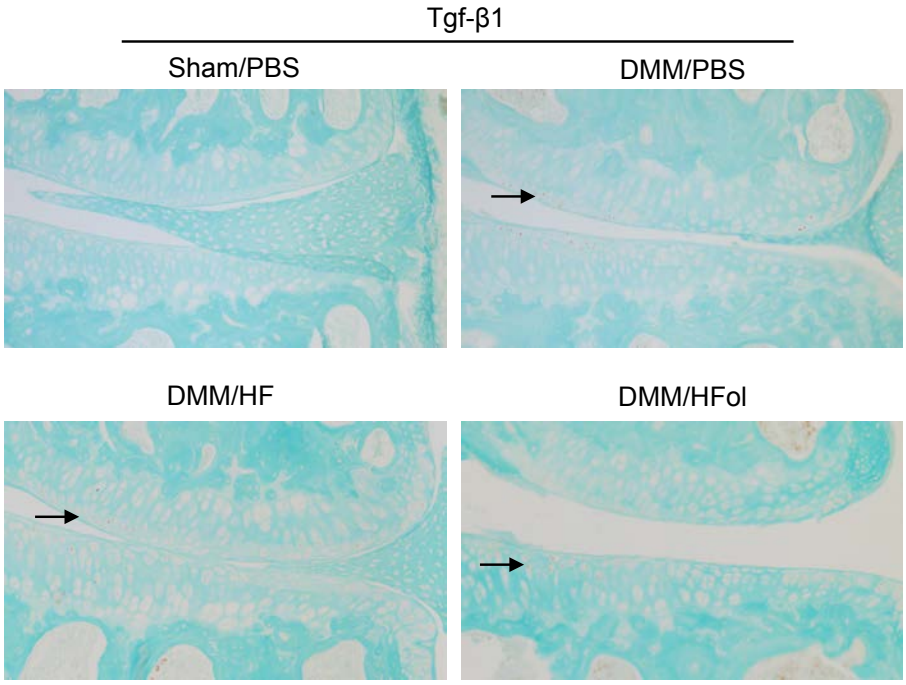

A rabbit polyclonal antibody (the final concentration of 1:200 dilution) against Tgf-β1 was used. The expression of Tgf-β1 was increased in DMM/PBS group (see brown-color staining cells in figure 9). The expression of Tgf-β1 was also detected in DMM/HF and DMM/HFol groups.

Figure 10. The expression of HtrA1 in mouse knee articular cartilages

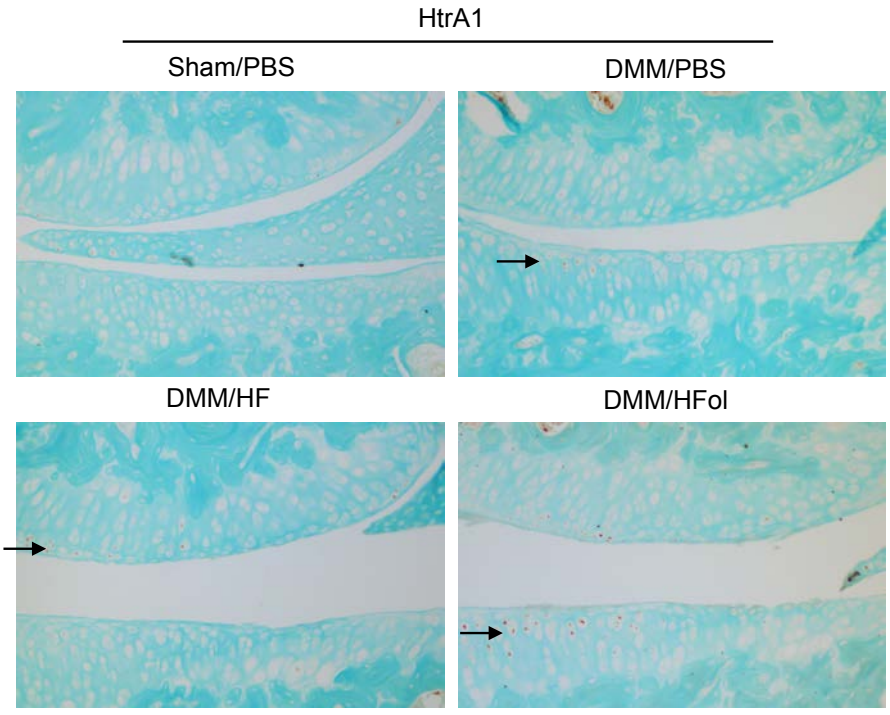

A rabbit polyclonal antibody (the final concentration of 1:200 dilution) against HtrA1 was used. We found the similar expression of patterns of HtrA1 to what was observed in the expression pattern of Tgf-β1 group, see figure 10).

Figure 11. The expression of Ddr2 in mouse knee articular cartilage

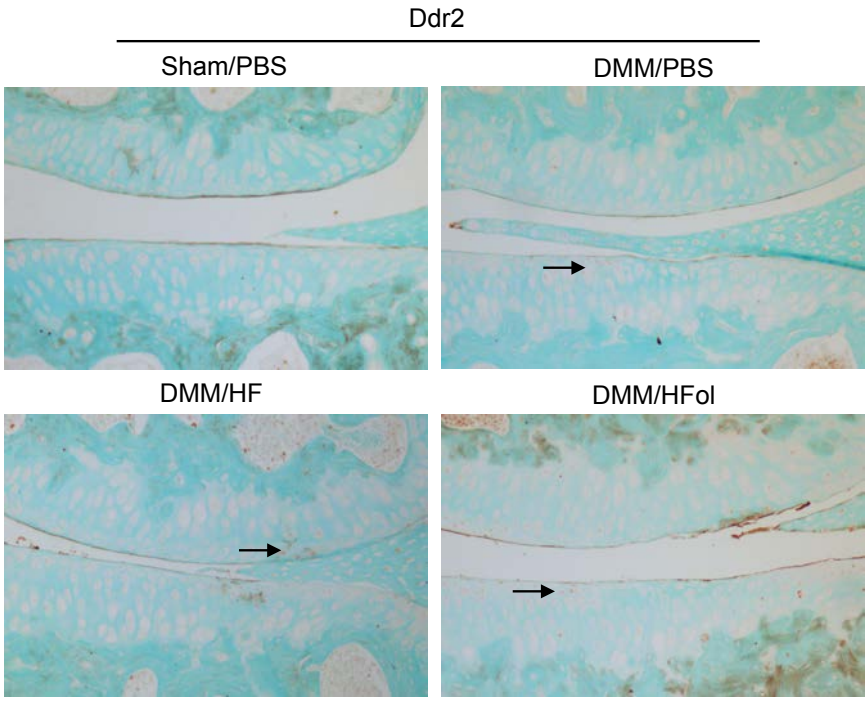

A rabbit polyclonal antibody against Ddr2 (a final concentration of 1:200 dilution) was used in this experiment. We found the similar expression of patterns of Ddr2 to what were observed in the expression patterns of Tgf-β1 and HtrA1 groups, see figures 10 and 11).

Conclusion: HF or HFol inhibits the up-regulation expression of Mmp-13 in the articular cartilage of mouse knee joints at 8 weeks after DMM. However, no evidence indicates that zinc-ZIP8-MTF1 axis and the TGF-β1-HTRA1-DDR2 pathway are involved in the inhibition expression of Mmp-13 by HF or HFol with the exception of one remaining question, whether or not HF or HFol inhibits induction of MMP-13 by DDR2.

Objective 3: To elucidate a possible mechanism by which the expression of Mmp-13 was inhibited in chondrocytes by HF/Hfol in vitro

Rationale: By immunohistostaining, no evidence indicates that HF or HFol inhibit the increased expression of Ddr2 in the joints. We are aware that the immunohistostaining technique that we used may not be sensitive enough to detect a subtle change of Ddr2 expression by HF or HFol treatment. Thus, we decided to carry out in vitro experiments to know whether or not HF or HFol could inhibit the expression of Ddr2, which leads to the down-regulated expression of Mm-13.

***Methods and results*:**
Preparation of type II collagen coated plates: make a type II collagen solution at the concentration of 10μg/ml. Add 1.5 ml of the above solution to each well of a 6-well plate and dry up in hood overnight.
Preparation of HFol: make the stock solution at the concentration of 0.1μM in media. Add 4 or 8 μl of the stock solution to each well containing 2, 000 μl media to make a final concentration of HFol is 200 nM or 400 nM in each well.
Articular chondrocyte culture: Mouse articular chondrocytes of knee joints from 6 days old mice were used in the experiment. Briefly, articular chondrocytes were isolated by digestion with Collagenase D at a concentration of 3mg/ml overnight. The chondrocytes were then collected and cultured on a cell-culture dish. The cells were harvested at about 90-100% confluence and seeded at a density of 2.5 x 10^5/well on 6-well collagen type II-coated plate with 2 ml of culture media. 20 μg of collagen type II was added to the culture media in each well. The cells were treated with or without HFol inhibitor for 18 hr.
Real time-PCR analysis: Total RNAs were isolated for cDNA synthesis. The cDNA was synthesized with oligo(dT). Real-time PCR conditions were optimized for maximal PCR efficiency by the adjustment of concentrations of PCR primers for Ddr2, forward 5'-CTGTCGGATGAGCAGGTTAT-3' and reverse 5'-CTCGGCTCCTTGCTGAAGAA-3' and for Mmp-13, forward 5'-GTGTGGAGTTATGATGATGT-3' and reverse 5-TGCGATTACTCCAGATACTG-3' and for Gapdh 5'-ACTGAGGACCAGGTTGTC-3' and reverse

5’-TGCTGTAGCCGTATTCATTG-3’. Real-time PCR was performed using the StepOnePlus, Applied Biosystems. PCR reaction was carried out at 95°C for 3 minutes followed by 50 cycles of 95°C for 30 seconds, 60°C for 30 seconds, and 72°C for 30 seconds, with a final extension at 72°C for 4 min. At the end of the PCR cycles, a melting curve, using a temperature range between 550C to 950C with +0.5°C intervals, was generated to test the specificity of the PCR product. A cDNA sample in the experiment was tested in triplicate.

This experiment was performed twice independently.

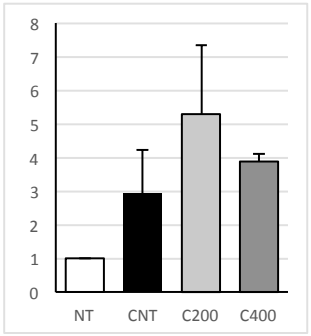

Figure 12. The level of *Ddr2* mRNAs in mouse chondrocytes. As shown in figure 12, the level of *Ddr2* mRNA was increased in HFol treatment, which indicates that HFol cannot inhibit up-regulation expression of Ddr2 in chondrocytes cultured on type II collagen-coated plates by HFol treatment, at both 200 nM and 400 nM. NT: non type II collagen-coated well and no HFol treatment, CNT: type II collagen-coated well and no HFol treatment, C200: type II collagen-coated well with HFol at 200 nM and C400: type II collagen-coated well with HFol at 400 nM.

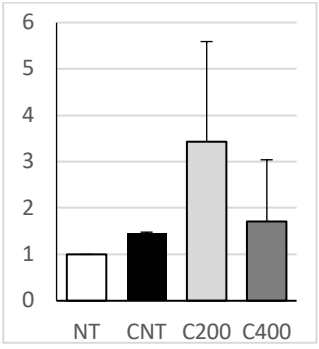

Figure 13. The level of *Mmp-13* mRNAs in mouse chondrocytes. As shown in figure 13, the level of *Mmp-13* mRNA was also increased in HFol treatment, which indicates that HFol cannot inhibit up-regulation expression of Mmp-13 in chondrocytes on type II collagen-coated plates by HFol treatment, at both 200 nM and 400 nM.

Conclusion: Results from this experiment are consistent with our previous observation that the level of DDR2 mRNA is increased in chondrocytes cultured on type II collagen-coated plates. This, in turn, induces MMP-13 in chondrocytes. However, HFol does not inhibit the increase in the levels of Ddr2 and Mmp-13 mRNAs in chondrocytes cultured on type II collagen-coated plates. This suggests that DDR2 may not be responsible for the down-regulation expression of MMP-13 in the articular cartilage of mouse knee joints at 8 weeks following DMM surgery by HFol treatment, which we observed in our previous histologic examination.

Objective iii. (Joint effort, Whitman and Li labs). To examine effects of HFol on early (2-4 week)changes in gene expression following DMM surgery, before frank cartilage changes are apparent. We performed DMM on the medial condyle of the right knee join of mice at the age of 10 weeks old. We started to administer HFol (10 μg/10g body weight) subcutaneously four days after the surgery. We treated the mice with either vehicle (PBS) or HFol every other day. The mice were then sacrificed at 2 or 4 weeks after DMM surgery.

There are ten mice in each experimental group, four groups at each time point. There were eighty mice in total.

	Sham		DMM	
post surgery	NT	HFol	NT	HFol
2 weeks	10	10	10	10
4 weeks	10	10	10	10

Two days after the last injection, knee joints of the mice were harvested and processed in RNALater solution. Articular cartilage was sliced off from the medial condyles of tibia and femur. The cartilage was stored in RNALater at -80°C. In order to get enough RNA from the articular cartilage, we pooled the cartilage from two mice, so there were five sets of tissues in each group. For RNA isolation, the cartilage was homogenized in Trizol with a motor-driven plastic pestle. Total RNAs were then isolated by using RNeasy Micro Kit (Qiagen). Gene-expression profile will be analyzed by real time-PCR.
Results: preliminary characterization of gene expression indicated overall consistency in RNA recovery among samples, but analysis of gene expression of genes of interest showed such great variability that significant changes could not be observed (Fig. 14, Fig. 15).

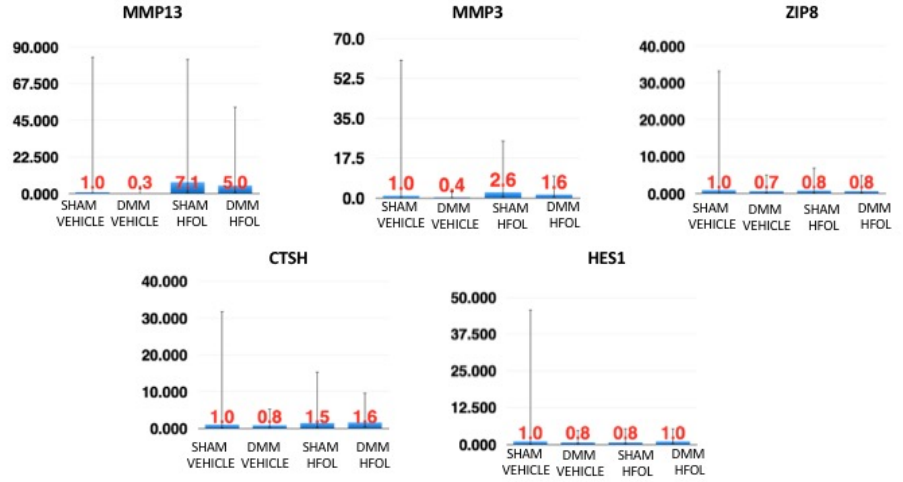

Figure 14. RT-Q-PCR analysis of mRNA from joints 2 weeks post DMM surgery

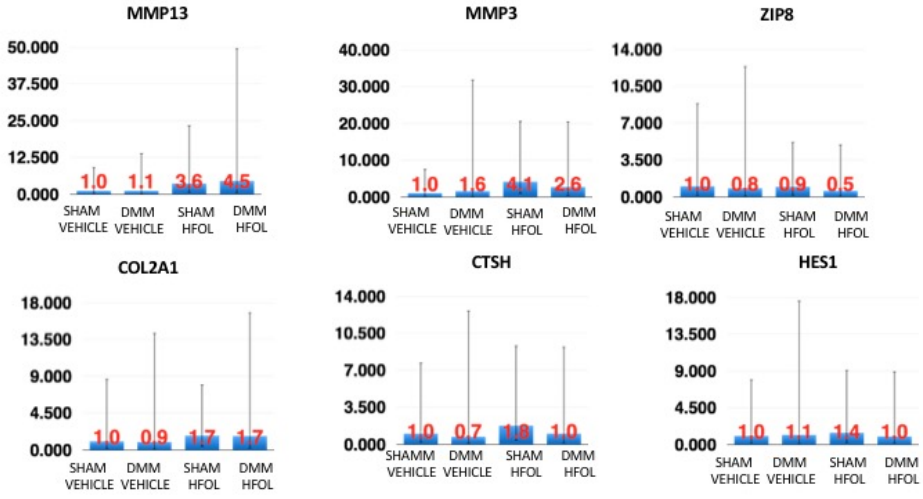

Figure 15. RT-Q-PCR analysis of mRNA from joints 2 weeks post DMM surgery

Objective iv. (Principal effort, Whitman Lab). Ex vivo assays for HF/Hfol action on the induction of tissue destruction effectors in chondrocytes and synovial cells. As outlined in previous reports, we have shown that HF and HFol block cytokine induction of tissue destructive effectors in primary chondrocytes and

synovial fibroblasts, two cell types with a central role in arthritis. Although we have found that HF and HFol substantially inhibit cytokines in primary chondrocytes or freshly isolated femoral cap cartilage, we have found that primary or established chondrocytes rapidly lose their cytokine responsiveness when place in tissue culture. We have also found that freshly isolated femoral caps are highly variable in their response to cytokines, and despite considerable effort we have not succeeded in making this a reliably reproducible test system. In contrast, both primary and established synoviocytes, from human and from mouse, maintain robust cytokine responses even after many passages in culture, making them much more amenable to mechanistic analyses than chondrocytes. Typical data from fresh primary mouse chondrocyte preparations are shown below, and are planned for inclusion in a manuscript in preparation on the efficacy of HF and Hfol for PTOA (**Fig. 16**). Despite promising initial results with isolated femoral caps (**Fig.17,18)**, we have not found reproducibility in this system to be adequate for publication. For primary and established synoviocytes, however, we have successfully delineated a novel pathway by which tRNA synthetase inhibitors or depletion of amino acids dramatically inhibit a broad pro-inflammatory, tissue destructive transcriptional program that is activated by cytokines and central to joint destruction in arthritis. These findings are described in detail in a manuscript to the journal eLife and appended to this report (Kim et al.), and are not restated here.

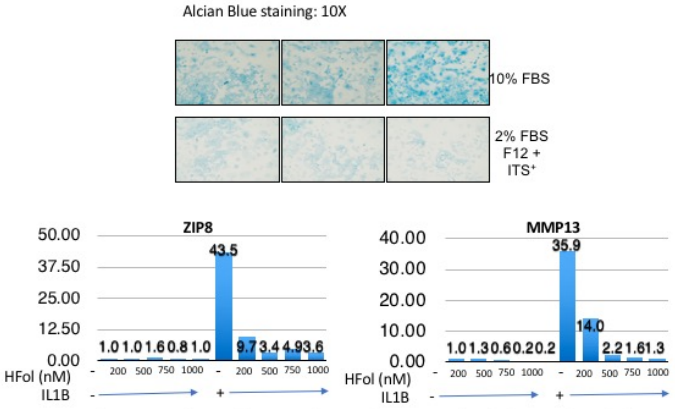

Fig. 16. Induction of OA effectors by cytokines, and inhibition by Hfol, in primary mouse chondrocytes by IL1ß. Chondrocytes were harvested from 6 day old mice and cultured for 4 days. Chondrogenic phenotype was established using Alcian blue staining (top panel). Chondrocytes were pretreated for 6 hours with indicated concentration of Hfol, then for 24 hours with IL1ß and analyzed by Q-RT-PCR. PGK1 was used as a housekeeping gene control

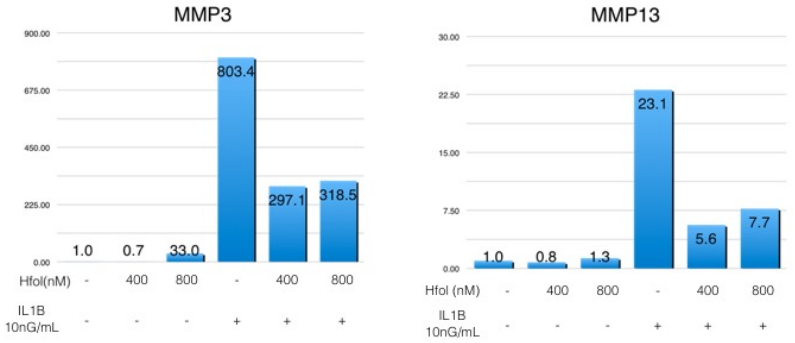

Fig. 17. Hfol Inhibits Cytokine Induced MMP expression in Isolated femoral cap articular cartilage. Fresh femoral cap joints (the femoral side of the hip joint) were surgically excised from 8 week old mice and culture for 24 hours, then treated overnight with Hfol, then for 48 hours and harvested for Q-RT-PCR analysis of gene expression

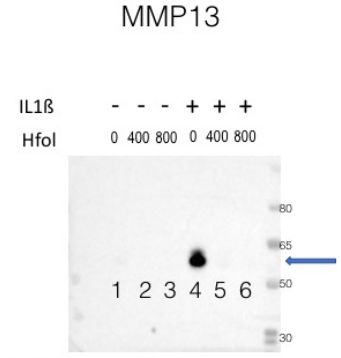

Fig. 18. Hfol Inhibits Cytokine Induced MMP13 secretion from isolated femoral cap articular cartilage. Femoral caps were isolated as in Fig,17 above, and conditioned medium isolated and analyzed for MMP13 by Western blot.

Training and professional development:
What opportunities for training and professional development has the project provided
Post-doctoral fellow training
Dr. Yeonjin Kim (Whitman lab), a postdoc who had a significant role in the first two years of the project, has now secured a research scientist position at a major pharmaceutical venture (Biocon) in her home country of South Korea.

Dr. Chenlu Liu was a post-doctoral fellow from West China University of Chengdu, China. She had been working on this project since Oct 1, 2016. She finished her training by the end of April, 2018. She carried out the experiments and joined the discussion and interpretation of the results. During this training, she learned how to design and perform experiments to test a hypothesis.

Dissemination of results to communities of interest? Results to date were presented at the CDMRP IPR meeting at Ft. Detrick in May 2017 to scientific and military participants associated with the CDMRP program . Key findings have also been presented as an invited platform presentation at: the 10th International Conference on Aminoacyl-tRNA Synthetases (Barcelona, Spain, 2016) and the 2017 IUBMB Focused Meeting on Aminoacyl-tRNA Synthetases (Clearwater Fl, 2017).

IMPACT: Our finding that HFol has a >4-fold improvement in therapeutic index over HF establishes Hfol as a new lead compound for the study of EPRS inhibitors as therapeutics in PTOA. We do not find, however, that maximal efficacy of Hfol is improved relative to HF, which was disappointing. Our manuscript (Kim et al.Appendix) regarding the mechanism of action of HF/HFol on cytokine responses in synoviocytes establishes a new class of potential drug targets for future mechanism based therapeutics for PTOA. Work in this manuscript establishes that the effects of pharmacological treatment with tRNA synthetase inhibitors on inflammotry responses mirrors the immunoregulatory/anti-inflammatory effects of local amino acid degradation in tissues. These findings have fundamental importance for our understanding of the mechanisms linking nutrient availability to inflammatory pathology and tissue destruction, in arthritis as well as other chronic disease states.

CHANGES/PROBLEMS. Despite the success of significant aspects of the planned work, a number of factors have contributed to the low publication productivity associated with this grant. These are:

1) The large number of surgeries and associated animal care for the second phase of in vivo studies took significantly longer than originally planned, thereby delaying achievement of milestones as originally planned. Unexpected departure of several personnel on the project (Kim, Jie) also delayed progress significantly as the labs involved are small and identifying and training new personnel has been problematic.

2) Difficulties in obtaining suitable HFol for these studies has also introduced a major delay (a Chinese CRO spent 6 months failing to produce usable material). Suitable HFol has subsequently been obtained, and all surgeries and treatments have now been completed.

3) Technical problems with the study of chondrocytes ex vivo. These cells appear to be quite vulnerable to stresses that change their behavior in culture, making them poorly reproducible tools for studying mechanism of HF/Hfol action. While we had hoped that freshly isolated chondrons would solve this problem, variability inherent to fresh surgical isolates has also made these problematic. For these reasons we have continued to focus on synoviocytes as the primary joint tissue for study ex vivo. Since a growing body of data point to synoviocytes as a key source of tissue damaging factors in arthritis, we feel that the study of these cells effectively advances our study of PTOA therapeutics.

4) Submission of a manuscript on the in vivo efficacy of HF/Hfol in the DMM model has been substantially complicated by the publication of several papers describing the efficacy of HF in OA, proposing a mechanism of HF action based on its effects on TGFß signaling. While these publications confirm our findings that HF is efficacious in models of arthritis, we believe their proposed model for HF action to be incorrect. The need for us to address this published model in our own publication significantly raises the bar for the data we will need to present regarding HF mechanism in our own publication. In addition, we have found that while the effects of Hfol on joint damage in the DMM model are statistically significant, they do not represent a statistically significant improvement in efficacy over HF, reducing impact of a potential publication.

5) An important component of the planned studies of HFol in vivo was the effect of Hfol on early markers of tissue damage following DMM surgery. We have found severe variability in RNA expression analysis across tissue samples (both sham and DMM operated, treated and untreated) that it will not be possible to publish statistically significant analysis of gene expression in these samples. This severely reduces the novel mechanistic component of our planned analyses of in vivo samples

6) The manuscript currently submitted to eLife encompasses an unusually large amount of data and broad body of work. Ordinarily this might have led to several smaller publications that would

already have been completed. Because of the fundamental importance of this work in identifying a novel mechanism by which nutrient sensing modifies inflammatory responses, we have chosen to pool these data into one high impact manuscript that is now submitted.

PRODUCTS. Data described above reflect work product that are a component of one manuscript (Kim et al. "Therapeutic tRNA Synthetase-inhibition Activates a Novel Pathway that Branches from the Canonical Amino Acid Response **")** that has been submitted for publication (appended), and a second manuscript currently being prepared for submission.

PARTICIPANTS & OTHER COLLABORATING ORGANIZATIONS
The following individuals have participated in the project.

Name: Project Role:	Malcolm Whitman, Ph.D Principal Investigator	**NO CHANGE**
Name: Project Role:	Tracy Keller Co-Investigator	**NO CHANGE**
Name: Project Role:	Yefu Li MD/PhD. Principal Investigator	**NO CHANGE**
Name: Project Role:	Lin Xu, MD/PhD. Co-Investigator	**NO CHANGE**
Name: Project Role	Fan Jie, PhD Research Assistant	**NO CHANGE**
Name: Project Role	Kristen Powers Research Scientist	**NO CHANGE**
Name: Project Role	Yeon Jin Kim, PhD. Postdoctoral scientist	**NO CHANGE**

Name: Edenius Maja, PhD.
Project Role: Postdoctoral scientist
Researcher Identifier: (leave blank):
Nearest person month worked: 10.0
Contribution to Project: Design and execution of experiments on HF effects in vitro, development of Q-PCR assays and execution of transcriptomics.
Funding Support:

Name: Chenlu Liu, DDS/PhD
Project Role: research scientist
Research Identifier: (leave Blank)
Nearest Person-Month Worked: 5
Contribution to Project Assist on surgery, care for mice and HF injections, tissues harvesting and subsequent analysis of tissues.
Finding Support:

Name: Beiyu Wang, MD/PhD
Project Role: research scientist
Research Identifier: (leave Blank)
Nearest Person-Month Worked: 5

Contribution to Project Assist on care for mouse tissues harvesting and subsequent analysis of tissues.
Funding Support:

1.) Special Reporting Requirements

None

2.) Appendices: Manuscript submitted to eLife is appended

Therapeutic tRNA Synthetase-inhibition Activates a Novel Pathway that Branches from the Canonical Amino Acid Response

Yeonjin Kim*, Mark S Sundrud*, Maja Edenius, Davide Zocco, Changqian Zhou, Kristen Powers, Erika H Noss, Michael B Brenner, Anjana Rao, Ralph Mazitschek, Chang-Yeol Yeo, Malcolm Whitman**, and Tracy L Keller**

ABSTRACT (154)

Signaling pathways that sense amino acid (aa) abundance are integral to tissue homeostasis and cellular defense. Our lab previously has shown that halofuginone (HF) inhibits the PRS catalytic activity of glutamyl-prolyl-tRNA synthetase (EPRS), thereby activating the Amino Acid Response (AAR). We now show that HF treatment selectively inhibits inflammatory responses in diverse cell types and that these therapeutic benefits occur in cells that lack GCN2, the signature effector of the AAR. Other aminoacyl-tRNA synthetase (aaRS) inhibitors also mimic key aspects of HF treatment in the absence of GCN2. We show here that HF-induced inflammatory suppression occurs without GCN2, but that this immunoregulation is sensitive to depletion of GCN1, an upstream AAR pathway component required for GCN2 activation. Together, these observations indicate that GCN1 constitutes a branch-point from the canonical AAR, and that aaRS inhibition activates a previously unrecognized aa sensor pathway that can modulate immune responses in diverse tissues without the AAR/GCN2 signaling cassette.

INTRODUCTION (~1320)

The ability to successfully respond to environmental stimuli, such as changing nutrient conditions, is essential to an organism's survival. Stringent control, a well-recognized example of programmatic adaption to nutrient limitation occurs in bacteria and utilizes the protein synthetic machinery for signal generation (Hauryliuk et al., 2015; Liu et al., 2015). Stringent control detects amino acid (aa) stress by sensing non-aminoacylated (uncharged) tRNA and responds by comprehensive transcriptional reprogramming that induces growth arrest, upregulates survival genes and increases virulence in pathogenic bacteria (Brown et al., 2016; Liu et al., 2015). In both prokaryotic and eukaryotic cells, aa-insufficiency leads to depletion of available aminoacylated tRNA for addition to growing peptide chains, resulting in the accumulation of stalled ribosomes that have an uncharged tRNA occupying the ribosomal A site (Brown et al., 2016; Sattlegger, 2005; Srivatsan and Wang, 2008). In mammalian cells, this uncharged tRNA accumulation signals aa-insufficiency through an arm of the Integrated Stress Response (ISR), called the Amino Acid Response (AAR) (Harding et al., 2003; Wek, 2018) (Baird and Wek, 2012; Brown et al., 2010). Our lab showed that the natural product derivative halofuginone (HF) targets human glutamyl-prolyl-tRNA synthetase (EPRS) and inhibits its proly-tRNA synthetase (PRS) activity to confer therapeutic benefits (Keller et al., 2012). Aminoacyl-tRNA synthetases (aaRSs), such as EPRS, are ubiquitous, essential protein synthetic enzymes that fuse an amino acid to its cognate tRNA. Both HF-inhibition of EPRS and cellular aa-insufficiency reduce aminoacyl tRNA levels, resulting in the concomitant accumulation of uncharged tRNA (Keller et al., 2012). HF is a therapeutic that prevents tissue damage in a wide variety of disease settings ((Carlson et al., 2014; Guo et al., 2014; Park et al., 2013; Pines, 2014) (Peng et al., 2012; Sundrud et al., 2009)). In our effort to understand how HF's inhibition of EPRS mediates a programmatic change in diverse inflamed tissues, we considered the evolutionarily conserved utilization of the protein synthetic apparatus for cellular adaptive signaling, as well as the immune motif of regulated aa-catabolism for inflammatory suppression.

Metabolic stress pathways and nutrient availability instruct immunity (Chang and Pearce, 2016; Walls et al., 2016) (Grohmann et al., 2017; Murray, 2016) (Hotamisligil, 2017; Tsalikis et al., 2013). Immune cells operate in both nutrient-rich and -restricted niches, such as the gut and tumor microenvironment, which impact their function (Buck et al., 2017). Competition for resources is intense in both inflamed and cancerous tissues, but, in each of these settings, multiple types of immune cells upregulate amino acid catabolizing enzymes, such as indoleamine 2,3-dioxygenase (IDO1) or arginase 1 (Arg1) (Lemos et al., 2019; Munn and Mellor, 2016; Murray, 2016) (Ravishankar et al., 2012). Amino acid depletion at sites of inflammation and in the tumor microenvironment, suppresses inflammation and antitumor immunity (Lemos et al., 2019) (Sharma et al., 2007) (Mondanelli et al., 2017) (Munn and Mellor, 2016). The mammalian immune system balances protective wound healing inflammatory responses with their timely resolution to safeguard tissue and organ integrity. It utilizes the

induced breakdown of amino acids to temper hyper-inflammatory innate responses, foster tolerance to self and promote tissue integrity (Cobbold et al., 2009; Grohmann et al., 2017; Murray, 2016; Walls et al., 2016). Amino acid availability is monitored by two recognized sensors: the AAR, and the mechanistic Target of Rapamycin Complex 1 (mTORC1) pathway (Walls et al., 2016; Wolfson and Sabatini, 2017). The AAR and mTORC1 pathways each have important regulatory roles in immune response and healthspan (Cobbold et al., 2009) (Munn et al., 2005) (Jones and Pearce, 2017) (Gallinetti et al., 2013) (Saxton and Sabatini, 2017) (Haigis and Yankner, 2019) (Kapahi et al., 2010). Both pathways sense and respond to cellular aa-restriction, but they are differentially activated and elicit distinct sets of transcriptional responses and biological effects. Whereas the mTORC1 pathway can sense amino acids directly (Wolfson and Sabatini, 2017) and is inhibited by aa-limitation, the AAR pathway is activated by insufficiency of any aa (Palii et al., 2009) (Tang et al., 2015), and is initiated by the accumulation of uncharged tRNAs (Zaborske et al., 2009) (Wek et al., 1989). Uncharged tRNAs bind to and activate the protein kinase GCN2 (Wek et al., 1989), resulting in GCN2 autophosphorylation and the phosphorylation of eIF2α, the shared component of the integrated stress response (ISR) (Harding et al., 2003; Hinnebusch, 1993) (Wek, 2018). Cellular treatment with an aaRS-inhibitor activates the AAR (Kilberg et al., 2005) (Keller et al., 2012), but does not affect mTORC1 signaling directly (Wang et al., 2008) (Sundrud et al., 2009), making it a useful means to distinguish between cellular responses that are triggered by uncharged tRNA accumulation and those that result from inhibition of the mTORC1 pathway.

The breadth of conditions for which HF has demonstrated therapeutic value, coupled with the fact that EPRS is a ubiquitous enzyme, suggest that this compound could act directly upon multiple tissue targets in an in vivo disease setting. HF is an effective therapy in animal models of autoimmune disease, ischemia-reperfusion, and fibrotic disease, including rheumatoid arthritis (RA) (Park et al., 2014), cardiac stress (Qin et al., 2017), scleroderma (Pines, 2003; Pines et al., 2001) and graft rejection (Levi-Schaffer et al., 1996; Oishi et al., 2016). HF also has progressed to Phase II clinical trials for the treatment of Duchenne muscular dystrophy (DMD) (Huebner et al., 2008; Turgeman et al., 2008). Because HF competes with proline for binding to PRS, addition of excess proline can reverse the effects of HF that are due to PRS inhibition (Keller et al., 2012). Using HF treatment coupled with proline rescue, we have shown that HF's inhibition of PRS catalytic activity is necessary for, and sufficient to explain, the therapeutic action of this compound in vitro (Keller et al., 2012). In prior studies, our labs found that HF treatment, or selective aa-depletion, potently inhibited the in vitro differentiation of $CD4^+$ T helper 17 (T_H17) cells, inhibited the pro-inflammatory function of mature T_H17 memory cells (Carlson et al., 2014), and inhibited progression of T_H17-driven experimental autoimmune encephalomyelitis (EAE), a mouse model of multiple sclerosis (Sundrud et al., 2009) (Carlson et al., 2014). In vitro studies using HF treatment of cytokine-stimulated cells clearly demonstrate that HF can act directly upon fibroblastic and immune cells to suppress tissue remodeling and inflammatory responses (McGaha et al., 2002; O'Connell et al., 2016; Pines, 2014; Qin et al., 2017; Xavier et al., 2004) (Keller et al., 2012). So, work from us, and others, shows that HF's therapeutic mechanism cannot be readily explained by the inhibition of a single cytokine or action upon a specific tissue (Guo et al., 2014; O'Connell et al., 2016; Peng et al., 2012; Qin et al., 2017).

We began this work wanting to better understand HF's therapeutic mechanism in structural cells. Structural and stromal cells play a key role in the tissue inflammatory process, contributing to the pathogenesis of disease both directly, through destructive remodeling of tissues, and indirectly, through the attraction and stimulation of immune cells (Nowarski et al., 2017) (Nguyen et al., 2017) (Valin and Pablos, 2015) (Buckley, 2011; Duffield et al., 2013). Characterized as an anti-fibrotic drug that can act directly upon stromal fibroblasts, HF suppresses extracellular matrix (ECM) production and deposition (Pines and Nagler, 1998). Much has been made of HF's ability to inhibit collagen deposition, and others have proposed the inhibition of TGFβ-stimulated Smad-signaling to be its primary mechanism of tissue action in this setting (Song et al., 2018) (McGaha et al., 2002; Pines, 2014; Xavier et al., 2004). To study how HF might mediate a programmatic change in inflamed structural tissues, our lab utilized an in vitro culture system of TNFα-stimulated fibroblast-like synoviocytes (FLS). FLS are the resident mesenchymal cells in the lining of synovial joints, which play a key role in the pathogenesis of rheumatoid arthritis (RA) (Noss and Brenner, 2008) (Bottini and Firestein, 2013). In the RA synovium, FLS become activated, expressing a well-characterized program of matrix metalloproteinases, inflammatory cytokines, and chemokines that attract and activate immune cells, promoting ongoing inflammation and tissue destruction (Bottini and Firestein, 2013) (Chang et al., 2010; Noss and Brenner, 2008) (Nguyen et al., 2017). FLS maintain their differentiated characteristics and distinctive responses to inflammatory cytokines after establishment in culture (Bottini and Firestein, 2013). Reflecting key differences in the disease pathologies of arthritis and fibrosis, activated FLS induce net collagen destruction, rather than collagen deposition in inflamed

tissues. This difference allows us to study our proposed therapeutic mechanism of HF action-- that HF acts to suppress inflammatory tissue remodeling in structural cells, apart from the more narrow, proposed mechanism-- that HF acts as an inhibitor of TGFβ-induced collagen deposition. For these reasons, FLS are an ideal complement to stromal fibroblasts for a broad study of HF's therapeutic tissue mechanism.

Using either primary RA-FLS or established FLS cultures, we find that HF suppresses a subset of TNFα-stimulated responses, mirroring HF's suppression of pro-inflammatory functions in mature T_H17 memory cells (Carlson et al., 2014). Importantly, we show here that HF-mediated suppression of diverse inflammatory programs, whether in TNFα-stimulated FLS, or IL-23-stimulated T_H17 memory cells, can occur in cells that lack GCN2, the signature effector of the AAR. We further show that treatment with borrelidin, a catalytic site inhibitor of threonyl-tRNA synthetase (TRS) (Ruan, 2004), recapitulates key aspects of HF treatment in activated FLS, also in the absence of GCN2. These data indicate that the inflammatory suppressive tissue benefits of HF treatment are a general property of aaRS inhibition, rather than a singular feature of EPRS inhibition. The durable capacity of multiple aaRS inhibitors to signal in cells that lack GCN2 indicates the presence of a previously unrecognized cellular pathway that senses the accumulation of uncharged tRNAs (Fig. S1). When FLS are depleted of the upstream AAR pathway component GCN1 (Marton et al., 1993), HF's suppression of the inflammatory response largely disappears. Therefore, transduction of an aa-insufficiency signal that regulates programmatic inflammatory suppression is unaffected by the removal of GCN2, but sensitive to the removal of GCN1-- thus defining a novel pathway that branches from the canonical AAR.

RESULTS

HF Suppresses a Distinct Subset of the TNFα-induced Program in FLS. To study the effects of HF treatment on cytokine-stimulated structural cells, we first treated primary RA-FLS with TNFα in the presence or absence of HF, and assayed for matrix metalloproteinase 13 (*MMP13*) expression, using Q-RT-PCR. In RA-FLS, TNFα strongly induced the expression of *MMP13,* a collagenase involved in the pathophysiology of arthritis (Goldring et al., 2011) (**Fig.1A**), and HF potently suppressed this induction. The suppression of TNFα-induced *MMP13* expression was reversed by the addition of excess L-proline to culture medium (**Fig.1A**), confirming the role of PRS inhibition in this treatment model. HF treatment of RA-FLS at therapeutic doses did not affect global protein synthesis over 24 hours (**Fig S2**), and cells that were pre-treated with HF remained refractory to TNFα-induced *MMP13* upregulation for up at least 72 hours (**Fig. S3**). These results indicate that EPRS-mediated HF treatment results in durable, selective reprogramming of RA-FLS that suppresses a key participant in the TNFα-driven tissue destructive response in arthritis.

To examine whether HF treatment could modify cellular response to other cytokines in our in vitro model of arthritis tissue response, we stimulated RA-FLS with IL-1ß, with or without HF. As in TNFα-stimulated RA-FLS, HF treatment inhibited IL-1ß-induced upregulation of *MMP13,* and this inhibition was alleviated by proline supplementation (**Fig. 1A**). Expanding our observations to the cytokine-stimulation of other structural cells, we treated TNFα- or IL-1ß- stimulated primary human endothelial cells (HUVEC) with HF, and saw HF inhibition of the cytokine-induction of VCAM-1 and E-selectin (**Fig. 1A, S4**), two critical mediators of vascular inflammation (Agarwal and Brenner, 2006; Kakkar and Lefer, 2004) (Marcos-Ramiro et al., 2014). Likewise, in lung fibroblasts, HF inhibited TGFß-driven induction of smooth muscle actin (SMA) and CTGF (**Fig. 1A, Fig. S4**), two key pro-fibrotic factors (Leask, 2008) (Krieg et al., 2007). In each of these cases, HF's suppression of pro-inflammatory and/or pro-fibrotic structural cell responses was opposed by the presence of excess proline (**Fig. 1A, S4**). These data demonstrate that HF acts via PRS inhibition to suppress the cytokine induction of key inflammatory and/or tissue remodeling responses in diverse cells.

To provide an unbiased look at the effects of HF on a program of inflammatory response, we performed RNA-seq and differential expression analysis on RA-FLS treated with TNFα, HF, or both. More than 80% (10/12) of genes induced $\geq$ 1000-fold by TNFα stimulation were suppressed at least 5-fold in HF-treated FLS, whereas only half (83/171) of the genes induced between 16- and 64-fold by TNFα stimulation, and only 5% of the total FLS transcriptome were similarly sensitive to HF treatment (**Fig. 1B, S5A**). Examples of TNFα-inducible genes in FLS that were inhibited by HF included: 1) several matrix degrading proteases (*MMP1*, *MMP3*, *MMP9*, *MMP13*, *CTSS*, *CTSK*), 2) a series of pro-inflammatory chemokines and cytokines (*e.g. TNFα, IL-33, CXCL9, CXCL10*), 3) *SLC39A8/ZIP8*, a zinc transporter implicated in RA-associated joint damage (Kim et al., 2014), and 4) the serum amyloids *SAA1* and *SAA2,* secreted factors known to promote T_H17 cell activation (Sano et al., 2016) (Atarashi et al., 2015) that we confirmed by Q-RT-PCR (**Fig. S6**). Conversely, HF treatment of RA-FLS induced the expression of a smaller number of genes that were repressed by TNFα (*e.g.*, 65 genes inhibited by

TNFα ≥ 10-fold) (**Fig. 1B, S5A; Supplementary File 1**). *HES1,* a repressor of transcriptional elongation that suppresses CXCL1 production and, consequently, neutrophil recruitment (Shang et al., 2016) is one notable example from this group. Underscoring a specificity of action, HF had no effect on the expression of several TNFα-inducible genes, including *PTGS2* and *CXCL3*, and enhanced the induction of *IL6*. These genes, like most of the TNFα-induced genes inhibited by HF, are transcriptional targets of NFκB-activation downstream of both TNFα and IL-1ß signaling (**Supplementary File 1, Fig. 1B, S5**) (Mestre et al., 2001) (Vanden Berghe et al., 1998), indicating that HF's inhibition of cytokine signaling is not associated with global inhibition of NFκB activation. Accordingly, gene ontology (GO)-based pathway enrichment analysis of TNFα-inducible genes in FLS that are either HF-sensitive or HF-insensitive revealed that HF treatment preferentially represses the subset of TNFα-induced genes that promote chronic inflammatory responses (*i.e*., recruitment/activation of leukocytes), compared to the TNFα-driven gene expression modules that increase innate immunity to bacterial and viral pathogens (**Fig. 1C**). Taken together, these observations indicate that HF can act therapeutically to suppress a cytokine-mediated program of inflammatory responses in quiescent structural cells.

HF treatment shares features with immunoregulated aa-catabolism. HF and aa-catabolism each trigger the accumulation of uncharged tRNA, which activates GCN2 signaling. Once considered to be the mechanistic core of IDO1 immunosuppression (Munn et al., 2005), the role of GCN2 signaling in this process has been challenged (Van de Velde et al., 2016) (Cobbold et al., 2009) (Jasperson et al., 2009). Because HF treatment overlaps with IDO1-induction, both in mechanism and therapeutic tissue response, we next asked: do TNFα-stimulated FLS respond to HF treatment in the absence of GCN2 signaling?

HF Suppression of TNFα-induced Responses Can Occur Without GCN2 Signaling. To address this point, we examined the effect of HF treatment on TNFα-induced responses in $GCN2^{-/-}$ or GCN2-depleted FLS. Phosphorylation of eIF2α by GCN2 kinase leads to transient reduction in cap-dependent mRNA translation, and a concomitant increase in translation of a subset of mRNAs, notably the transcription factor ATF4 (Donnelly et al., 2013) (Harding et al., 2000). Whereas, broad translational inhibition conserves cellular amino acid stores, upregulated translation of ATF4 mediates expression of genes involved in amino acid transport and biosynthesis that constitute the adaptive response to aa-stress, such as TRIB3, ASNS, and SESN2 (Kilberg et al., 2005) (Ye et al., 2015) (Ohoka et al., 2005). To assess the presence or absence of intact AAR signaling, we assayed several AAR responses and genes. We show here that HF does not promote phosphorylation eif2α or induction of ATF4 in *Gcn2*$^{-/-}$ FLS (**Fig.S7)**, confirming that HF activation of the eIF2α signaling cassette is strictly GCN2-dependent **(Fig.S7)**. Surprisingly, the ability of HF to suppress TNFα-induction of *Mmp13* or *Mmp1a* expression was unaffected in primary FLS from *Gcn2*$^{-/-}$ (also known as *Eif2ak4*$^{-/-}$) mice (**Fig.2A**). Furthermore, HF-suppression of MMP13- and MMP1a-expression in TNFα-stimulated $Gcn2^{-/-}$ FLS was reversed by the addition of excess proline (**Fig.2**), validating PRS inhibition as the mechanism of action. HF effects on TNFα-induced responses were, likewise, unaffected by shRNA-mediated depletion of GCN2 in primary human RA-FLS (**Fig.S8)**, and depletion of GCN2 did not affect HF-dependent suppression of TGFß-induced Col1A1 upregulation in dermal fibroblasts (**Fig.S9**). To confirm that the GCN2-eif2α-ATF4 signaling cassette is dispensable for many HF effects on cytokine responses, we ectopically expressed GADD34, a constitutively-active fragment eif2α phosphatase regulatory subunit (Novoa et al., 2001), in immortalized K4 human FLS (Haas et al., 1997). GADD34 expression eliminated both baseline and HF-stimulated eif2α phosphorylation, but had no effect on HF's capacity to suppress TNFα-induction of MMP13 and CXCl10 (**Fig.S10**), confirming that GCN2 signaling is not required for key HF-treatment responses in FLS.

Transcriptomic analysis of *wild-type* vs. GCN2-depleted K4 FLS that were treated with TNFα, HF, or both (**Fig.2B, C**; **Supplementary File S2**), revealed that GCN2 is broadly dispensable for HF action on TNFα-induced responses. GCN2-depletion markedly reduced HF-induction of AAR response genes (**Fig.3B left panel**), confirming an effective functional knockdown of GCN2. HF-mediated inhibition of TNFα-responsive genes, in contrast, was either unaffected or slightly enhanced following GCN2 knockdown (**Fig.2C**). Furthermore, GCN2-depletion had no systematic impacts on TNFα-induced gene expression in the absence of HF (**Fig.2B**, right panel). Together, these findings indicate that GCN2 is not required for HF-mediated inflammatory suppression in FLS.

aaRS-inhibition Recapitulates HF-treatment in GCN2-depleted Cells**.** Inhibition of the catalytic activity of any aaRS, such as PRS, leads to the accumulation of non-aminoacylated tRNA, activating the AAR via GCN2 phosphorylation (Kilberg et al., 2005) (Keller et al., 2012) (Sundrud et al., 2009). We demonstrate here, however, that HF inhibition of PRS, as confirmed by proline rescue, suppresses a TNFα-mediated program of inflammatory

responses in the absence of GCN2 signaling, making the tissue mechanism of HF action unclear. We, therefore, considered whether the observed therapeutic effects were unique to EPRS, possibly stemming from a non-canonical EPRS activity (Mukhopadhyay et al., 2009) (Guo and Schimmel, 2013) incidental to catalytic PRS inhibition, or a general feature of aaRS-inhibition and, thus, elicited by uncharged tRNA accumulation. Previously, we showed that selective amino acid depletion and treatment with the TRS-inhibitor borrelidin (Fang et al., 2015) inhibits T_H17 cell differentiation comparably to HF (Sundrud et al., 2009). Recently, others have shown that borrelidin, or leucinol, treatment mimics the anti-fibrotic effects of HF in human cardiac fibroblasts, inhibiting type I collagen deposition, as well as Col1A1 gene and protein expression (Qin et al., 2017). Therefore, we tested the effects of borrelidin on cytokine responses in primary and established FLS. In primary human RA-FLS, both HF and borrelidin inhibited TNFα-induction of MMP13 and CXCL10 (**Fig.3A**) at doses matched to reflect similar activation of the AAR pathway (**Fig.S11**). Borrelidin treatment, like HF treatment, enhanced TNFα-induction of IL6 (**Fig.S12**), confirming that the distinctive specificity of HF action to inhibit some TNFα-stimulated responses, but not others is shared by a different aaRS inhibitor. We then compared the effects of borrelidin and HF treatment in GCN2-depleted K4 FLS; depletion of GCN2 was confirmed by a substantial reduction in borrelidin-induced TRIB3 compared to control K4 cells. Like HF treatment, borrelidin treatment suppressed TNFα-induction of MMP13 and CXCL10 in these cells, as in control K4s (**Fig.3B**). Additionally, we demonstrated inhibition of TNFα-induced gene expression in FLS following histidine deprivation (**Fig S13**). Collectively, these findings establish that any number of cellular treatments that cause the accumulation of uncharged tRNAs can suppress TNFα-stimulated responses in FLS, in the absence of GCN2 signaling. HF's therapeutic program of inflammatory suppression, therefore, is a general feature of aaRS-inhibition, shared with aa-catabolism, and the cellular aa-insufficiency signal of uncharged tRNA accumulation can be sensed and transduced without the canonical AAR/GCN2 signaling cassette.

HF effects on Pro-inflammatory T_H17 Cells Occur in Gcn2 $^{-/-}$ cells. Next, we sought to establish whether GCN2 signaling is required for each of our previously reported, HF-mediated observations in T cells: 1) inhibition of cytokine-directed T_H17 differentiation, and 2) inhibition of pro-inflammatory functions in mature T_H17 memory cells. Using T cells obtained from *Gcn2* $^{-/-}$ mice (Munn et al., 2005), we confirmed that, in these cells, HF neither induces eif2α phosphorylation (**Fig. S14A**), nor does HF induce of a cluster of adaptive AAR-associated responses, including expression aa-transport and -biosynthesis genes. (**Fig. S14B**). Strikingly, HF treatment inhibits T_H17 differentiation with similar potency in wild type and *Gcn2*$^{-/-}$ cells (**Fig. 4A,C**); this inhibition is rescued by addition of proline (**Fig. 4B**). Naïve $CD4^+$ T cells from *Gcn2*$^{-/-}$ mice show no overt functional defects *in vitro (***Fig, S14***),* indicating that, consistent with prior work, *Gcn2* is dispensable for most basic T cell functions , *in vitro. (*Sundrud) (Munn et al., 2005).

In addition to blocking the differentiation of naïve T cell precursors into T_H17 cells, we have previously shown that HF suppresses the pro-inflammatory response of already-differentiated T_H17 'memory' cells to IL-23 (Carlson et al., 2014). *In vivo*, T_H17 memory cells are distinguished from other memory T cell subsets by the expression of the mucosal chemokine receptor, CCR6, and, unlike in naive T cells, TCR stimulation is sufficient to induce basal IL-17A expression in T_H17 memory cells (Ramesh et al., 2014) (Carlson et al., 2014) (Acosta-Rodriguez et al., 2007). IL-23 stimulation further enhances pro-inflammatory function of T_H17 memory cells, and is required for T_H17 cell-driven autoimmunity *in vivo* (Cua et al., 2003) (Lee et al., 2012). Wild type and *Gcn2* $^{-/-}$ mice harbored similar numbers and percentages of endogenous T_H17 memory cells (data not shown), which allowed us to address the role of Gcn2 in HF-dependent regulation of T_H17 memory cell function. As in wild type T_H17 memory cells (Carlson et al., 2014), those lacking GCN2 expressed IL-17A following TCR stimulation, and upregulated IL-17A further in the presence of IL-23 (**Fig. 4C**). HF suppressed IL-23-induced IL-17A expression in *Gcn2* $^{-/-}$ T_H17 memory cells, leaving intact basal IL-17A expression, and this suppression was again abolished by provision of excess proline. (**Fig. 4C).**

Both IL-6-mediated T_H17 differentiation and IL-23-dependent memory T_H17 cell function proceeds through the transcription factor Stat3 (Durant et al., 2010). We have previously shown that HF inhibits Stat3 activation (*i.e.*, Tyr705 phosphorylation) downstream of multiple cytokines in wild type T_H cells, including IL-6, IL-23 and IL-27, and that this inhibition is associated with decreased Stat3 protein, but not mRNA, levels (Carlson et al., 2014). Indeed, HF also decreased Stat3 protein levels in *Gcn2* $^{-/-}$ T_H17 cells in both dose-dependent and proline-responsive manners (**Fig. 4D**, *left*; data not shown). Consistent with post-transcriptional regulation, HF reduced Stat3 protein abundance in *Gcn2* $^{-/-}$ Th17 cells without impacting *Stat3* mRNA levels (**Fig. 4D**, *right*). Thus, all aspects of HF-dependent Th17 regulation that we have previously described in wild type cells occur in cells lacking GCN2.

To better understand the relative contribution of GCN2-dependent and GCN2-independent pathways in the response of T_H17 cells to HF, we performed microarray time-course experiments, in which wild type or *Gcn2* $^{-/-}$naïve $CD4^+$ T cells were stimulated in T_H17-polarizing conditions +/- HF, and RNA was isolated at various time-points post-activation (e.g., 4, 18, 72 hr). Whereas more than half of all genes acutely affected by HF-treatment in wild type cells at 4 hr (39/71) represented canonical AAR-associated genes that were induced by HF in wild type, but not *Gcn2* $^{-/-}$, T cells, the vast majority of HF-regulated genes evident at 18 hr (120/177) and 72 hr (122/143) were suppressed equivalently in wild type and *Gcn2* $^{-/-}$ T_H17 cells (**Fig. 4E, 4F**) (**Table S3**). Key molecules involved in T_H17 cell differentiation and pro-inflammatory function—*Il23r*, *Tgfb3*, *Il17a*—were among these genes suppressed by HF in the absence of GCN2 (**Fig. 4E, 4F**) (Lee et al., 2012). These findings indicate that, in the absence of GCN2 signaling, HF-mediated inhibition of EPRS suppresses key aspects of pro-inflammatory cytokine programs responsible for the differentiation of T_H17 cells.

HF effects on Cytokine Responses are Sensitive to Depletion of GCN1. GCN1 was originally identified in yeast as an AAR pathway gene required for activation of GCN2 (Marton et al., 1993). We, therefore, examined whether mammalian GCN1 (GCN1L1) might have a role in mediating the effects of HF inhibition on TNFα-stimulated inflammatory responses, distinct from its recognized role in GCN2 activation. To test this possibility, we used shRNA mediated knockdowns of GCN1 or GCN2, matched with respect to their effects on AAR pathway readouts, to compare the effects of each depletion on HF therapeutic responses (**Fig. 5A**). Depletion of GCN1 or GCN2, each with 2 independently targeted shRNAs (**Fig**. **5A)**, reduced HF-induced GCN2 phosphorylation (**Fig**. **5A**), and reduced HF induction of the AAR-responsive transcription factor TRIB3 (**Fig. 5B).** GCN1 depletion, but not GCN2-depletion, largely prevented the ability of HF to suppress its characteristic subset TNFα-responsive genes (**Fig. 5B**), with either of two independently targeted shRNAs. To date, our CRISPR-mediated inactivation of GCN1 drastically reduced proliferation of K4 synovial cells to an extent that made them unsuitable for comparison to control cells (data not shown), which is consistent with findings in other cell types (Wang et al., 2015) (Hart et al., 2015). These knockdown data indicate that GCN1 mediates an inflammatory-suppressive response to HF inhibition, distinct from its role in the activation of GCN2, and points to a novel upstream branch-point in the canonical AAR pathway (**Fig.S1).**

DISCUSSION (2270, 43 in Headings)

In our effort to understand how the EPRS-inhibitor HF mediates programmatic change in diverse inflamed tissues, we discovered a novel nutrient stress pathway that senses aa-limitation using the cell's protein synthetic apparatus to induce a program of inflammatory suppression. This pathway, which we call the Amino Acid Immune Regulating (AAIR) pathway, branches from the canonical AAR, as demonstrated by data that it signals in cells that lack GCN2, but is sensitive to the removal of the upstream AAR pathway component GCN1(Fig. S1). aaRS-inhibitors, like HF, act as aa-restriction mimetics by triggering the cellular accumulation of uncharged tRNAs. This new pathway shares the activation mechanism of the AAR, which means that it is ubiquitous and can be induced by inhibition of any aaRS or the limitation of any single amino acid.

HF Treatment Shares Features with Immunoregulated aa-catabolism. A tissue's nutrient environment, specifically amino acid availability, influences immune function (Buck et al., 2017) (Grohmann et al., 2017) (Murray, 2016 {Hotamisligil, 2017 #3805) (Walls et al., 2016) (Lemos et al., 2019) (Chang and Pearce, 2016) (Tsalikis et al., 2013). Immune cell activation, differentiation and expansion of effector populations, and the production and release of cytokines are metabolically demanding processes; immune cells are uniquely sensitive to the presence or absence of nutrients to meet their functional needs (Buck et al., 2017) (Johnson et al., 2016) (Chang and Pearce, 2016). As well as being sensitive to the nutrient microenvironment, however, the immune system creates aa-insufficiency by upregulating the expression of aa-catabolizing enzymes to effect inflammatory suppression (Murray, 2016) (Grohmann et al., 2017) (Lemos et al., 2019). In mammalian cells, catabolism of tryptophan and arginine is fundamental to this immunoregulation (Grohmann et al., 2017; Murray, 2016) (Grohmann et al., 2017; Lemos et al., 2019) (Geiger et al., 2016) Mellor, 2008 #732}. Multiple immune cell types upregulate IDO1 (which catalyzes the rate-limiting step of tryptophan catabolism), or Arg1 (which degrades arginine) at sites of pathological inflammation or wounding (Fouda et al., 2018; Gause et al., 2013; Herbert et al., 2010; Murray, 2016; Pesce et al., 2009). The molecular mechanism of IDO1-induced immunosuppression is incompletely understood, but it involves both the generation of bioactive kynurenines (tryptophan catabolites that are aryl hydrocarbon receptor ligands) and signaling through aa-stress pathways, like the AAR and mTORC1, each of which contribute to IDO's physiological impact, to unknown extents (Belladonna et al., 2009; Fallarino et al., 2012; Munn et al., 2005; Munn and Mellor, 2013). In Interferon-γ-stimulated dendritic cells (DCs), induction

of IDO1 dampens tissue inflammation and confers immunosuppressive and tolerogenic properties. Depletion of tryptophan in the DC and local environment causes potent suppression of pro-inflammatory effector T cell proliferation and functional anergy (Cobbold et al., 2009; Munn et al., 2005; Van de Velde et al., 2016). Signaling through aa-stress pathways, triggered by amino acid depletion, is thought to collaborate with kynurenine-activated aryl hydrocarbon receptor (AhR) signaling to promote de novo T_{REG} differentiation and expansion (Belladonna et al., 2009; Fallarino et al., 2012; Munn and Mellor, 2013). Conversely, the upregulation of IDO1 and several other aa-catabolizing enzymes can be induced DC subsets (Cobbold et al., 2009; Mellor and Munn, 2004) via ligation of T_{REG}-expressed CTLA-4 with CD80/CD86. These IDO-competent, aa-catabolizing DCs lose their T cell stimulatory properties and instead acquire potent regulatory and suppressive functions, comprising an important component of peripheral tolerance (Belladonna et al., 2009; Cobbold et al., 2009; Fallarino et al., 2012; Mellor and Munn, 2004; Munn and Mellor, 2013).

HF treatment and aa-catabolizing enzymes, such as IDO1, have overlapping mechanisms of action and shared tissue consequences. Previously, we showed that HF treatment potently inhibits cytokine-directed T_H17 differentiation (Keller et al., 2012) and suppresses IL-23-stimulated pro-inflammatory functions in mature T_H17 memory cells (Carlson et al., 2014). We now show that these HF-mediated T cell effects can occur in cells that lack GCN2. HF and other aaRS-inhibitors are powerful tools with which to parse the aa-catabolic signal; they act as aa-restriction mimetics by triggering the cellular accumulation of uncharged tRNA, but, unlike aa-catabolism, they neither generate bioactive catabolites, nor do they directly inhibit the mTORC1 pathway. Although GCN2 signaling plays ~~several~~ distinct ~~and important~~ roles in the immune system (McGaha, 2015; Ravindran et al., 2014; Ravindran et al., 2016; Van de Velde et al., 2016; Walls et al., 2016) (Rodriguez et al., 2007), GCN2-independent responses both to IDO1-induced tryptophan catabolism (Cobbold et al., 2009; Jasperson et al., 2008; Van de Velde et al., 2016), and to general amino acid restriction have been reported (Chaveroux et al., 2009; De Vito et al., 2018; Deval et al., 2009; Shan et al., 2014). Furthermore, evidence that IDO-induced tryptophan depletion has a central role in local immunosuppression (Muller et al., 2008; Munn et al., 2005), and reinforcement of peripheral tolerance is at apparent odds with the absence of a prominent immunologic phenotype in either IDO-null or GCN2-null mice (Cobbold et al., 2009; Murray, 2016). It has been noted that this discrepancy suggests redundancy in the signaling networks that govern these processes (Cobbold et al., 2009). One example of such redundancy is the observation that T_{REGS} stimulate the expression of multiple aa-consuming enzymes within dendritic cells (DCs) and successful skin grafts (Cobbold et al., 2009). Whereas GCN2 kinase signaling was once thought to be the core mechanism that mediates proliferative arrest and anergy in T cells (Munn et al., 2005), several studies now directly challenge the notion that immunoregulated aa-catabolism acts through AAR pathway activation (Cobbold et al., 2009; Jasperson et al., 2009), or that GCN2 is required for sensing aa-depletion in T cells (Cobbold et al., 2009) (Van de Velde et al., 2017). Cobbold et al showed that the in vitro restriction of a single amino acid was sufficient to suppress the proliferation of T cells in response to antigen, and that this response could occur in cells that lack GCN2 (Cobbold et al., 2009). Likewise, Van de Velde et al (Van de Velde et al., 2017) demonstrated that GCN2-deficient T cells retain the capacity to sense and respond to tryptophan limitation. To date, studies of aa-depletion- or IDO1-induced immunosuppression in the GCN2-null context have focused on the mechanism of mTORC1 pathway inhibition (Cobbold et al., 2009; Murray, 2016; Van de Velde et al., 2017), and on tissue responses to kynurenine metabolites (Jasperson et al., 2009). Our discovery of a novel aa-sensor pathway that doesn't signal through GCN2 activation provides an additional potential explanation for observed immunoregulation in the GCN2-null context, and prompts further study of the IDO1 mechanism in critical pathological contexts, such as the chronic inflammatory or tumor microenvironment. Knocking down GCN1 in key immune cell populations will be important future work.

Structural Cells Respond to aaRS-treatment**.** Over the last 25 years, HF has been studied extensively as an anti-fibrotic drug (Pines and Nagler, 1998) (Pines, 2014), and used to treat a variety of fibrotic manifestations in animal models (Oishi et al., 2016; Pines et al., 2001; Qin et al., 2017; Turgeman et al., 2008; Xavier et al., 2004). More recently, HF has been used effectively for the treatment of autoimmune disease in animal models of EAE, RA, psoriasis and scleroderma, consistent with its activity as a potent inhibitor of T_H17 differentiation. We've used the competition between HF and proline for binding to their common target, the PRS catalytic site, to demonstrate that HF's therapeutic effects in immune and structural tissues are solely attributable to EPRS target inhibition (Fig.2) (Keller et al., 2012). In vitro experiments demonstrate that HF acts directly upon structural cells. HF treatment of fibroblasts decreases collagen deposition, suppresses collagen transcription and protein levels (McGaha et al., 2002; Qin et al., 2017), and inhibits TGFβ-stimulated induction of fibrotic markers, such as

smooth muscle actin and CTGF(Fig.2). We now show that HF potently, and selectively, inhibits a TNFα-driven tissue remodeling program that involves collagen destruction in cultured FLS. These data demonstrate that EPRS inhibition can modulate different inflammatory and/or tissue remodeling programs in diverse cell types, as indicated by: 1) HF's inhibition of T_H17 cell differentiation, 2) HF's inhibition of ECM deposition and TGFβ-stimulated induction of fibrotic markers in fibroblastic cells, and 3) HF's inhibition of TNFα-mediated inflammatory and matrix-degrading program in cultured FLS.

HF is not the only aaRS-inhibitor that can elicit these characteristic tissue effects. Borrelidin treatment both inhibits the differentiation of T_H17 cells (Keller et al., 2012), and suppresses pro-fibrotic markers in lung fibroblasts (Whitman lab, unpub). Qin et al (Qin et al., 2017) recently showed that HF, borrelidin and leucinol inhibit collagen deposition in cardiac fibroblasts, and that these effects can be rescued by the addition of proline, threonine, and leucine, respectively. We show here that treatment of cytokine-stimulated FLS with borrelidin, or starvation for the amino acid histidine, can mimic key aspects of HF's inflammatory suppression program in FLS. These data demonstrate that the effects of HF, whether inhibiting the deposition of ECM, the degradation of cartilage, or the differentiation and function of a pro-inflammatory T helper cell subset, are part of broader homeostatic signal that is a shared feature of other aaRS-inhibitors, and of aa-restriction, in general. For this reason, we looked for evidence that endogenously-regulated aa-catabolism can impact structural cells and instruct tissue remodeling behavior.

Immunoregulated Arginine-depletion Drives Fibrosis Resolution. Type 2 (T_H2) immune responses provide host protection against parasites, such as helminth infection, control inflammation, and promote wound repair (Gause et al., 2013). In wild-type mice, infection with *Schistosoma mansoni* results in a protective granuloma formation, and a T_H2 response sufficient to kill schistosome eggs (Allen and Sutherland, 2014). This T_H2 response is associated with a strong activation of the arginine-degrading enzyme Arg1 in M2 macrophages by Th2 cytokines (Herbert et al., 2010). This potent induction of Arg1, combined with upregulation of arginine import, make M2 macrophages a big sink for the tissue-depletion of arginine. In mice that are deficient in macrophage-specific Arg1 ($Arg1^{\Delta M}$), however, schistosomiasis results in a non-resolving granulomatous pathology, unrestricted Th2 cell proliferation and marked liver fibrosis (Pesce et al., 2009). These data demonstrate that Arg1-expressing macrophages function as suppressors of fibrosis, and governors of T_H2-dependent inflammation (Murray, 2016). We surmise that aaRS-inhibitors mimic the endogenous effects of upregulated aa-catabolism**,** suppressing T cell proliferation and fibrosis**,** by inducing aa-stress pathway signals, including the novel pathway described here.

aaRS-inhibition Suppresses Inflammatory Programs in T cells and FLS without GCN2. The convergence of findings in T cells and FLS points strongly to a common pathway linking HF inhibition of EPRS to the suppression of inflammatory programs in both immune and structural cells. Transcriptomic analyses of HF-treated T cells cultured under T_H17-polarizing conditions establish that HF inhibits a broad program of genes in these cells (Supplementary File 3). HF's inhibition of pro-inflammatory function of mature T_H17 memory cells proceeds via post-transcriptional and transcriptional suppression mechanisms. Using either primary RA-FLS or established FLS cultures, we show that HF also potently suppresses key IL1ß- and/or TNFα-driven transcriptional responses. In T cells cultured under T_H17-polarizing conditions, IL-23-stimulated T_H17 memory cells and cytokine-stimulated FLS, HF exerts its inflammatory suppressive effects in cells that lack GCN2. RNA-Seq analyses of TNFα-stimulated FLS, show that HF suppresses a distinct subset of TNFα's fully-induced transcriptome, potently inhibiting some genes, while inducing or not affecting others. Gene ontology analysis indicates that HF preferentially suppresses gene programs that are involved in chronic inflammation, over those regulating acute response to pathogens (Fig 1C), further demonstrating patterned specificity.

In multiple cell types, stimulated with different cytokines that produce diverse programmatic outputs, we see that aa-restriction (histidine deprivation) and the application of aa-restriction mimetics (HF, borrelidin) directed toward different aaRS targets (HRS, EPRS, TRS, respectively) leads to the potent suppression of inflammatory and tissue remodeling parameters. The dose for onset of HF-induced tissue benefit tracks reliably with AAR pathway activation, but can occur cells that lack GCN2. Taken together, these data suggest the presence of a signaling pathway that shares the AAR's activation strategy, but branches from the AAR upstream from GCN2. So, we considered AAR pathway components upstream from GCN2 as potential candidates to transduce the observed inflammatory-suppressive signal.

How are uncharged tRNAs sensed in cells without GCN2? Currently, GCN2 is the only protein in mammalian cells that is known to sense and transduce an uncharged tRNA-based signal (Castilho et al., 2014). The AAR detects aa-stress through the build-up of uncharged tRNAs that activate GCN2, by binding to a histidyl-tRNA synthetase (HRS)-like domain in its C-terminus (Wek et al., 1989). GCN2 then responds by autophosphorylation

and phosphorylation of eIF2α (Harding et al., 2003) (Kilberg et al., 2005). Our findings demonstrate that perturbations that cause the cellular accumulation of uncharged tRNAs also induce an inflammatory suppressive program in cells that lack GCN2, thus indicating the presence of a novel pathway that must sense and respond to this stress signal.

In *Saccharomyces cerevisiae,* as in *E. coli* (Brown et al., 2016), uncharged tRNA is detected in the context of the stalled ribosome (Sattlegger and Hinnebusch, 2000) (Sattlegger, 2005). In aa-starved yeast, neither general amino acid control nor GCN2 signaling can be activated in response to uncharged tRNA, without GCN2 binding to GCN1 (Marton et al., 1993), which forms a complex with GCN20 (Marton et al., 1997). The GCN1-GCN20 complex binds the ribosome and is positioned near its A-site where GCN1 is thought to alter its function, possibly facilitating the transfer of uncharged tRNA to GCN2 for binding and activation of the AAR/ISR pathway (Sattlegger and Hinnebusch, 2000). The requirement of GCN1 for GCN2 activation also has been demonstrated recently in mammalian cells (Silva et al., 2016). Consistent with these data, we show here that GCN1 is required for GCN2/AAR pathway activation in K4 human FLS cells. In mice, GCN1-null germline mutation results in early embryonic lethality (K.Itoh, H. Yamazaki, Hirosaki University Graduate School of Medicine, personal communication), whereas GCN2-null mice survive to fertile maturity (Munn et al., 2005), pointing to a critical role for GCN1 in mammals distinct from its function in GCN2 regulation. Because GCN1 is genetically upstream from GCN2 in the mammalian AAR pathway, it is a potential candidate for a branch-point and transducer of the HF-induced inflammatory-suppressive signal. Significantly, we find that therapeutic HF-suppression of TNFα-stimulated FLS is sensitive to the removal of GCN1, indicating that GCN1 constitutes a branch-point in the canonical AAR pathway. GCN1 lacks any recognized enzymatic activity or tRNA-binding motif, and may act as a scaffold to bind a sensor of A-site-resident tRNA, transducing an aa-stress signal that broadly alters tissue inflammation and remodeling. Determining exactly how uncharged tRNA is sensed and coupled to downstream signaling will be important future work.

Do People and Plants Share an Immune Pathway? The AAR is the oldest arm of the ISR, conserved to plants (Zhang et al., 2003), worms (Hirose and Horvitz, 2014), and yeast (Hinnebusch, 1993). Studies in *Arabidopsis thaliana (A. thaliana)* also point to branching in the AAR pathway, and a GCN2-independent role for GCN1 in pathogen defense and abiotic stress (Izquierdo et al., 2018) (Faus et al., 2018) (Luna et al., 2014). In 2014, Luna *et al* (Luna et al., 2014) established that aspartyl-tRNA synthetase (AtDRS) is the critical target for the defense priming agent β-aminobutyric acid (BABA), a non-proteinogenic amino acid that is widely used to protect agricultural yield against a broad range of crop stress. This group showed that BABA inhibits the catalytic activity of AtDRS, leading both to defense priming and to the major undesirable effect of BABA-treatment, inhibition of plant growth. Strikingly, growth-inhibition was relieved in BABA-treated plants that lack AtGCN2, but BABA-priming of immune defense was unaffected by loss of AtGCN2. Like animals and fungi, *A. thaliana* have a GCN1 orthologue, AtGCN1/ILITHYIA (ILA) that is required for AtGCN2 activation (Izquierdo et al., 2018) (Faus et al., 2018) (Wang et al., 2017). Although Luna *et al* did not examine the possible involvement of AtGCN1 in BABA-primed immunity, two independent lines of investigation have generated AtGCN1 mutants (Izquierdo et al., 2018) (Faus et al., 2018). In addition to mediating adaptation to aa-deprivation and the activation of GCN2/eIF2α-phosphorylation, various other AtGCN1 mutants fail to phenocopy the loss of AtGCN2, and impact plant immunity and defense, as well as adaptation to several abiotic stress responses (Izquierdo et al., 2018) (Faus et al., 2018; Monaghan and Li, 2010).Considered together, these observations suggest that the signaling apparatus that allows amino acid deprivation to modulate immune function and cellular defense through GCN1 arose early in the evolution of immunity in multicellular organisms. Studies addressing this topic will be exciting future work.

Impact. We report here the identification of a novel mammalian pathway that senses aa-insufficiency, and has regulatory impact on cellular immune and inflammatory responses. Like stringent control and the AAR, this pathway utilizes the cell's protein synthetic machinery to signal via the accumulation of uncharged tRNA. We previously showed that HF inhibition of PRS catalytic activity is sufficient to explain the therapeutic action of this compound (Keller et al., 2012), and now we show that HF's tissue effects cannot be attributed solely to canonical AAR pathway activation. Our work, and an important body of work by others, demonstrate that perturbations which cause the cellular accumulation of uncharged tRNAs, aa-restriction and the inhibition of aaRSs, can reproduce key features of HF's therapeutic action (Peng et al., 2012; Sundrud et al., 2009) (Keller et al., 2012) (Qin et al., 2017). Using T_H17-polarized T cells and TNFα-stimulated FLS, we now establish that HF treatment mediates suppression of distinct inflammatory programs in immune and structural cells, notably in cells that lack the signature AAR effector GCN2. We provide here a fuller understanding of the tissue mechanism of aaRS-inhibitors for the treatment of human disease, both by characterizing HF's suppression of disease-relevant

inflammatory and tissue remodeling programs, and by identifying a novel mode of therapeutic action, activation of a pathway we call the AAIR (Fig S1). Our work points to the tremendous therapeutic potential of aaRS-inhibitors due to their capacity to promote restoration of immune and tissue homeostasis in diverse cell types. We identify here a branch-point in the AAR at GCN1 that is important for transduction of a novel immunoregulatory signal. Future work is required, however, to discover how signaling pathway components that are common to all cells transduce an aa-insufficiency signal that regulates diverse tissue-specific inflammatory and remodeling programs.

MATERIAL and METHODS

Cell culture and media.

Human RA synoviocytes were provided by Dr Erika Noss (Brighman and Women's Hospital). Briefly, human synovial tissues from patients with RA were obtained by after synoviectomy or joint replacement surgery performed as part of indicated clinical care at Brigham and Women's Hospital. Synovial fibroblasts were released from synovial tissue by mincing followed by collagenase digestion (1mg/ml, collagenase type IV, Worthington Biochemicals) were purified by serial passage as previously described (Agarwal et al.), and were used in experiments between passages 6 and 10. Primary synoviocytes were cultured at 37°C under an atmosphere containing 10% CO2 in DMEM supplemented with 10% FBS, 2mM L-Glutamine, 1mM Sodium Pyruvate (Lonza), 1X MEM Non-Essential Amino Acid (Lonza), 1X MEM Amino Acid (Hyclone), 55μM 2-Mercaptoethanol (Gibco), 50μg/mL Gentamycin (Amresco) and 1X Penicillin/Streptomycin/Amphotericin B (Lonza). For gene expression analysis, 80% sub-confluent cells were left in serum reduced media (0.2% FBS) for 24-48 hours, treated with HF (300 nM) and/or proline (2mM) for 16 hours and treated with TNFα (10ng/ml) for 4 hours.

Immortalized K4 synoviocytes were a kind gift from Dr Evelyn Murphy (University College Dublin). Cells were cultured at 5% CO2 at 37°C in DMEM supplemented with 10% FBS, L-glutamine, sodium pyruvated, and antibiotics. For TNFα-stimulated experiments, cells were shifted into K4 cell media with 0.2% FBS instead of 10%FBS 24 hours before the HF treatment.

Human lung fibroblasts (LL29, AnHa), were purchased from the American Type Culture Collection (ATCC, Manassas, VA) and cultured DMEM + 10%FBS. Cells were put into DMEM with reduced (0.2%) FBS 24 hours before treatment with 200nM HF-/+ 2mM proline for 6 hours, and then TGFß for 16 hours. Cells were used before 12th passage.

Human Vascular Endothelial Cells (HUVEC, Lonza EGM (CC-2517)) were cultured in EGM-2 (CC-3162, Lonza). For experiments, cells were serum starved in 0.2% FBS for 24hr, treated with 200nM HF and 2mM proline for 16hr, and then treated 10ng/mL TNFa for 4hr.

Normal human dermal fibroblasts (NHDF) were purchased from Lonza (CC-2511) and according to the manufacturer's instructions. For later passages, cells were cultured in Dulbecco's modified Eagle's medium (DMEM) supplemented with 10% fetal bovine serum (FBS, Gibco), 2mM L-glutamine (Life Technologies) and 1X of penicillin and streptomycin (Lonza). For gene expression experiments, NHDF cells were plated on collagen type 1 plates (BD biosciences), serum-starved in serum-reduced media (0.2 % FBS) for 24 hours, treated with HF and/or proline (2mM; Sigma-Aldrich) and/or TGF beta (10ng/ml; R&D Systems) for 48 hours and re-treated for additional 48 hours. NHDF cells were used between passage 4 and 12.

***GCN2$^{-/-}$* FLS isolation and culture**. Primary cell cultures were obtained from wild type and general control nonderepressible 2 GCN2$^{-/-}$ (*eif2ak4$^{-/-}$*) mice purchased from Jackson Laboratories (Bar Harbor, Maine) (stock no. 008240). Primary murine synoviocytes isolated as previously described (Agarwal et al, 2006). Murine synoviocytes were cultured in the same media used for human primary synoviocytes. For treatment, murine synoviocytes were cultured in serum-reduced media (2%) for 72 hours , as further lowering FBS concentration reduced cell viability.

Primary CD4^{+} T cells from wild type (C57Bl/6J; stock no. 000664) or Gcn2$^{-/-}$ (*eif2ak4$^{-/-}$*) mice were isolated, treated +/- HF +/- L-proline, and cultured as previously described (Carlson et al., 2014). Briefly, "naïve" CD4+CD25- T cells were magnetically isolated from single cell splenocyte suspensions using an EasySep mouse CD4+ T cell enrichment kit (Stem Cell Technologies, Cat. #: 19752). A biotinylated anti-mouse CD25 antibody (clone PC61.5, from eBioscience) was added at 1 μg/mL to the biotinylated antibody cocktail prior to incubation with streptavidin beads. These cells were activated with plate-coated anti-CD3ε (Clone: 145-2C11, 0.3 μg/mL) and anti-CD28 (Clone: 37.51, 0.5 μg/mL) antibodies (both from Bio X Cell), and treated with additives (HF, L-proline) and/or Th17 polarizing cytokines (TGFβ + IL-6) at the time of activation. For Th17 polarization, activated T cells were cultured with recombinant human TGFβ (0.3 μg/mL; cat #: 240-B) and recombinant mouse IL-6 (3 μg/mL; cat. #: 406-ML) (both from R&D systems). Activated T cells were removed from antibody-coated wells after 48 hours; non-polarized cells (no cytokines) were expanded in media containing 10 μg/mL recombinant human IL-2 (eBioscience, cat. #: BMS334). TGFβ and IL-6 were re-added to Th17-polarized cell cultures at 48 hours, and

these cells were expanded in the absence of IL-2. Cells were expanded until day 4, and cytokine expression was determined by intracellular staining as previously described (Carlson et al., 2014) following 3-4 hr stimulation with phorbol 12-myristate 13-acetate (PMA, 10 nM,, cat. #: P8139) and ionomycin (1 μM, cat. #: I3909) in the presence of brefeldin A (10 μg/mL, cat. #: B7651) (all from Sigma-Aldrich). For some experiments, CD4+CD25- T cells activated in Th17-polarizing conditions were collected at different time points for analysis of protein or mRNA expression. CCR6+ memory (CD3+CD4+CD25-CD62LloCD44hi) T cells were FACS-sorted from single cell splenocyte suspensions as previously described (Carlson et al., 2014). These cells were activated in 96-well round-bottom tissue culture plates (Corning) with anti-CD3/anti-CD28-coated beads (Invitrogen; 3 beads:1 cell) plus 10 μg/mL recombinant human IL-2. Recombinant human IL-23 (20 ng/ml; R&D Systems, cat. #: 1290), as well as HF and/or L-proline were added as indicated. These cells were stimulated for 3-4 hr with PMA and ionomycin in the presence of brefeldin A after 48 hours for analysis of intracellular cytokine expression.

Cell lysates and Western blot

Primary or established FLS were harvested in RIPA buffer (150 mM NaCl, 1% NP40, 0.5% Sodium deoxycholate, 0.1% SDS, 50 mM Tris-HCl pH 8.0) plus 1X complete protease and phosphatase inhibitors (Roche Applied Science). Cultured T cells were harvested at the indicated time points, washed once in PBS, and lysed on ice at 5–10 x 10^7 cells/ml in Laemmli sample buffer (Bio- Rad) supplemented with protease inhibitor tablets (Roche) and phosphatase inhibitors. T cell lysates were cleared by centrifugation at 12,000 x g for 10 min at 4℃, and stored at -80°C. Cell lysates were quantified by BCA (Pierce) or Bradford (Bio-Rad) assays according to manufacturer's instructions. Blotted nitrocellulose membranes were blocked with 5% non-fat milk for 1 hour and probed with for primary antibodies as described (Keller et al., 2012).

Antibodies and Q-RT-PCR probes

Antibodies against total GCN2 (Cat. #3302), total eif2 (Cat#5324) and peif2 (Cat #3398) were purchased from Cell Signaling Technologies (Danvers, MA). Antibody against ATF4 (10835-1-AP) was from ProteinTech. Antibody against cytoplasmic actin was from Sigma (Clone AC-40). Anti-GCN1L1 was from Novus (NB100-97851). HF and HFol were prepared as described previously (Keller et al., 2012). Amino acids L-proline, L-threonine and the threonyl-tRNA synthetase inhibitor borrelidin were purchased from Sigma-Aldrich (Cat #5607, #T8625 and #B1936 respectively). The selective inhibitor of c-jun N-terminal kinase (JNK) SP600125 and the mTOR inhibitor Torin1 were purchased from Sigma-Aldrich (Cat. #S5567) and Tocris (Cat. #4247) respectively.

Quantitative reverse polymerase chain reaction (qPCR) and high-density qPCR microarray.

For gene expression studies, RNA was extracted using Trizol reagent according to the manufacturer's instructions (Invitrogen), and retro-transcribed to cDNA using the High Capacity cDNA Reverse Transcription kit (Applied Biosystems). Transcriptional analysis was performed using the Universal Probe Library System (UPL; Roche) on a LightCycler 480 Real-Time PCR machine. The following primers and probes were used:

- *Human ACTA2* (α-SMA): probe 21. FW primer: gcactgccttggtgtgtg; RW primer: tcccattcccaccatcac
- *Human COL1A1*: probe 21. FW primer: ccctctggagcctctggt; RW primer: gagtccatctttgccaggag
- *Human CXCL2:* probe 69. FW primer: cccatggttaagaaaatcatcg; RW primer: cttcaggaacagccaccaat
- *Human CXCL9:* probe 56. FW primer: ttgaatcactgctcacactgc; RW primer: gacgttcgggtgggatct
- *Human CXCL10:* probe 34. FW primer: gaaagcagttagcaaggaaaggt; RW primer: gacatatactccatgtagggaagtga
- *Human MMP1:* probe 7. FW primer: gctaacctttgatgctataactacga; RW primer: tttgtgcgcatgtagaatctg
- *Human MMP3:* probe 46. FW primer: ctccaaccgtgaggaaaatc; RW primer: catggaatttctcttctcatcaaa
- *Human MMP13:* probe 73. FW primer: ccagtctccgaggagaaaca; RW primer: aaaaacagctccgcatcaac
- *Human MMP14:* probe 15. FW primer: tggtctcggaccatgtctc; RW primer: aggtagccatattgctgtagcc
- *Human PGK1 (control for primary cells):* probe 56. FW primer: ggaagcgggtcgttatgag; RW primer: attgtccaagcagaatttgatg
- *Human GAPDH (control for Immortalized cells):* probe 60. FW primer: agccacatcgctcagacac; RW primer: gcccaatacgaccaaatcc
- *Human TRB3: probe16. FW primer: tccagatcgtgcaactgct. RW primer: cttcctggacggggtaca*
- Human ACTA2: probe 21. FW primer: gcactgccttggtgtgtg. RW primer: tcccattcccaccatcac
- *Mouse ACTA2* (α-SMA): probe 56. FW primer: caaccgggagaaaatgacc; RW primer: cagttgtacgtccagaggcata
- *Mouse COL1A1:* probe 15. FW primer: catgttcagctttgtggacct; RW primer: gcagctgacttcagggatgt.
- *Mouse CXCL9:* probe 1. FW primer: cttttcctcttgggcatcat; RW primer: gcatcgtgcattccttatca.
- *Mouse CXCL10:* probe 56. FW primer: aatgaaagcgtttagccaaaaa; RW primer: aggggagtgatggagagagg.
- *Mouse MMP1a:* probe 69. FW primer: tgacaccacttacgttccaaa; RW primer: tcaaatgggttgttgtcacc
- *Mouse MMP13:* probe 89. FW primer: gccagaacttcccaaccat; FW primer: tcagagcccagaattttctcc
- *Mouse TBP1 (control):* probe 107. primer FW: ggcggtttggctaggttt; primer RW: gggttatcttcacacaccatga

Probe and primers were designed using the ProbeFinder software (https://www.roche-applied-science.com/sis/rtpcr/upl/index.jsp?id=uplct_030000). Relative gene expression (fold change) levels were obtained using the ΔΔCt method and normalizing to the control genes.

For high-density qPCR microarray assay, 1ug of RNA was retro-transcribed as previously described, mixed with SIBR Green Master Mix (Roche) and loaded on the Oncology SmartChip (Wafergen). The Oncology SmartChip contains over 1200 cancer-related genes, 10 endogenous and 5 exogenous control genes for RT-PCR analysis. After 30 cycles of amplification, results were collected and analyzed using the Bio-Gazzelle software for cluster analysis. Relative gene expression (fold change) levels were obtained using the ΔΔCt method and normalizing to the control gene GAPDH.

Stable knock-down of GCN1 and GCN2 in K4 synoviocytes and human RA synoviocytes
Lentiviral-transduction was performed using the following pLKO.1 lentiviral constructs encoding shRNA against human GCN2: Clone ID: TRCN0000078652 (Open Biosystems); human GCN1: Clone ID: TRCN0000154964 (Open Biosystems). Scrambled shRNA (Addgene plasmid #1864). Lentiviruses were generated in 293T cells by Effectene (Qiagen) mediated co-transfection of the pLKO.1 plasmid, the psPAX2 packaging vector and the pMD2.G, VSV-G envelope expressing plasmid in a 2:1.5:1 ratio. 16 hours after transfection, the transfected 293T cells rinsed with PBS, and then they grew in the growth media for K4 synoviocytes or RA synoviocytes. At 48 hours post transfection, the lentiviral supernatant was harvested, spun at 2000xg for 5 mimutes at 4℃, filtered with 0.45μM syringe filter. K4 synoviocytes or RA synoviocytes were treated with the lentiviral suprnatant with 5μg/mL polybrene. 6 hours after infection, the transduced cells rinsed with PBS, and then they grew in the fresh growth media. Next day, the lentiviral infection process was repeated. The transduced cells were selected with 2μg/mL puromycin for 48~72 hours. After selection, cells grew in growth media with 0.25ug/mL puromycin.

Transduced K4 synoviocytes or RA synoviocytes were left in serum-reduced media (0.2% FBS) for 24 hours, treated with HF (100nM or 200nM, respectively) for 16 hours and with TNFα (10ng/ml) for additional 6 hours. Western blot and gene expression analyses were performed as previously described. Results are representative of three independent experiments.

Stable cells expressing GADD34 in K4 synoviocytes
Retroviral-transduction was performed using the retroviral constructs encoding GADD34 C-terminal: haA1.pBABEpu was a gift from David Ron (Addgene plasmid # 21813 ; http://n2t.net/addgene:21813 ; RRID:Addgene_21813). eGFP gene was used for negative control. Retroviruses were generated in 293T cells by Effectene (Qiagen) mediated co-transfection of the retrovial plasmid, the MLVβ gal-pol packaging vector and the pCMV-VSVG envelope expressing plasmid in a 4.5:4.5:1 ratio. 16 hours after transfection, the transfected 293T cells rinsed with PBS, and then they grew in the growth media for K4 synoviocytes. At 48 hours post transfection, the retroviral supernatant was harvested, spun at 2000xg for 5 mimutes at 4℃, filtered with 0.45μM syringe filter. K4 synoviocytes were treated with the retroviral suprnatant with 5μg/mL polybrene. 6 hours after infection, the transduced cells rinsed with PBS, and then they grew in the fresh growth media. Next day, the retroviral infection process was repeated. The transduced cells were selected with 2μg/mL puromycin for 48~72 hours. After selection, cells grew in growth media with 0.25ug/mL puromycin. Transduced K4 synoviocytes were left in serum-reduced media (0.2% FBS) for 24 hours, treated with HF (100nM~200nM) for 16 hours and with TNF-α(10ng/ml) for additional 6 hours.

RNA-seq. RNA-seq was performed on primary human FLS (Supplementary File 1) or K4 FLS (Supplementary File 2). Primary FLS were left in serum-reduced media (0.2% FBS) for 24hours, pre-treated for 16 hrs with 300 nM HF or vehicle, and then treated for 8 or 24 hours with 10 ng/ml TNFα or vehicle. K4 FLS stably transformed with lentiviral shRNAs (scrambled or GCN2 shRNA #2) as described above were cultured in serum-reduced media (0.2% FBS) for 24 hours, then treated for 24 hours with 250 nM halofuginol, an HF derivative with similar activity to HF as an EPRS inhibitor (Keller et al., 2012), or vehicle, and then with 10 ng/ml TNFα for 8 hours. Biological duplicates were collected for each condition. RNA quantity and quality was checked using a Bioanalyzer at the Biopolymers Facility, Harvard Medical School. Poly-A enriched libraries were prepared with the TruSeq Stranded mRNA Library Prep Kit, sequenced using a single-end approach with 100 bp reads at a total sequencing depth of 30 million reads on an Illumina 4000 instrument, and mapped to the genome by the JP Sulzberger Columbia Genome Center. Pairwise DEseq2 analysis of differentially expressed genes was performed on the Galaxy web platform (4) Normalized gene expression was analyzed using the GenePattern software suite (http://genepattern.broadinstitute.org), and visualized via the MultiPlot module. For analysis, only annotated genes displaying real normalized expression values (> 0) in all replicate samples were used (n = 12,973). Effects of HF treatment on genes that were decreased, not affected, or increased by TNFα treatment (≥10-fold) were analyzed in Prism (GraphPad); statistical significance was determined by One-way ANOVA.

T cell Microarrays and data analyses. Total RNA was sent to the Boston University Microarray Resource Facility. All procedures were performed as described in GeneChip® Whole Transcript (WT) Sense Target Labeling Assay Manual (Affymetrix, Santa Clara, CA, current version available at www.affymetrix.com) and Ambion® WT Expression Kit Protocol (Life Technologies, current version available at http://tools.invitrogen.com/content/sfs/manuals/cms_064619.pdf). Differentially expressed genes (≥ 2.5-fold) were analyzed using the Hieracrchical Clustering module in GenePattern (http://www.broadinstitute.org/cancer/software/genepattern). Microarray data are publically available at Gene Expression Omnibus (GEO, Accession: GSE47478).

^{35}S Methionine Experiments

Primary human RA synoviocytes were seeded in each well of a 6 well-plate, serum starved as described for TNF treatment studies above, pre-treated with HF and labelled with 1 µCi/well S^{35}-labelled methionine in DMEM containing 0.2% FBS for 24 hours. Incorporation of S^{35}-methionine. Label incorporated into protein was isolated by total protein precipitation with trichloroacetic acid as described (Link and LaBaer, 2011), and incorporated radioactivity determined as counts per minute using a liquid scintillation counter. Cell labelings were performed in triplicate. Background (unincorporated ^{35}S methionine) was measured in parallel trichloroacetic acid precipitations using an identical amount of ^{35}S methionine added to TCA/cell mixture after harvest.

Statistical analysis

Analysis was performed using Prism Graphpad software. The unpaired Student's t-test and the one-way ANOVA with Bonferroni's post hoc analysis were used to determine statistically significant differences between groups. P-Values of less than 0.05 were considered statistically significant.

REFERENCES

Acosta-Rodriguez, E.V., Rivino, L., Geginat, J., Jarrossay, D., Gattorno, M., Lanzavecchia, A., Sallusto, F., and Napolitani, G. (2007). Surface phenotype and antigenic specificity of human interleukin 17-producing T helper memory cells. Nat Immunol *8*, 639-646.

Agarwal, S.K., and Brenner, M.B. (2006). Role of adhesion molecules in synovial inflammation. Current Opinion in Rheumatology *18*, 268-276.

Allen, J.E., and Sutherland, T.E. (2014). Host protective roles of type 2 immunity: parasite killing and tissue repair, flip sides of the same coin. Semin Immunol *26*, 329-340.

Atarashi, K., Tanoue, T., Ando, M., Kamada, N., Nagano, Y., Narushima, S., Suda, W., Imaoka, A., Setoyama, H., Nagamori, T.*, et al.* (2015). Th17 Cell Induction by Adhesion of Microbes to Intestinal Epithelial Cells. Cell *163*, 367-380.

Baird, T.D., and Wek, R.C. (2012). Eukaryotic initiation factor 2 phosphorylation and translational control in metabolism. Advances in nutrition (Bethesda, Md) *3*, 307-321.

Belladonna, M.L., Orabona, C., Grohmann, U., and Puccetti, P. (2009). TGF-beta and kynurenines as the key to infectious tolerance. Trends Mol Med *15*, 41-49.

Bottini, N., and Firestein, G.S. (2013). Duality of fibroblast-like synoviocytes in RA: passive responders and imprinted aggressors. Nat Rev Rheumatol *9*, 24-33.

Brown, A., Fernandez, I.S., Gordiyenko, Y., and Ramakrishnan, V. (2016). Ribosome-dependent activation of stringent control. Nature *534*, 277-280.

Brown, M.V., Reader, J.S., and Tzima, E. (2010). Mammalian aminoacyl-tRNA synthetases: cell signaling functions of the protein translation machinery. Vascul Pharmacol *52*, 21-26.

Buck, M.D., Sowell, R.T., Kaech, S.M., and Pearce, E.L. (2017). Metabolic Instruction of Immunity. Cell *169*, 570-586.

Buckley, C.D. (2011). Why does chronic inflammation persist: An unexpected role for fibroblasts. Immunology letters *138*, 12-14.

Carlson, T.J., Pellerin, A., Djuretic, I.M., Trivigno, C., Koralov, S.B., Rao, A., and Sundrud, M.S. (2014). Halofuginone-Induced Amino Acid Starvation Regulates Stat3-Dependent Th17 Effector Function and Reduces Established Autoimmune Inflammation. The Journal of Immunology.

Castilho, B.A., Shanmugam, R., Silva, R.C., Ramesh, R., Himme, B.M., and Sattlegger, E. (2014). Keeping the eIF2 alpha kinase Gcn2 in check. BBA - Molecular Cell Research, 1-61.
Chang, C.H., and Pearce, E.L. (2016). Emerging concepts of T cell metabolism as a target of immunotherapy. Nat Immunol *17*, 364-368.
Chang, S.K., Gu, Z., and Brenner, M.B. (2010). Fibroblast-like synoviocytes in inflammatory arthritis pathology: the emerging role of cadherin-11. Immunological reviews *233*, 256-266.
Chaveroux, C., Jousse, C., Cherasse, Y., Maurin, A.-C., Parry, L., Carraro, V., Derijard, B., Bruhat, A., and Fafournoux, P. (2009). Identification of a Novel Amino Acid Response Pathway Triggering ATF2 Phosphorylation in Mammals. Molecular and Cellular Biology *29*, 6515-6526.
Cobbold, S.P., Adams, E., Farquhar, C.A., Nolan, K.F., Howie, D., Lui, K.O., Fairchild, P.J., Mellor, A.L., Ron, D., and Waldmann, H. (2009). Infectious tolerance via the consumption of essential amino acids and mTOR signaling. Proceedings of the National Academy of Sciences of the United States of America *106*, 12055-12060.
Cua, D.J., Sherlock, J., Chen, Y., Murphy, C.A., Joyce, B., Seymour, B., Lucian, L., To, W., Kwan, S., Churakova, T.*, et al.* (2003). Interleukin-23 rather than interleukin-12 is the critical cytokine for autoimmune inflammation of the brain. Nature *421*, 744-748.
De Vito, A., Lazzaro, M., Palmisano, I., Cittaro, D., Riba, M., Lazarevic, D., Bannai, M., Gabellini, D., and Schiaffino, M.V. (2018). Amino acid deprivation triggers a novel GCN2-independent response leading to the transcriptional reactivation of non-native DNA sequences. PLoS One *13*, e0200783.
Deval, C., Chaveroux, C., Maurin, A.-C., Cherasse, Y., Parry, L., Carraro, V., Milenkovic, D., Ferrara, M., Bruhat, A., Jousse, C.*, et al.* (2009). Amino acid limitation regulates the expression of genes involved in several specific biological processes through GCN2-dependent and GCN2-independent pathways. FEBS Journal *276*, 707-718.
Donnelly, N., Gorman, A.M., Gupta, S., and Samali, A. (2013). The eIF2alpha kinases: their structures and functions. Cell Mol Life Sci *70*, 3493-3511.
Duffield, J.S., Lupher, M., Thannickal, V.J., and Wynn, T.A. (2013). Host Responses in Tissue Repair and Fibrosis. Annual Review of Pathology: Mechanisms of Disease *8*, 241-276.
Durant, L., Watford, W.T., Ramos, H.L., Laurence, A., Vahedi, G., Wei, L., Takahashi, H., Sun, H.W., Kanno, Y., Powrie, F.*, et al.* (2010). Diverse targets of the transcription factor STAT3 contribute to T cell pathogenicity and homeostasis. Immunity *32*, 605-615.
Fallarino, F., Grohmann, U., and Puccetti, P. (2012). Indoleamine 2,3-dioxygenase: from catalyst to signaling function. Eur J Immunol *42*, 1932-1937.
Fang, P., Yu, X., Jeong, S.J., Mirando, A., Chen, K., Chen, X., Kim, S., Francklyn, C.S., and Guo, M. (2015). Structural basis for full-spectrum inhibition of translational functions on a tRNA synthetase. Nature Communications, 1-11.
Faus, I., Ninoles, R., Kesari, V., Llabata, P., Tam, E., Nebauer, S.G., Santiago, J., Hauser, M.T., and Gadea, J. (2018). Arabidopsis ILITHYIA protein is necessary for proper chloroplast biogenesis and root development independent of eIF2alpha phosphorylation. J Plant Physiol *224-225*, 173-182.
Fouda, A.Y., Xu, Z., Shosha, E., Lemtalsi, T., Chen, J., Toque, H.A., Tritz, R., Cui, X., Stansfield, B.K., Huo, Y.*, et al.* (2018). Arginase 1 promotes retinal neurovascular protection from ischemia through suppression of macrophage inflammatory responses. Cell Death Dis *9*, 1001.
Gallinetti, J., Harputlugil, E., and Mitchell, J.R. (2013). Amino acid sensing in dietary-restriction-mediated longevity: roles of signal-transducing kinases GCN2 and TOR. The Biochemical journal *449*, 1-10.
Gause, W.C., Wynn, T.A., and Allen, J.E. (2013). Type 2 immunity and wound healing: evolutionary refinement of adaptive immunity by helminths. Nat Rev Immunol *13*, 607-614.
Geiger, R., Rieckmann, J.C., Wolf, T., Basso, C., Feng, Y., Fuhrer, T., Kogadeeva, M., Picotti, P., Meissner, F., Mann, M.*, et al.* (2016). L-Arginine Modulates T Cell Metabolism and Enhances Survival and Anti-tumor Activity. Cell *167*, 829-842 e813.

Goldring, M.B., Otero, M., Plumb, D.A., Dragomir, C., Favero, M., El Hachem, K., Hashimoto, K., Roach, H.I., Olivotto, E., Borzi, R.M.*, et al.* (2011). Roles of inflammatory and anabolic cytokines in cartilage metabolism: signals and multiple effectors converge upon MMP-13 regulation in osteoarthritis. Eur Cell Mater *21*, 202-220.
Grohmann, U., Mondanelli, G., Belladonna, M.L., Orabona, C., Pallotta, M.T., Iacono, A., Puccetti, P., and Volpi, C. (2017). Amino-acid sensing and degrading pathways in immune regulation. Cytokine Growth Factor Rev *35*, 37-45.
Guo, L.-W., Wang, B., Goel, S.A., Little, C., Takayama, T., Shi, X.D., Roenneburg, D., DiRenzo, D., and Kent, K.C. (2014). Halofuginone Stimulates Adaptive Remodeling and Preserves Re-Endothelialization in Balloon-Injured Rat Carotid Arteries. Circulation Cardiovascular interventions.
Guo, M., and Schimmel, P. (2013). Essential nontranslational functions of tRNA synthetases. Nature Chemical Biology *9*, 145-153.
Haas, C., Aicher, W.K., Dinkel, A., Peter, H.H., and Eibel, H. (1997). Characterization of SV40T antigen immortalized human synovial fibroblasts: maintained expression patterns of EGR-1, HLA-DR and some surface receptors. Rheumatol Int *16*, 241-247.
Haigis, M.C., and Yankner, B.A. (2019). The Aging Stress Response. Molecular Cell *40*, 333-344.
Harding, H.P., Novoa, I., Zhang, Y., Zeng, H., Wek, R., Schapira, M., and Ron, D. (2000). Regulated translation initiation controls stress-induced gene expression in mammalian cells. Mol Cell *6*, 1099-1108.
Harding, H.P., Zhang, Y., Zeng, H., Novoa, I., Lu, P.D., Calfon, M., Sadri, N., Yun, C., Popko, B., Paules, R.*, et al.* (2003). An integrated stress response regulates amino acid metabolism and resistance to oxidative stress. Molecular Cell *11*, 619-633.
Hart, T., Chandrashekhar, M., Aregger, M., Steinhart, Z., Brown, K.R., MacLeod, G., Mis, M., Zimmermann, M., Fradet-Turcotte, A., Sun, S.*, et al.* (2015). High-Resolution CRISPR Screens Reveal Fitness Genes and Genotype-Specific Cancer Liabilities. Cell *163*, 1515-1526.
Hauryliuk, V., Atkinson, G.C., Murakami, K.S., Tenson, T., and Gerdes, K. (2015). Recent functional insights into the role of (p)ppGpp in bacterial physiology. Nat Rev Microbiol *13*, 298-309.
Herbert, D.R., Orekov, T., Roloson, A., Ilies, M., Perkins, C., O'Brien, W., Cederbaum, S., Christianson, D.W., Zimmermann, N., Rothenberg, M.E.*, et al.* (2010). Arginase I suppresses IL-12/IL-23p40-driven intestinal inflammation during acute schistosomiasis. J Immunol *184*, 6438-6446.
Hinnebusch, A.G. (1993). Gene-specific translational control of the yeast GCN4 gene by phosphorylation of eukaryotic initiation factor 2. Mol Microbiol *10*, 215-223.
Hirose, T., and Horvitz, H.R. (2014). The Translational Regulators GCN-1 and ABCF-3 Act Together to Promote Apoptosis in C. elegans. PLoS Genetics *10*, e1004512.
Hotamisligil, G.S. (2017). Inflammation, metaflammation and immunometabolic disorders. Nature *542*, 177-185.
Huebner, K.D., Jassal, D.S., Halevy, O., Pines, M., and Anderson, J.E. (2008). Functional resolution of fibrosis in mdx mouse dystrophic heart and skeletal muscle by halofuginone. AJP: Heart and Circulatory Physiology *294*, H1550-H1561.
Izquierdo, Y., Kulasekaran, S., Benito, P., Lopez, B., Marcos, R., Cascon, T., Hamberg, M., and Castresana, C. (2018). Arabidopsis nonresponding to oxylipins locus NOXY7 encodes a yeast GCN1 homolog that mediates noncanonical translation regulation and stress adaptation. Plant Cell Environ *41*, 1438-1452.
Jasperson, L.K., Bucher, C., Panoskaltsis-Mortari, A., Mellor, A.L., Munn, D.H., and Blazar, B.R. (2009). Inducing the tryptophan catabolic pathway, indoleamine 2,3-dioxygenase (IDO), for suppression of graft-versus-host disease (GVHD) lethality. Blood *114*, 5062-5070.
Jasperson, L.K., Bucher, C., Panoskaltsis-Mortari, A., Taylor, P.A., Mellor, A.L., Munn, D.H., and Blazar, B.R. (2008). Indoleamine 2,3-dioxygenase is a critical regulator of acute graft-versus-host disease lethality. Blood *111*, 3257-3265.

Johnson, M.O., Siska, P.J., Contreras, D.C., and Rathmell, J.C. (2016). Nutrients and the microenvironment to feed a T cell army. Semin Immunol *28*, 505-513.
Jones, R.G., and Pearce, E.J. (2017). MenTORing Immunity: mTOR Signaling in the Development and Function of Tissue-Resident Immune Cells. Immunity *46*, 730-742.
Kakkar, A.K., and Lefer, D.J. (2004). Leukocyte and endothelial adhesion molecule studies in knockout mice. Curr Opin Pharmacol *4*, 154-158.
Kapahi, P., Chen, D., Rogers, A.N., Katewa, S.D., Li, P.W., Thomas, E.L., and Kockel, L. (2010). With TOR, less is more: a key role for the conserved nutrient-sensing TOR pathway in aging. Cell Metab *11*, 453-465.
Keller, T.L., Zocco, D., Sundrud, M.S., Hendrick, M., Edenius, M., Yum, J., Kim, Y.-J., Lee, H.-K., Cortese, J.F., Wirth, D.F.*, et al.* (2012). Halofuginone and other febrifugine derivatives inhibit prolyl-tRNA synthetase. Nature Chemical Biology *8*, 311-317.
Kilberg, M., Pan, Y.-X., Chen, H., and Leung-Pineda, V. (2005). NUTRITIONAL CONTROL OF GENE EXPRESSION: How Mammalian Cells Respond to Amino Acid Limitation*. Annual Review of Nutrition *25*, 59-85.
Kim, J.-H., Jeon, J., Shin, M., Won, Y., Lee, M., Kwak, J.-S., Lee, G., Rhee, J., Ryu, J.-H., Chun, C.-H.*, et al.* (2014). Regulation of the Catabolic Cascade in Osteoarthritis by the Zinc-ZIP8-MTF1 Axis. Cell *156*, 730-743.
Krieg, T., Abraham, D., and Lafyatis, R. (2007). Fibrosis in connective tissue disease: the role of the myofibroblast and fibroblast-epithelial cell interactions. Arthritis Research & Therapy *9 Suppl 2*, S4.
Leask, A. (2008). Targeting the TGFbeta, endothelin-1 and CCN2 axis to combat fibrosis in scleroderma. Cellular Signalling *20*, 1409-1414.
Lee, Y., Awasthi, A., Yosef, N., Quintana, F.J., Xiao, S., Peters, A., Wu, C., Kleinewietfeld, M., Kunder, S., Hafler, D.A.*, et al.* (2012). Induction and molecular signature of pathogenic TH17 cells. Nat Immunol *13*, 991-999.
Lemos, H., Huang, L., Prendergast, G.C., and Mellor, A.L. (2019). Immune control by amino acid catabolism during tumorigenesis and therapy. Nat Rev Cancer.
Levi-Schaffer, F., Nagler, A., Slavin, S., Knopov, V., and Pines, M. (1996). Inhibition of collagen synthesis and changes in skin morphology in murine graft-versus-host disease and tight skin mice: effect of halofuginone. The Journal of investigative dermatology *106*, 84-88.
Link, A.J., and LaBaer, J. (2011). Trichloroacetic acid (TCA) precipitation of proteins. Cold Spring Harb Protoc *2011*, 993-994.
Liu, K., Bittner, A.N., and Wang, J.D. (2015). Diversity in (p)ppGpp metabolism and effectors. Curr Opin Microbiol *24*, 72-79.
Luna, E., van Hulten, M., Zhang, Y., Berkowitz, O., Lopez, A., Petriacq, P., Sellwood, M.A., Chen, B., Burrell, M., van de Meene, A.*, et al.* (2014). Plant perception of beta-aminobutyric acid is mediated by an aspartyl-tRNA synthetase. Nat Chem Biol *10*, 450-456.
Marcos-Ramiro, B., Garcia-Weber, D., and Millan, J. (2014). TNF-induced endothelial barrier disruption: beyond actin and Rho. Thromb Haemost *112*, 1088-1102.
Marton, M.J., Crouch, D., and Hinnebusch, A.G. (1993). GCN1, a translational activator of GCN4 in Saccharomyces cerevisiae, is required for phosphorylation of eukaryotic translation initiation factor 2 by protein kinase GCN2. Mol Cell Biol *13*, 3541-3556.
Marton, M.J., Vazquez de Aldana, C.R., Qiu, H., Chakraburtty, K., and Hinnebusch, A.G. (1997). Evidence that GCN1 and GCN20, translational regulators of GCN4, function on elongating ribosomes in activation of eIF2alpha kinase GCN2. Mol Cell Biol *17*, 4474-4489.
McGaha, T.L. (2015). IDO-GCN2 and Autophagy in Inflammation. 1-2.
McGaha, T.L., Phelps, R.G., Spiera, H., and Bona, C. (2002). Halofuginone, an inhibitor of type-I collagen synthesis and skin sclerosis, blocks transforming-growth-factor-beta-mediated Smad3 activation in fibroblasts. The Journal of investigative dermatology *118*, 461-470.
Mellor, A.L., and Munn, D.H. (2004). IDO expression by dendritic cells: tolerance and tryptophan catabolism. Nat Rev Immunol *4*, 762-774.

Mestre, J.R., Mackrell, P.J., Rivadeneira, D.E., Stapleton, P.P., Tanabe, T., and Daly, J.M. (2001). Redundancy in the signaling pathways and promoter elements regulating cyclooxygenase-2 gene expression in endotoxin-treated macrophage/monocytic cells. J Biol Chem *276*, 3977-3982.
Monaghan, J., and Li, X. (2010). The HEAT repeat protein ILITYHIA is required for plant immunity. Plant Cell Physiol *51*, 742-753.
Mondanelli, G., Bianchi, R., Pallotta, M.T., Orabona, C., Albini, E., Iacono, A., Belladonna, M.L., Vacca, C., Fallarino, F., Macchiarulo, A.*, et al.* (2017). A Relay Pathway between Arginine and Tryptophan Metabolism Confers Immunosuppressive Properties on Dendritic Cells. Immunity *46*, 233-244.
Mukhopadhyay, R., Jia, J., Arif, A., Ray, P.S., and Fox, P.L. (2009). The GAIT system: a gatekeeper of inflammatory gene expression. Trends in Biochemical Sciences *34*, 324-331.
Muller, A.J., Sharma, M.D., Chandler, P.R., Duhadaway, J.B., Everhart, M.E., Johnson, B.A., 3rd, Kahler, D.J., Pihkala, J., Soler, A.P., Munn, D.H.*, et al.* (2008). Chronic inflammation that facilitates tumor progression creates local immune suppression by inducing indoleamine 2,3 dioxygenase. Proc Natl Acad Sci U S A *105*, 17073-17078.
Munn, D., Sharma, M., Baban, B., Harding, H., Zhang, Y., Ron, D., and Mellor, A. (2005). GCN2 Kinase in T Cells Mediates Proliferative Arrest and Anergy Induction in Response to Indoleamine 2,3-Dioxygenase. Immunity *22*, 633-642.
Munn, D.H., and Mellor, A.L. (2013). Indoleamine 2,3 dioxygenase and metabolic control of immune responses. Trends Immunol *34*, 137-143.
Munn, D.H., and Mellor, A.L. (2016). IDO in the Tumor Microenvironment: Inflammation, Counter-Regulation, and Tolerance. Trends Immunol *37*, 193-207.
Murray, P.J. (2016). Amino acid auxotrophy as a system of immunological control nodes. Nat Immunol *17*, 132-139.
Nguyen, H.N., Noss, E.H., Mizoguchi, F., Huppertz, C., Wei, K.S., Watts, G.F.M., and Brenner, M.B. (2017). Autocrine Loop Involving IL-6 Family Member LIF, LIF Receptor, and STAT4 Drives Sustained Fibroblast Production of Inflammatory Mediators. Immunity *46*, 220-232.
Noss, E.H., and Brenner, M.B. (2008). The role and therapeutic implications of fibroblast-like synoviocytes in inflammation and cartilage erosion in rheumatoid arthritis. Immunol Rev *223*, 252-270.
Novoa, I., Zeng, H., Harding, H.P., and Ron, D. (2001). Feedback inhibition of the unfolded protein response by GADD34-mediated dephosphorylation of eIF2alpha. J Cell Biol *153*, 1011-1022.
Nowarski, R., Jackson, R., and Flavell, R.A. (2017). The Stromal Intervention: Regulation of Immunity and Inflammation at the Epithelial-Mesenchymal Barrier. Cell *168*, 362-375.
O'Connell, D.J., Kolde, R., Sooknah, M., Graham, D.B., Sundberg, T.B., Latorre, I., Mikkelsen, T.S., and Xavier, R.J. (2016). Simultaneous Pathway Activity Inference and Gene Expression Analysis Using RNA Sequencing. Cell Syst *2*, 323-334.
Ohoka, N., Yoshii, S., Hattori, T., Onozaki, K., and Hayashi, H. (2005). TRB3, a novel ER stress-inducible gene, is induced via ATF4-CHOP pathway and is involved in cell death. EMBO J *24*, 1243-1255.
Oishi, H., Martinu, T., Sato, M., Matsuda, Y., Hirayama, S., Juvet, S.C., Guan, Z., Saito, T., Cypel, M., Hwang, D.M.*, et al.* (2016). Halofuginone treatment reduces interleukin-17A and ameliorates features of chronic lung allograft dysfunction in a mouse orthotopic lung transplant model. J Heart Lung Transplant *35*, 518-527.
Palii, S.S., Kays, C.E., Deval, C., Bruhat, A., Fafournoux, P., and Kilberg, M.S. (2009). Specificity of amino acid regulated gene expression: analysis of genes subjected to either complete or single amino acid deprivation. Amino Acids *37*, 79-88.
Park, M.-K., Park, J.-S., Park, E.-M., Lim, M.-A., Kim, S.-M., Lee, D.-G., Baek, S.-Y., Yang, E.-J., Woo, J.-W., Lee, J.*, et al.* (2013). Halofuginone ameliorates autoimmune arthritis by regulating the balance between Th17 and regulatory T cells and inhibiting osteoclastogenesis. Arthritis & Rheumatism, n/a-n/a.

Park, M.K., Park, J.S., Park, E.M., Lim, M.A., Kim, S.M., Lee, D.G., Baek, S.Y., Yang, E.J., Woo, J.W., Lee, J.*, et al.* (2014). Halofuginone ameliorates autoimmune arthritis in mice by regulating the balance between Th17 and Treg cells and inhibiting osteoclastogenesis. Arthritis Rheumatol *66*, 1195-1207.
Peng, W., Robertson, L., Gallinetti, J., Mejia, P., Vose, S., Charlip, A., Chu, T., and Mitchell, J.R. (2012). Surgical Stress Resistance Induced by Single Amino Acid Deprivation Requires Gcn2 in Mice. Science Translational Medicine *4*, 118ra111-118ra111.
Pesce, J.T., Ramalingam, T.R., Mentink-Kane, M.M., Wilson, M.S., El Kasmi, K.C., Smith, A.M., Thompson, R.W., Cheever, A.W., Murray, P.J., and Wynn, T.A. (2009). Arginase-1-expressing macrophages suppress Th2 cytokine-driven inflammation and fibrosis. PLoS Pathog *5*, e1000371.
Pines, M. (2003). Halofuginone to treat fibrosis in chronic graft-versus-host disease and scleroderma. Biology of Blood and Marrow Transplantation *9*, 417-425.
Pines, M. (2014). Halofuginone for fibrosis, regeneration and cancer in the gastrointestinal tract. World Journal of Gastroenterology *20*, 14778.
Pines, M., Domb, A., Ohana, M., Inbar, J., Genina, O., Alexiev, R., and Nagler, A. (2001). Reduction in dermal fibrosis in the tight-skin (Tsk) mouse after local application of halofuginone. Biochemical Pharmacology *62*, 1221-1227.
Pines, M., and Nagler, A. (1998). Halofuginone: a novel antifibrotic therapy. General pharmacology *30*, 445-450.
Qin, P., Arabacilar, P., Bernard, R.E., Bao, W., Olzinski, A.R., Guo, Y., Lal, H., Eisennagel, S.H., Platchek, M.C., Xie, W.*, et al.* (2017). Activation of the Amino Acid Response Pathway Blunts the Effects of Cardiac Stress. J Am Heart Assoc *6*.
Ramesh, R., Kozhaya, L., McKevitt, K., Djuretic, I.M., Carlson, T.J., Quintero, M.A., McCauley, J.L., Abreu, M.T., Unutmaz, D., and Sundrud, M.S. (2014). Pro-inflammatory human Th17 cells selectively express P-glycoprotein and are refractory to glucocorticoids. J Exp Med *211*, 89-104.
Ravindran, R., Khan, N., Nakaya, H.I., Li, S., Loebbermann, J., Maddur, M.S., PARK, Y., Jones, D.P., Chappert, P., Davoust, J.*, et al.* (2014). Vaccine Activation of the Nutrient Sensor GCN2 in Dendritic Cells Enhances Antigen Presentation. Science (New York, NY) *343*, 313-317.
Ravindran, R., Loebbermann, J., Nakaya, H.I., Khan, N., Ma, H., Gama, L., Machiah, D.K., Lawson, B., Hakimpour, P., Wang, Y.C.*, et al.* (2016). The amino acid sensor GCN2 controls gut inflammation by inhibiting inflammasome activation. Nature *531*, 523-527.
Ravishankar, B., Liu, H., Shinde, R., Chandler, P., Baban, B., Tanaka, M., Munn, D.H., Mellor, A.L., Karlsson, M.C.I., and mcgaha, T.L. (2012). Tolerance to apoptotic cells is regulated by indoleamine 2,3-dioxygenase. Proceedings of the National Academy of Sciences, 1-6.
Rodriguez, P.C., Quiceno, D.G., and Ochoa, A.C. (2007). L-arginine availability regulates T-lymphocyte cell-cycle progression. Blood *109*, 1568-1573.
Ruan, B. (2004). A unique hydrophobic cluster near the active site contributes to differences of borrelidin inhibition among threonyl-tRNA synthetases. Journal of Biological Chemistry, 7.
Sano, T., Huang, W., Hall, J.A., Yang, Y., Chen, A., Gavzy, S.J., Lee, J.Y., Ziel, J.W., Miraldi, E.R., Domingos, A.I.*, et al.* (2016). An IL-23R/IL-22 Circuit Regulates Epithelial Serum Amyloid A to Promote Local Effector Th17 Responses. Cell *164*, 324.
Sattlegger, E. (2005). Polyribosome Binding by GCN1 Is Required for Full Activation of Eukaryotic Translation Initiation Factor 2 Kinase GCN2 during Amino Acid Starvation. Journal of Biological Chemistry *280*, 16514-16521.
Sattlegger, E., and Hinnebusch, A.G. (2000). Separate domains in GCN1 for binding protein kinase GCN2 and ribosomes are required for GCN2 activation in amino acid-starved cells. EMBO J *19*, 6622-6633.
Saxton, R.A., and Sabatini, D.M. (2017). mTOR Signaling in Growth, Metabolism, and Disease. Cell *168*, 960-976.

Shan, J., Balasubramanian, M.N., Donelan, W., Fu, L., Hayner, J., Lopez, M.C., Baker, H.V., and Kilberg, M.S. (2014). A MEK-Dependent Transcriptional Program Controls Activation of the Early Growth Response 1 (EGR1) Gene During Amino Acid Limitation. Journal of Biological Chemistry.
Shang, Y., Coppo, M., He, T., Ning, F., Yu, L., Kang, L., Zhang, B., Ju, C., Qiao, Y., Zhao, B.*, et al.* (2016). The transcriptional repressor Hes1 attenuates inflammation by regulating transcription elongation. Nat Immunol *17*, 930-937.
Sharma, M.D., Baban, B., Chandler, P., Hou, D.-Y., Singh, N., Yagita, H., Azuma, M., Blazar, B.R., Mellor, A.L., and Munn, D.H. (2007). Plasmacytoid dendritic cells from mouse tumor-draining lymph nodes directly activate mature Tregs via indoleamine 2,3-dioxygenase. Journal of Clinical Investigation *117*, 2570-2582.
Silva, R.C., Sattlegger, E., and Castilho, B.A. (2016). Perturbations in actin dynamics reconfigure protein complexes that modulate GCN2 activity and promote an eIF2 response. J Cell Sci *129*, 4521-4533.
Song, D.G., Kim, D., Jung, J.W., Nam, S.H., Kim, J.E., Kim, H.J., Kim, J.H., Lee, S.J., Pan, C.H., Kim, S.*, et al.* (2018). Glutamyl-prolyl-tRNA synthetase induces fibrotic extracellular matrix via both transcriptional and translational mechanisms. FASEB J, fj201801344RR.
Srivatsan, A., and Wang, J.D. (2008). Control of bacterial transcription, translation and replication by (p)ppGpp. Current opinion in microbiology *11*, 100-105.
Sundrud, M.S., Koralov, S.B., Feuerer, M., Calado, D.P., Kozhaya, A.E., Rhule-Smith, A., Lefebvre, R.E., Unutmaz, D., Mazitschek, R., Waldner, H.*, et al.* (2009). Halofuginone inhibits TH17 cell differentiation by activating the amino acid starvation response. Science *324*, 1334-1338.
Tang, X., Keenan, M.M., Wu, J., Lin, C.A., Dubois, L., Thompson, J.W., Freedland, S.J., Murphy, S.K., and Chi, J.T. (2015). Comprehensive profiling of amino acid response uncovers unique methionine-deprived response dependent on intact creatine biosynthesis. PLoS Genet *11*, e1005158.
Tsalikis, J., Croitoru, D.O., Philpott, D.J., and Girardin, S.E. (2013). Nutrient sensing and metabolic stress pathways in innate immunity. Cell Microbiol *15*, 1632-1641.
Turgeman, T., Hagai, Y., Huebner, K., Jassal, D.S., Anderson, J.E., Genin, O., Nagler, A., Halevy, O., and Pines, M. (2008). Prevention of muscle fibrosis and improvement in muscle performance in the mdx mouse by halofuginone. Neuromuscular disorders : NMD *18*, 857-868.
Valin, A., and Pablos, J.L. (2015). The Role of the Transcriptional Regulation of Stromal Cells in Chronic Inflammation. Biomolecules *5*, 2723-2757.
Van de Velde, L.A., Guo, X.J., Barbaric, L., Smith, A.M., Oguin, T.H., 3rd, Thomas, P.G., and Murray, P.J. (2016). Stress Kinase GCN2 Controls the Proliferative Fitness and Trafficking of Cytotoxic T Cells Independent of Environmental Amino Acid Sensing. Cell Rep *17*, 2247-2258.
Van de Velde, L.A., Subramanian, C., Smith, A.M., Barron, L., Qualls, J.E., Neale, G., Alfonso-Pecchio, A., Jackowski, S., Rock, C.O., Wynn, T.A.*, et al.* (2017). T Cells Encountering Myeloid Cells Programmed for Amino Acid-dependent Immunosuppression Use Rictor/mTORC2 Protein for Proliferative Checkpoint Decisions. J Biol Chem *292*, 15-30.
Vanden Berghe, W., Plaisance, S., Boone, E., De Bosscher, K., Schmitz, M.L., Fiers, W., and Haegeman, G. (1998). p38 and extracellular signal-regulated kinase mitogen-activated protein kinase pathways are required for nuclear factor-kappaB p65 transactivation mediated by tumor necrosis factor. J Biol Chem *273*, 3285-3290.
Walls, J., Sinclair, L., and Finlay, D. (2016). Nutrient sensing, signal transduction and immune responses. Semin Immunol *28*, 396-407.
Wang, L., Li, H., Zhao, C., Li, S., Kong, L., Wu, W., Kong, W., Liu, Y., Wei, Y., Zhu, J.K.*, et al.* (2017). The inhibition of protein translation mediated by AtGCN1 is essential for cold tolerance in Arabidopsis thaliana. Plant Cell Environ *40*, 56-68.
Wang, T., Birsoy, K., Hughes, N.W., Krupczak, K.M., Post, Y., Wei, J.J., Lander, E.S., and Sabatini, D.M. (2015). Identification and characterization of essential genes in the human genome. Science *350*, 1096-1101.

Wang, X., Fonseca, B.D., Tang, H., Liu, R., Elia, A., Clemens, M.J., Bommer, U.A., and Proud, C.G. (2008). Re-evaluating the roles of proposed modulators of mammalian target of rapamycin complex 1 (mTORC1) signaling. J Biol Chem *283*, 30482-30492.
Wek, R.C. (2018). Role of eIF2alpha Kinases in Translational Control and Adaptation to Cellular Stress. Cold Spring Harb Perspect Biol *10*.
Wek, R.C., Jackson, B.M., and Hinnebusch, A.G. (1989). Juxtaposition of domains homologous to protein kinases and histidyl-tRNA synthetases in GCN2 protein suggests a mechanism for coupling GCN4 expression to amino acid availability. Proc Natl Acad Sci U S A *86*, 4579-4583.
Wolfson, R.L., and Sabatini, D.M. (2017). The Dawn of the Age of Amino Acid Sensors for the mTORC1 Pathway. Cell Metab *26*, 301-309.
Xavier, S., Piek, E., Fujii, M., Javelaud, D., Mauviel, A., Flanders, K.C., Samuni, A.M., Felici, A., Reiss, M., Yarkoni, S*., et al.* (2004). Amelioration of radiation-induced fibrosis: inhibition of transforming growth factor-beta signaling by halofuginone. The Journal of biological chemistry *279*, 15167-15176.
Ye, J., Palm, W., Peng, M., King, B., Lindsten, T., Li, M.O., Koumenis, C., and Thompson, C.B. (2015). GCN2 sustains mTORC1 suppression upon amino acid deprivation by inducing Sestrin2. Genes Dev *29*, 2331-2336.
Zaborske, J.M., Narasimhan, J., Jiang, L., Wek, S.A., Dittmar, K.A., Freimoser, F., Pan, T., and Wek, R.C. (2009). Genome-wide Analysis of tRNA Charging and Activation of the eIF2 Kinase Gcn2p. Journal of Biological Chemistry *284*, 25254-25267.
Zhang, Y., Dickinson, J.R., Paul, M.J., and Halford, N.G. (2003). Molecular cloning of an arabidopsis homologue of GCN2, a protein kinase involved in co-ordinated response to amino acid starvation. Planta *217*, 668-675.

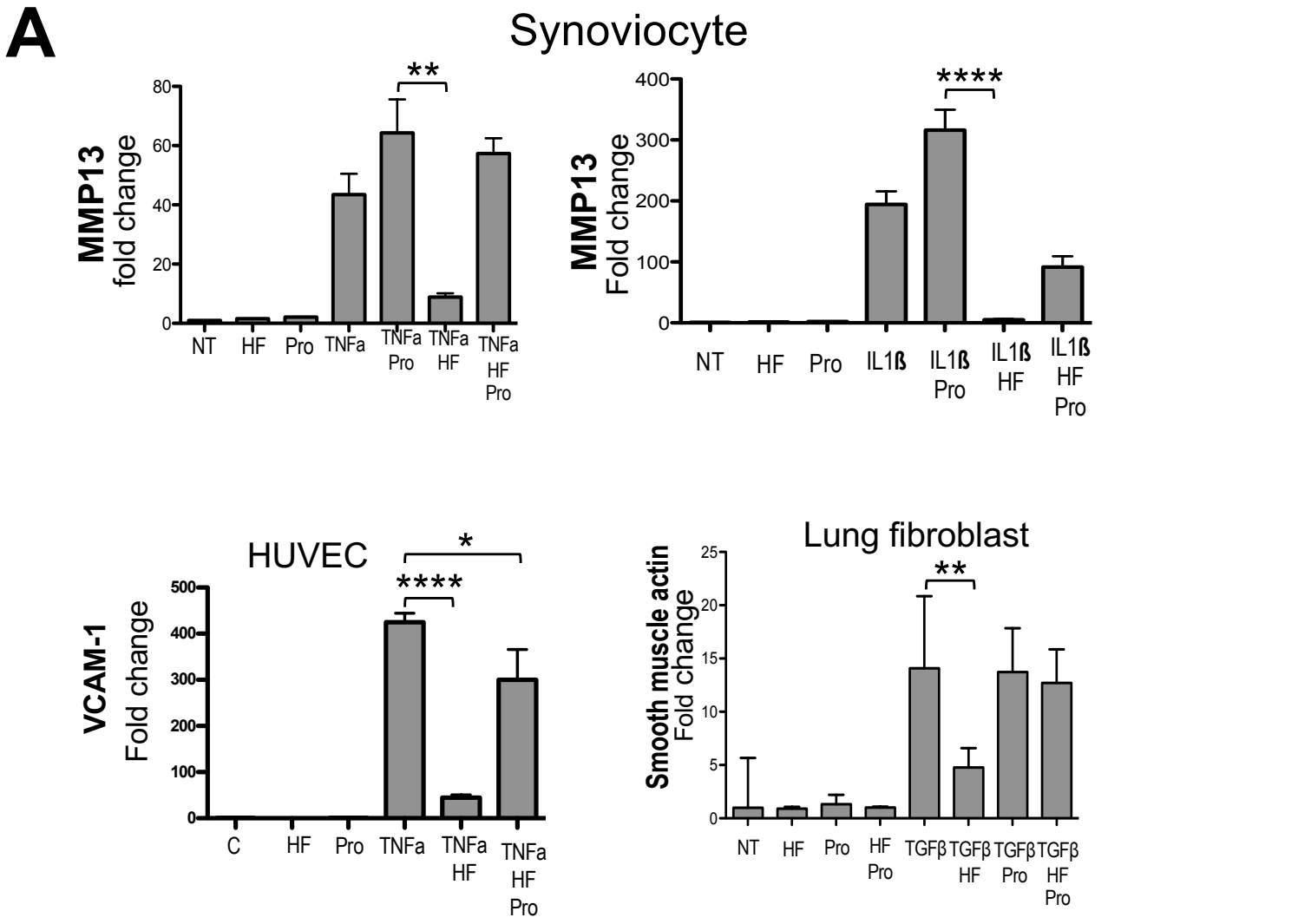
A
Synoviocyte
MMP13
fold change
**
NT
HF
Pro
TNFa
TNFa Pro
TNFa HF
TNFa HF Pro
MMP13
Fold change
****
NT
HF
Pro
IL1ß
IL1ß Pro
IL1ß HF
IL1ß HF Pro
HUVEC
VCAM-1
Fold change
*
****
C
HF
Pro
TNFa
TNFa HF
TNFa HF Pro
Lung fibroblast
Smooth muscle actin
Fold change
**
NT
HF
Pro
HF Pro
TGFβ
TGFβ HF
TGFβ Pro
TGFβ HF Pro

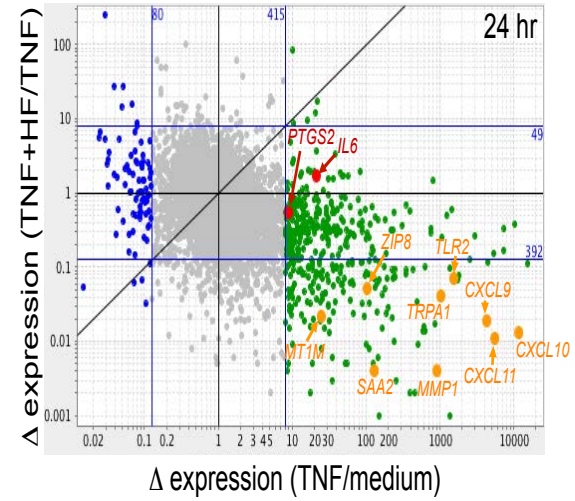
B
24 hr
PTGS2
IL6
ZIP8
TLR2
CXCL9
TRPA1
MT1M
SAA2
MMP1
CXCL11
CXCL10
Δ expression (TNF+HF/TNF)
Δ expression (TNF/medium)

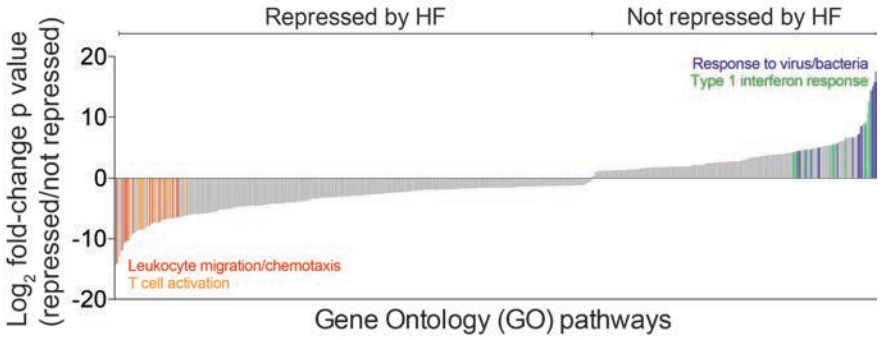
C
Repressed by HF
Not repressed by HF
Response to virus/bacteria
Type 1 interferon response
Leukocyte migration/chemotaxis
T cell activation
Log2 fold-change p value
(repressed/not repressed)
Gene Ontology (GO) pathways

Fig.1. HF inhibits multiple cytokine responses in a range of primary cell types. A) top row: HF inhibition of MMP13 induction by TNFα (left) or IL1ß (right) in human fibroblast like synoviocytes (RA-FLS). Human RA-FLS were pre-treated with 200 nM HF and/or proline (2 mM) (Pro) overnight and treated with 10ng/mL TNFα for 6 hours and mRNA analyzed for MMP13 expression by Q-RT-PCR **Bottom row** : left panel, HUVEC were treated and analyzed for gene expression as described for FLS above; right panel, human LL29 lung fibroblasts were pre-treated with HF and/or proline (Pro) for 6 hours and treated with TGFß for 24 hours and analyzed for gene expression as above. Results are representative of three independent experiments. Statistical Analysis: significance was analyzed using 1 way ANOVA – multiple comparisons (Dunnett test); comparisons are indicated by brackets. *: P<0.1; **:P<0.01; ***:P<0.001; ****:P<0.0001.

B. **RNA-seq analysis of HF effects on TNFα responses.** *Left* – selective regulation of TNFα -inducible pro-inflammatory gene expression in FLS, determined by RNA -seq. after 24 hr culture in media alone, TNFα, or TNFα plus HF. Data are presented as fold-change/fold-change plot; x-axis shows the change (D) in normalized gene expression (reads per kilobase per million reads, RPKM) in TNFα-treated *vs.* untreated FLS (TNF/medium); y-axis shows Δ gene expression in FLS treated with TNFα plus HF *vs.* TNFα alone (TNF+HF/TNF). Only genes with real RPKM values (> 0) are shown (*n* = 12,973). Blue- and green-highlighted genes are reduced or increased by TNFα treatment (10-fold), respectively. Examples of TNFα-inducible genes that are not affected (highlighted red) or suppressed (highlighted orange) by HF treatment are indicated by arrowhead and text. **C. Analysis of TNFα -induced pathways in FLS that are sensitive or insensitive to HF treatment.** Gene ontology (GO) term enrichment analysis, presented as Log2 fold-change in P adjusted values of TNFα -induced pathways that are repressed or not repressed in the presence of HF. 554 GO terms (i.e., pathways) were enriched in either or both gene sets (see Supplementary file x for details); examples of GO terms more strongly enriched in the "repressed by HF" (i.e., leukocyte migration/chemotaxis—red; T cell activation—orange) or "not repressed by HF" (response to virus/bacteria—blue; type 1 interferon response—green) gene sets are highlighted.

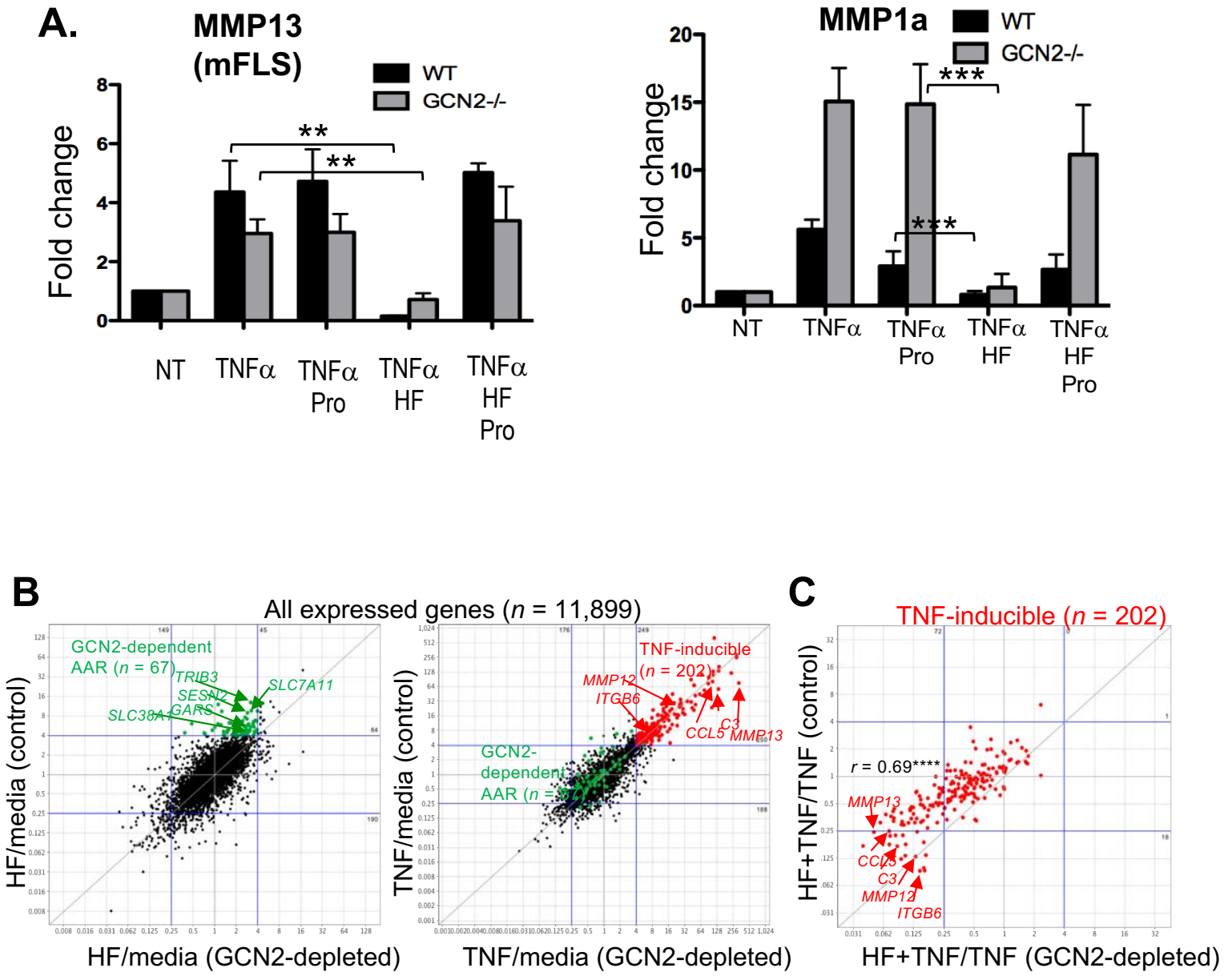

Fig.2. HF regulates cytokine responses in cells lacking GCN2. A) FLS from Wt and GCN2-/- mice were pre-treated with HF and/or proline (Pro) and treated with TNFα for 6 hours. Transcript levels of target genes were quantified by qPCR . Results are representative of three independent experiments. **B)** Summary of results from RNA-Seq transcriptomics comparing HF and TNF action in wild type and GCN2 depleted K4 synoviocytes. Left panel: GCN2 depletion reduces HF induction of canonical AAR genes (highlighted in green); right panel: GCN2 depletion has no significant effect on TNFα induced genes (highlighted in red); **C**) GCN2 depletion either has no effect, or enhances, HF effects on TNFα induced genes.

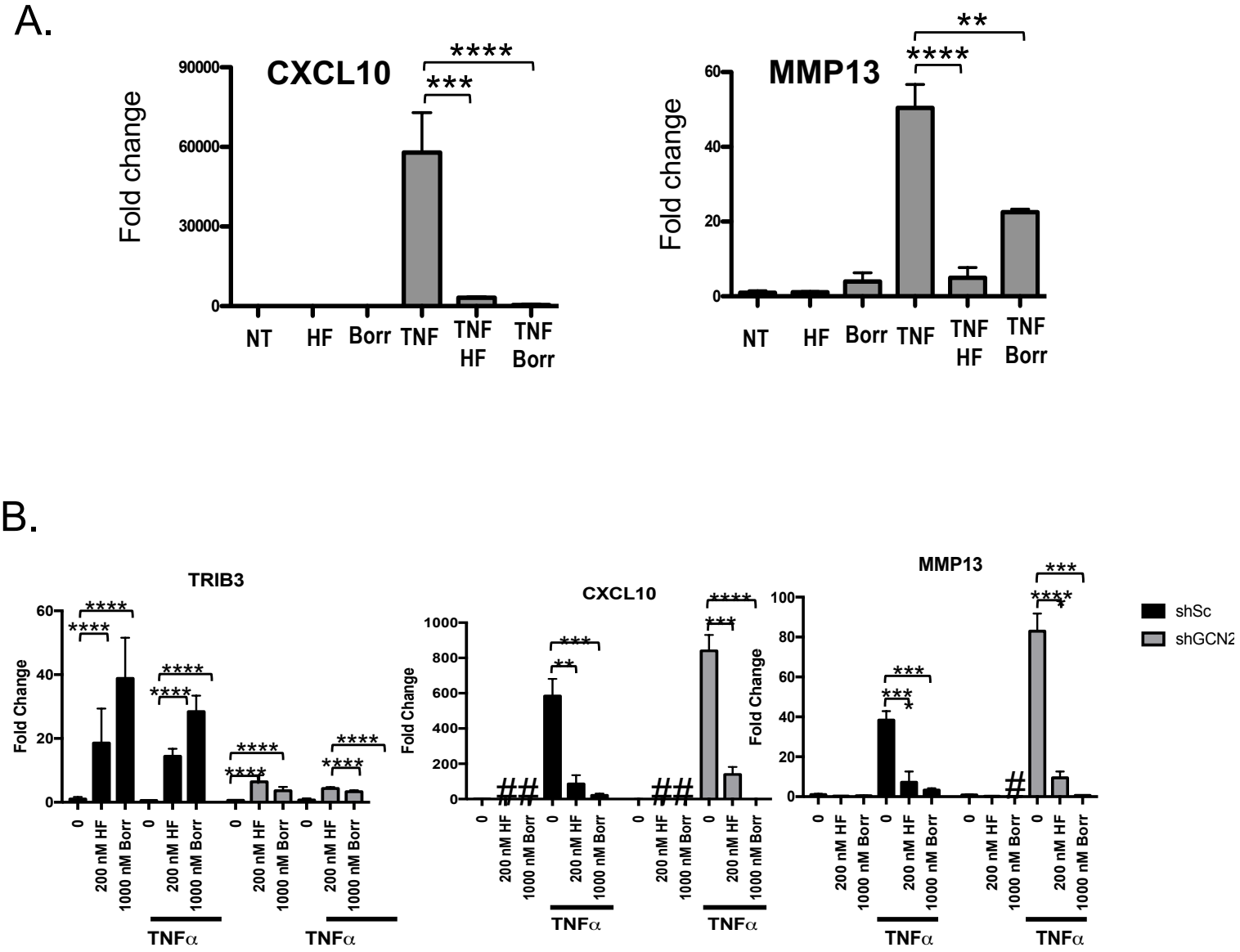

Fig.3. Borrelidin blocks responses to TNFα in wild type and GCN2 depleted cells. **A)** Human RA-FLS were pre-treated with 300 nM HF or 1μM Borrelidin (Borr) for 16 hours , and treated with 10ng/mL TNFα. Transcript levels of MMP13 and CXCL10 were quantified by qRT-PCR and normalized to PGK1. Results are representative of three independent experiments. Statistical analysis: significance was evaluated by 1 way ANOVA test for the comparisons indicated. **B)** wt or shRNA GCN2 depleted K4 fibroblasts were pre-treated with 1000 nM Borrelidin or 200 nM HF for 16 hours, and then treated with 10 ng/mL TNFα for 6 hours. Transcript levels were quantified by qRT-PCR and normalized to GAPDH levels. Statistical Analysis: *P* values were determined as follows: For MMP13 and TRIB3: Means of biological triplicates were analyzed by ANOVA followed by post hoc analysis for multiple group comparisons with the level of significance for comparison set at $p<0.05$. For CXCL10: Means of biological triplicates were analyzed by a student's T-test comparing HF or Borrelidin treatment to untreated in the presence of cytokine stimulation. #: In indicated sample for at least one replicate gene expression was undetectable in the absence of cytokine stimulation.

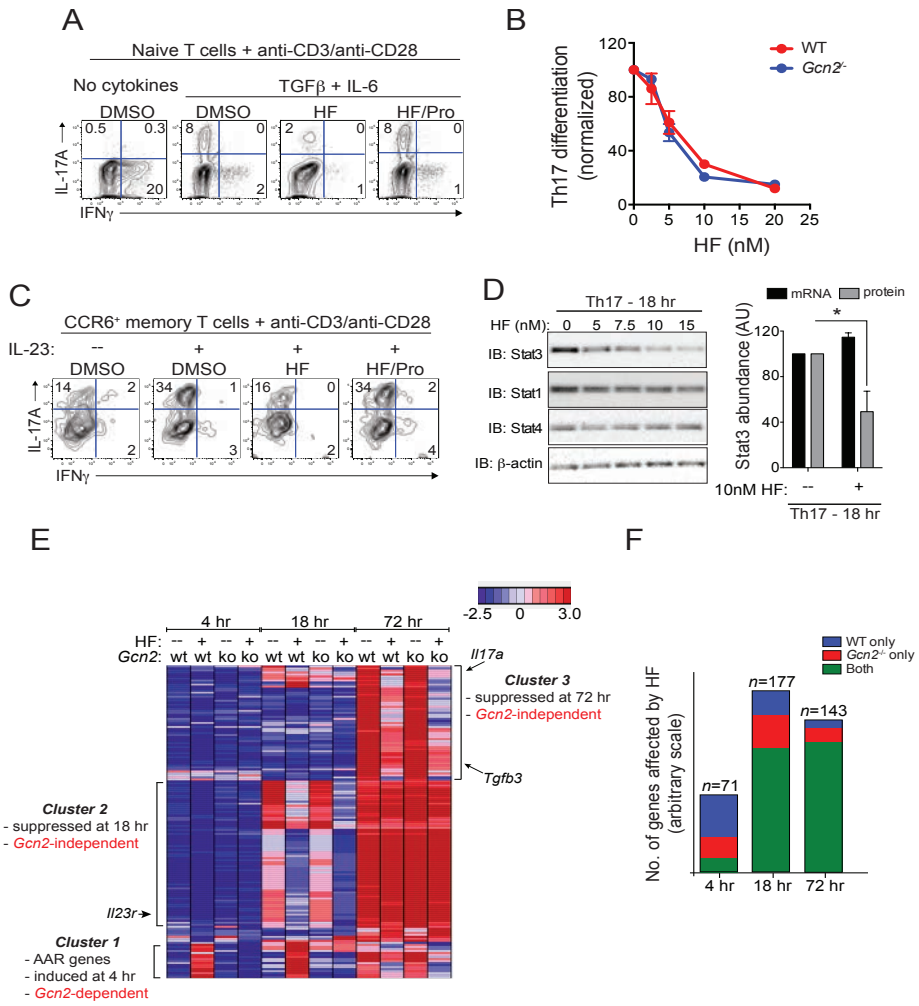

Fig. 4. HF regulates Th17 differentiation and effector function in the absence of Gcn2. (A) FACS analysis of IL-17A and IFNγ expression in Gcn2-deficient CD4+ T cells 4 days after activation in the absence (no cytokines) or presence of Th17-polarizing cytokines (TGFβ + IL-6). Th17-polarized cells were treated with vehicle (DMSO), 10 nM HF, or 10 nM HF plus 50 μM L-proline (HF/Pro) as indicated. Representative of 3 experiments. (B) Dose-response of HF on wild type (red) or Gcn2-deficient (blue) Th17 differentiation. Percentages of IL-17A+ cells (+ SEM; n = 3) were determined by intracellular staining and FACS analysis as in (A) and are normalized to DMSO-treated cells. (C) FACS analysis of cytokine (IL-17A, IFNγ) expression in Gcn2-deficient CCR6+ memory Th17 cells 2 days after in vitro-stimulation (anti-CD3/anti-CD28) in the presence or absence of IL-23. Cells were treated with vehicle (DMSO), 10 nM HF, or 10 nM HF plus 50 □M L-proline (HF/Pro) as indicated. Representative of 3 experiments. (D) Left, Stat protein levels, determined by western blot, in Gcn2-deficient CD4+ T cells stimulated in Th17-polarizing conditions as in (A) for 18 hr. Cells were treated with titrating concentrations of HF. Representative of 3 experiments. Right, relative abundance (+ SEM; n = 3) of Stat3 protein or Stat3 mRNA in Gcn2-deficient CD4+ T cells stimulated in Th17-polarizing conditions for 18 hr +/- 10 nM HF. Stat3 protein levels determined by western blot as above; Stat3 mRNA levels were determined by microarray. Abundance shown as fold change in HF- vs. DMSO-treated samples. (E) Hierarchical clustering of differentially-expressed genes (> 2.5-fold change) in wild type and Gcn2-deficient CD4+ T cells cultured for the indicated times in Th17-polarizing conditions +/- 10 nM HF. Gene clusters (1, 2, 3) are indicated by text; examples of genes within clusters are indicated by text and arrowhead; based on mean gene expression values obtained from biological duplicates. (F) Proportion of genes affected by HF (10 nM) in wild type CD4+ T cells, Gcn2-deficient T cells, or both, determined by microarray as in (E).

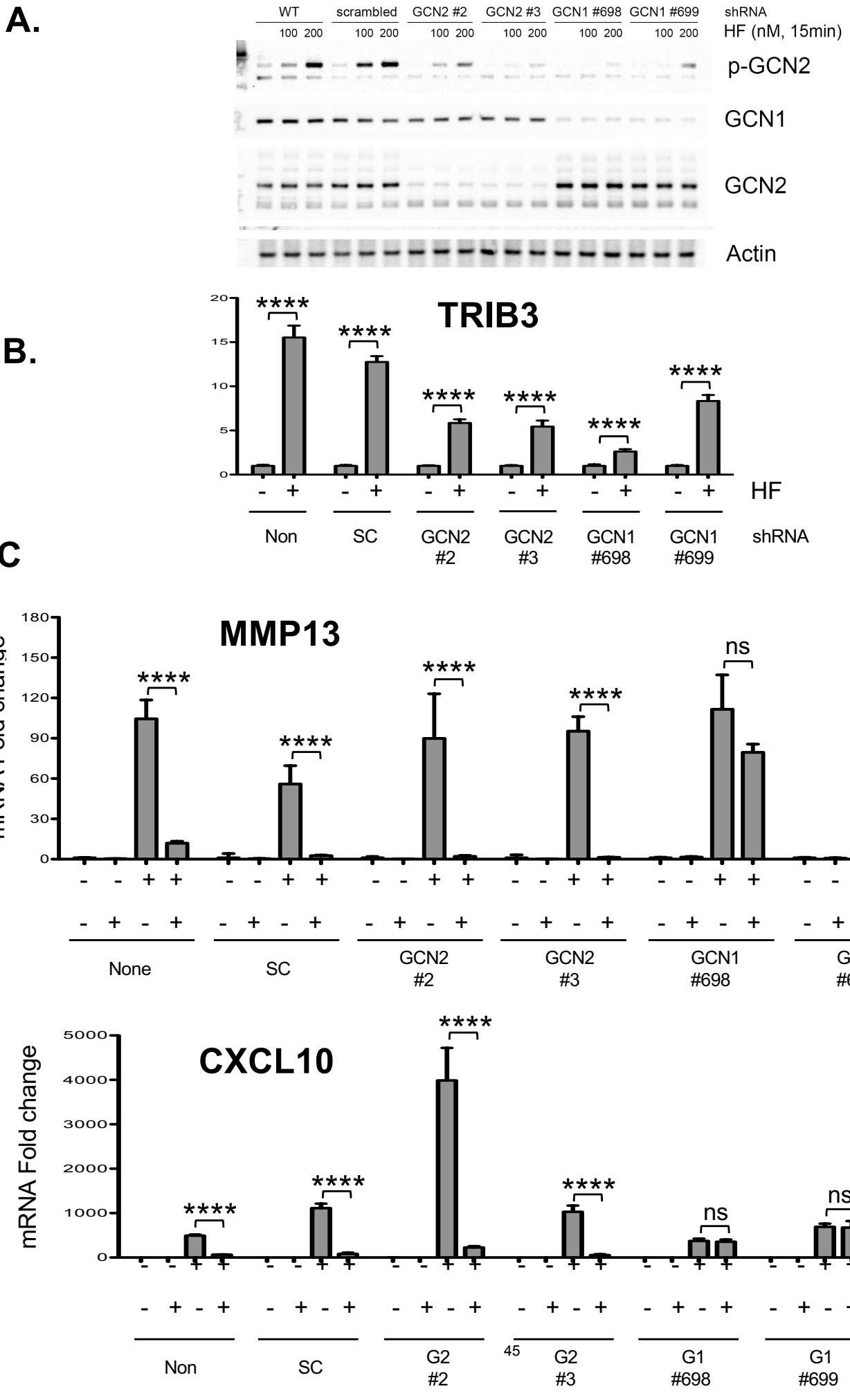
A.
WT
scrambled
GCN2 #2
GCN2 #3
GCN1 #698
GCN1 #699
shRNA
100 200
HF (nM, 15min)
p-GCN2
GCN1
GCN2
Actin
B.
TRIB3
HF
Non
SC
GCN2 #2
GCN2 #3
GCN1 #698
GCN1 #699
shRNA
C
MMP13
mRNA Fold change
TNFα
HF
None
SC
GCN2 #2
GCN2 #3
GCN1 #698
GCN1 #699
shRNA
CXCL10
mRNA Fold change
TNFα
HF
Non
SC
G2 #2
G2 #3
G1 #698
G1 #699
shRNA

Figure 5. HF Inhibition of cytokine responses is sensitive to depletion of GCN1, but not GCN2. A) Characterization of protein expression and GCN2 phosphorylation in GCN1 and GCN2 depleted K4 cells**.** K4 were transfected with a lentiviral vector carrying two independently targeted shRNAs against GCN2 (#2 or #3) or GCN1 (#698 or #699), and protein expression and GCN2 phosphorylation examined by Western blot 15' after HF treatment. Scrambled shRNA (SC) infected cells and uninfected cells were used as a negative controls. **B**) Evaluation of knockdown effects on induction of the AAR marker Trib3**.** GCN2 or GCN1 knockdown cells were treated with HF (100 nM) and/or TNFα (10 ng/mL). For transcript levels of TRIB3, cells treated with HF for 6 hours. **B**) **Evaluation of knockdown effects on HF inhibition of TNF induced genes.** For transcript levels of MMP13 (top, or CXCL10 (bottom), cells were pre-treated with HF and treated with TNFα for 6 hours. Transcript levels of target genes were quantified by qPCR, and normalized to GAPDH. Results are representative of three independent experiments. Statistical analysis: significance was analyzed using 2 way ANOVA for multiple comparisons (Bonferroni test); comparison indicated with brackets.

Supplement

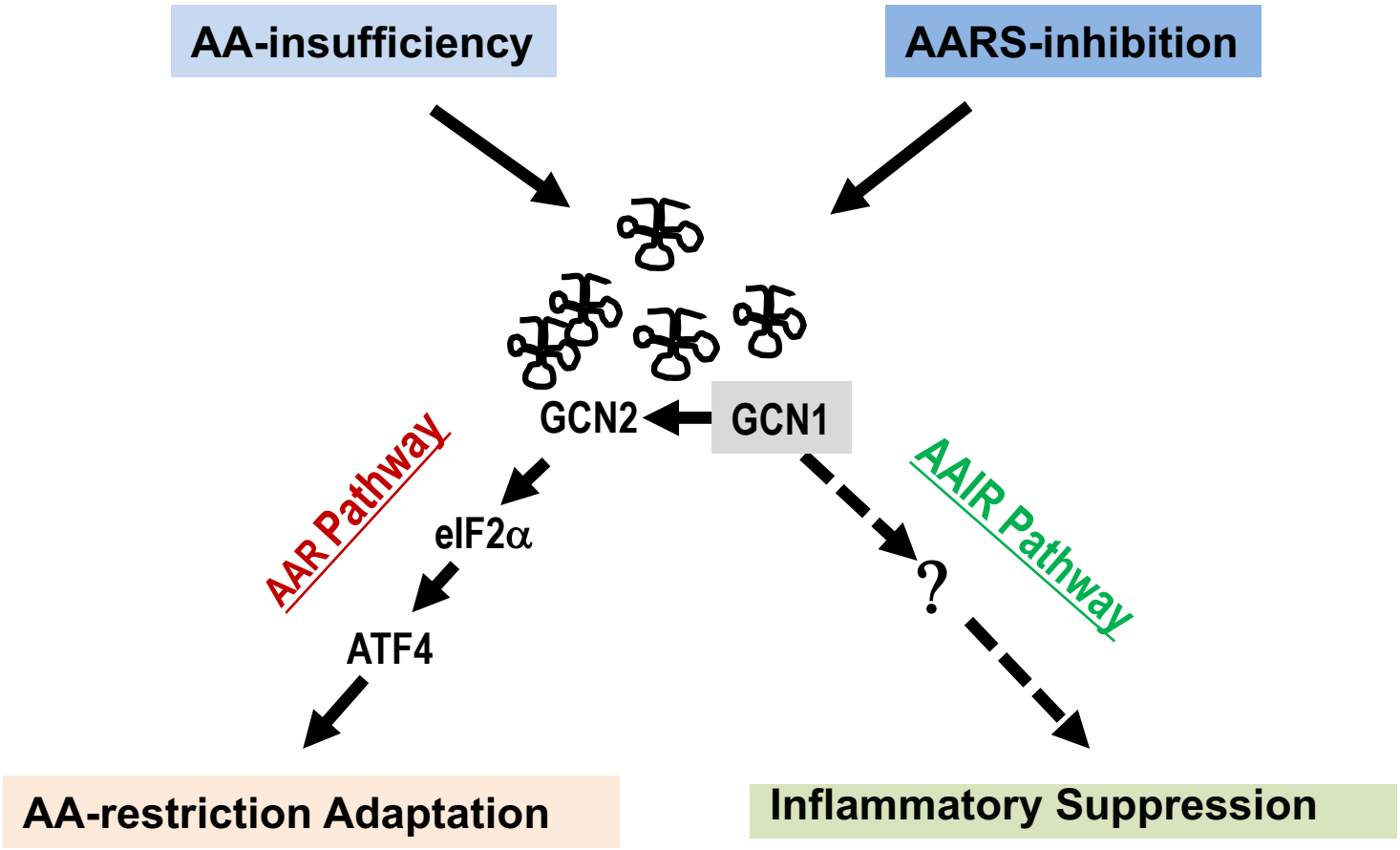

Fig. S1. (Related to Fig.5). Model of Novel Pathway responsive to uncharged tRNA accumulation. AA-insufficiency or AARS-inhibition leads to accumulation of uncharged tRNAs, which, in turn, activate downstream signals to inhibit cytokine-induced inflammatory responses (dashed line indicates proposed new pathway.) GCN1 is a shared component of both pathways, being required for GCN2 activation by uncharged tRNA.

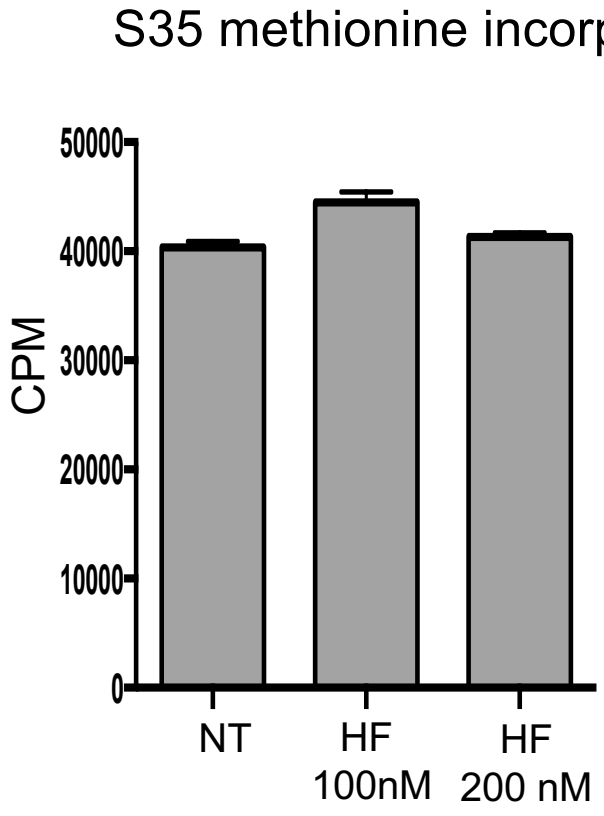

Fig.S2 (related to Fig.1). HF does not significantly inhibit general protein translation over 24 hours in quiescent cells. Human RA FLS were rendered quiescent by serum reduction as in Figure 1, and labelled with ^{35}S-labelled methionine in DMEM+0.2% FBS for 24 hours in the presence of indicated concentrations of HF. TCA precipitable counts per minute were measured in triplicate.

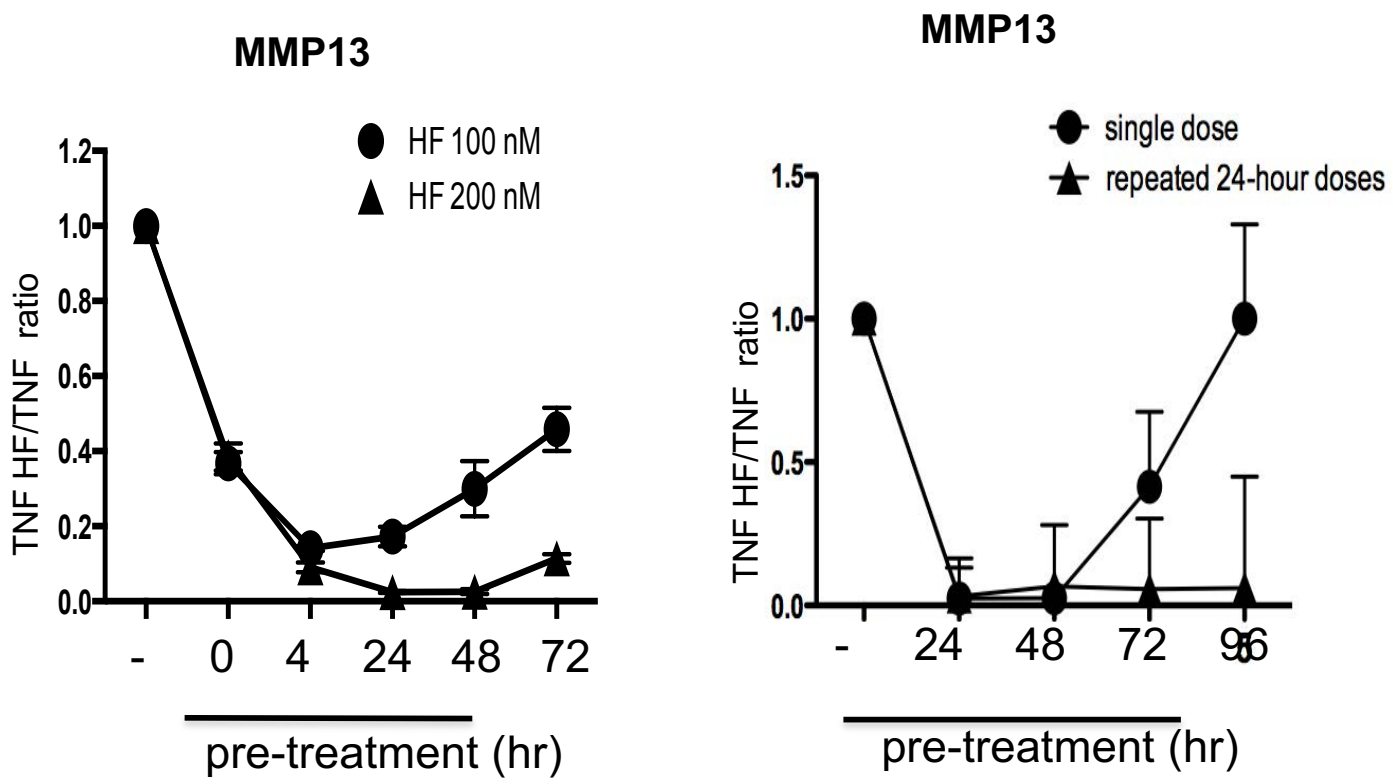

Figure S3 (related to Fig.1). HF induces a sustained change in cell responses. Human RA synoviocytes were serum starved as before, pre-treated with a single or multiple 24-hour doses of HF (200 nM) at the time indicated and treated with TNFα (10 ng/ml) for 6 hours. Results were normalized to control gene (PGK1) and reproduced in triplicate in 4 different cell lines from RA patients.

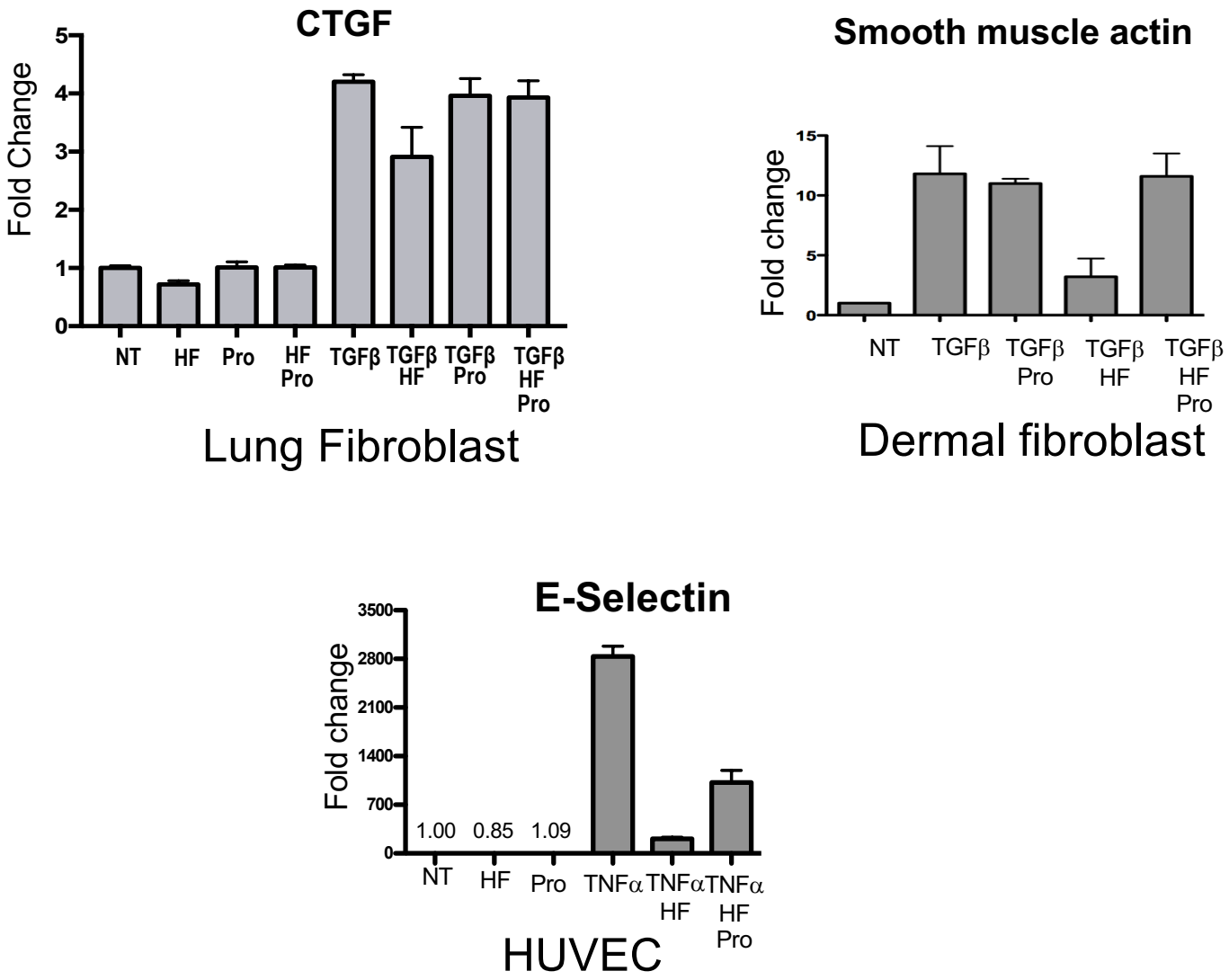

Fig.S4 (Related to Fig.1). HF affects multiple effectors of inflammation and remodeling in different primary cell types. Cells were treated and analyzed as described in legend to Fig.1A.

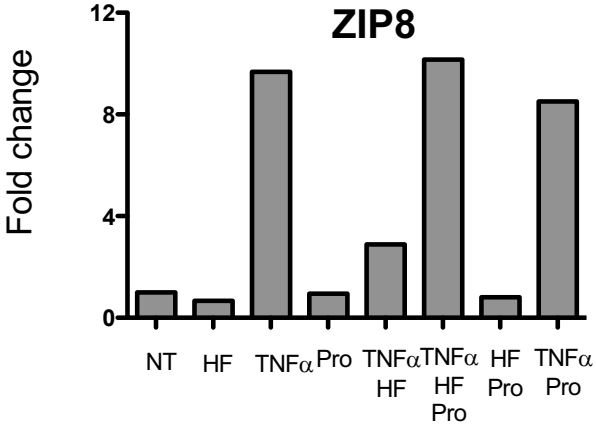

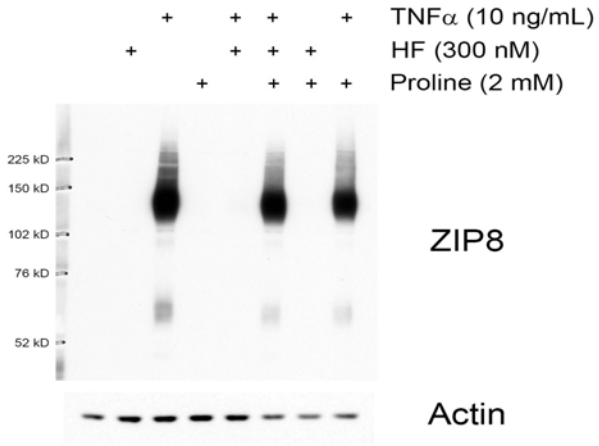

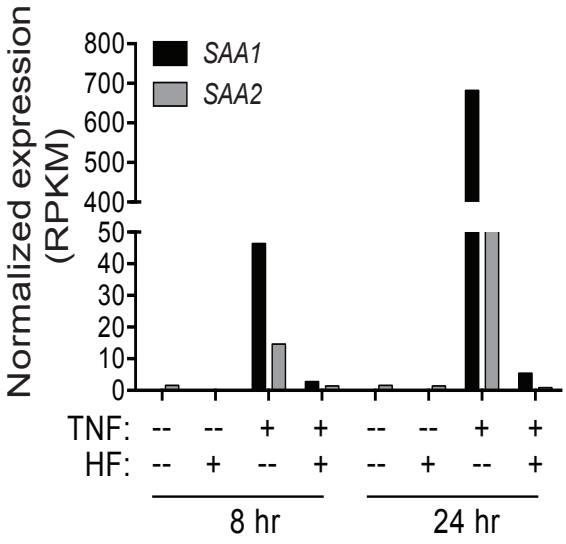

Figure S5 (related to Fig.1). HF inhibits TNFα induction of mediators of arthritis in synoviocytes. **A)** HF inhibition of ZIP8 mRNA and protein induction by TNFa. Human RA-FLS were pre-treated with 200 nM HF and/or 2 mM proline (Pro) for 16 hours, and treated with TNFα or IL1ß for 6 hours. Transcript levels were quantified by qRT-PCR and normalized to phosphoglycerate kinase 1 (PGK1) levels. Protein levels were measured by Western Blot. Results are representative of three independent experiments. B) HF inhibition of TNF induced SAA1 and SAA2 in K4 fibroblasts. Cells were treated as described in Figure 1; normalized RPKM values from biological replicate RNAseq analyses are shown. C) Validation of RNAseq data in K4 synoviocytes by Q-RT-PCR.

A

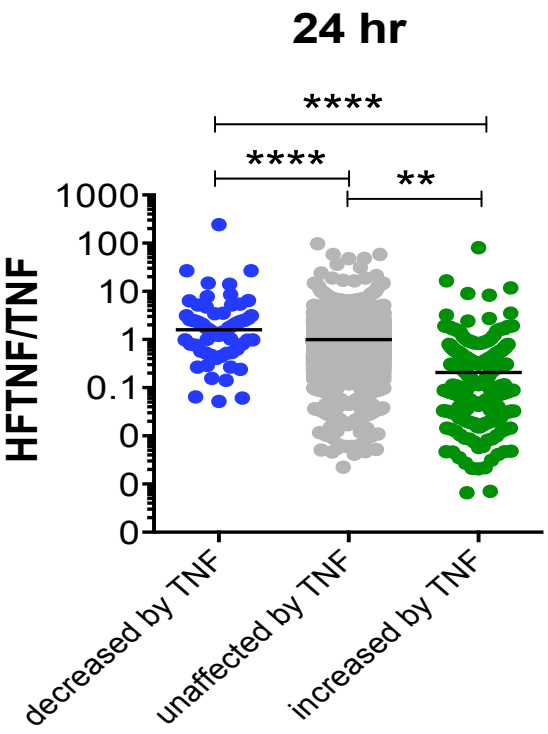

B

	Fold Induction by TNF	Fold Inhibition by TNF
CXCL10	11725	80
MX2	10341	2.7
CXCL11	5526	97
RSAD2	5394	6.7
CCL5	4511	8.9
CXCL9	4267	54
CMPK2	3016	3.9
BST2	1838	13
UBD	1742	15
TLR2	1551	15
GBP4	1376	11
IL8	1241	2
TRPA1	1037	25
MMP1	914.1	286
IDO1	867.9	60
HERC5	766.7	3.1
OASL	756.8	3.5
ELOVL7	640.4	10
ANO9	616.8	65
NOD2	588.1	74
PIK3AP1	493.5	30
CHRNA1	389.7	500
CXCL5	355.9	1.5
BATF2	346.9	13
SLCO2A1	311.8	2.8
HRASLS2	257.1	313
TNFAIP6	246.6	11
SIGLEC1	241.4	7.1
MX1	241.1	1.9
CD38	240.8	14
ISG15	234.7	3.3
IL4I1	231.1	14
SLCO5A1	226.9	11
CR1L	226.4	50
IFI27	220.4	3.2
CNTN2	203.7	36
SSTR2	195.1	15
GCH1	188.8	6.8
FLJ23865	188	8
IFI44L	184.4	2.3
LGI2	169.4	25
MEFV	166.6	68
RCSD1	152.1	*
PCLO	150.1	15
IL1RN	145.5	167
TRIM14	144.9	2.4
MCOLN2	144.3	17
ALK	140.9	42
BATF3	135.2	2.2
CX3CL1	133	20
TNFRSF9	132.7	8.3
SAA2	131.4	244
HCK	126.6	6.1
ALOX15B	126.3	213
TNFSF13B	120.1	6.9
CXCL1	114.3	2.7
LIPG	113.2	31
IFIT2	112.3	8.4
FRMD3	109.7	135
LGALS9	109.3	13
HERC6	104.2	3.6
SLC39A8	104.2	20
TSPAN33	100.6	13
HLA-F	99.85	4.2
CCR1	99.83	111
RET	96.81	13
GRIP2	96.01	45
EBI3	90.5	8.8
OAS2	88.12	2.9
C3AR1	88.08	32
CXCL6	85.73	9.1
OAS3	83.98	1.9
CXCL3	83.93	0.5
IFI6	81.52	2.8
C20orf118	70.87	6.3
IFIT1	70.66	3.8
TNFSF10	68.35	43
RASGEF1B	68.18	18
RSPO3	67.93	3.7
MEOX1	65.71	8.3
USP18	65.53	2.4
CTSS	65.3	9.1
HSD11B1	65.26	1.8
IL32	61.98	1.6
ADORA2A	61.8	30
GBP1P1	61.74	3.6
IGSF1	59.89	16
IFIT3	58.65	4
CFB	57.31	9.1
NEURL3	55.27	200
GRB7	54.76	3.2
MEP1B	54.55	5.5
KDR	53.42	4.5
FGF13	52.61	217
ADAP1	52.41	1.2
SPARCL1	52.09	5.3
KIF5C	51.78	15
ELF3	49.84	22
IFI44	49.66	2.5
CLDN1	49.2	0.3
MYH16	48.6	2.7

Fig. S6 (related to Fig.1B). HF effects on TNFα induced genes in RA-FLS. A) Opposing effects of TNFα and HF on FLS gene expression. Effects of HF treatment on the expression of genes that are strongly decreased (≥ 10-fold, blue), not affected (within 10-fold, grey), or strong induced ((≥ 10-fold, green) by TNFα stimulation after 24 hr (compared to cells cultured in media alone). Data are presented as fold-change in TNFα + HF- *vs.* TNFα only-treated cells. B) HF effects on top 100 most TNFα responsive genes. Data summarized from transcriptomics (Supp. Table 1), 8 hr time point. Red highlights mark TNFα induced genes inhibited >30 fold, yellow marks genes inhibited <3 fold, and green marks genes enhanced by HF. *No reads detected under +HF condition, fold inhibition therefore undefined.

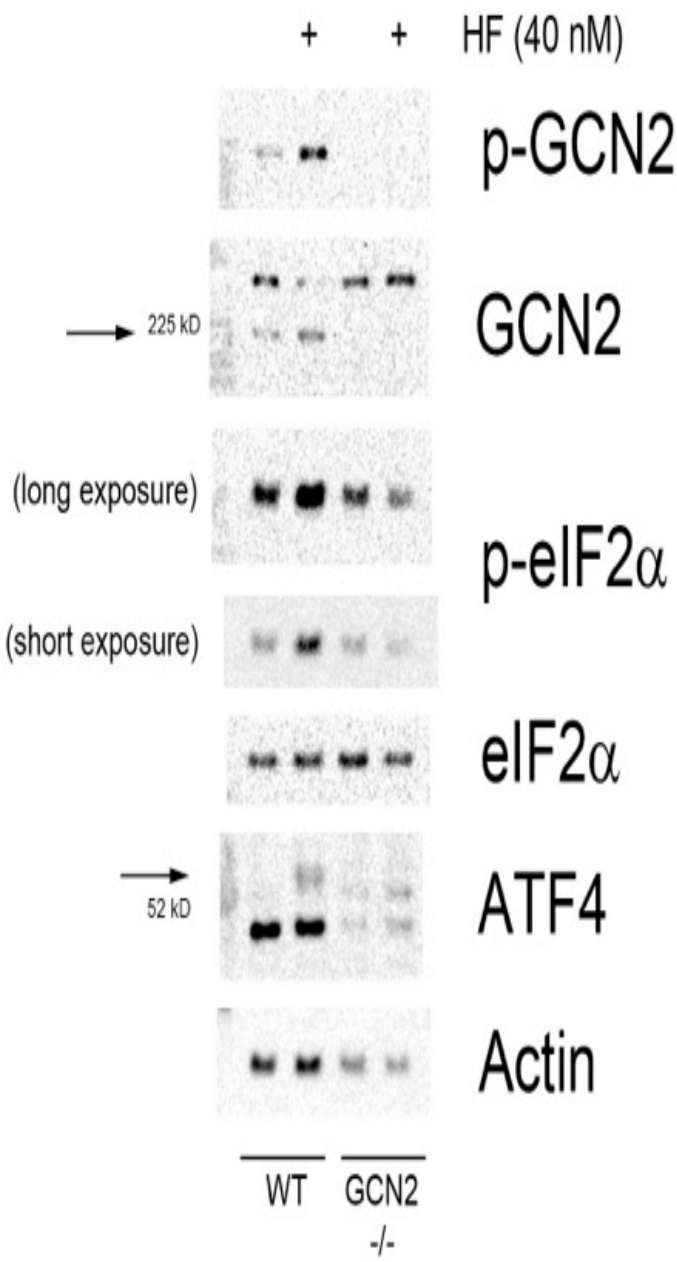

Fig. S7 (related to Fig.3). **Mouse GCN2-/- synoviocytes lack canonical GCN2 signaling.** Mouse primary fibroblast-like synoviocytes from wild type (WT) and GCN2 knockout (GCN2-/-) were serum starved (2% FBS) for 72 hours, treated with 40 nM HF for 2 hours (for GCN2 and eIF2α) or 5 hours (for ATF4), and analyzed by western blotting for total GCN2, phosphorylated GCN2 (on Thr899), total eIF2α, phosphorylated eIF2α (on Ser51), and ATF4.

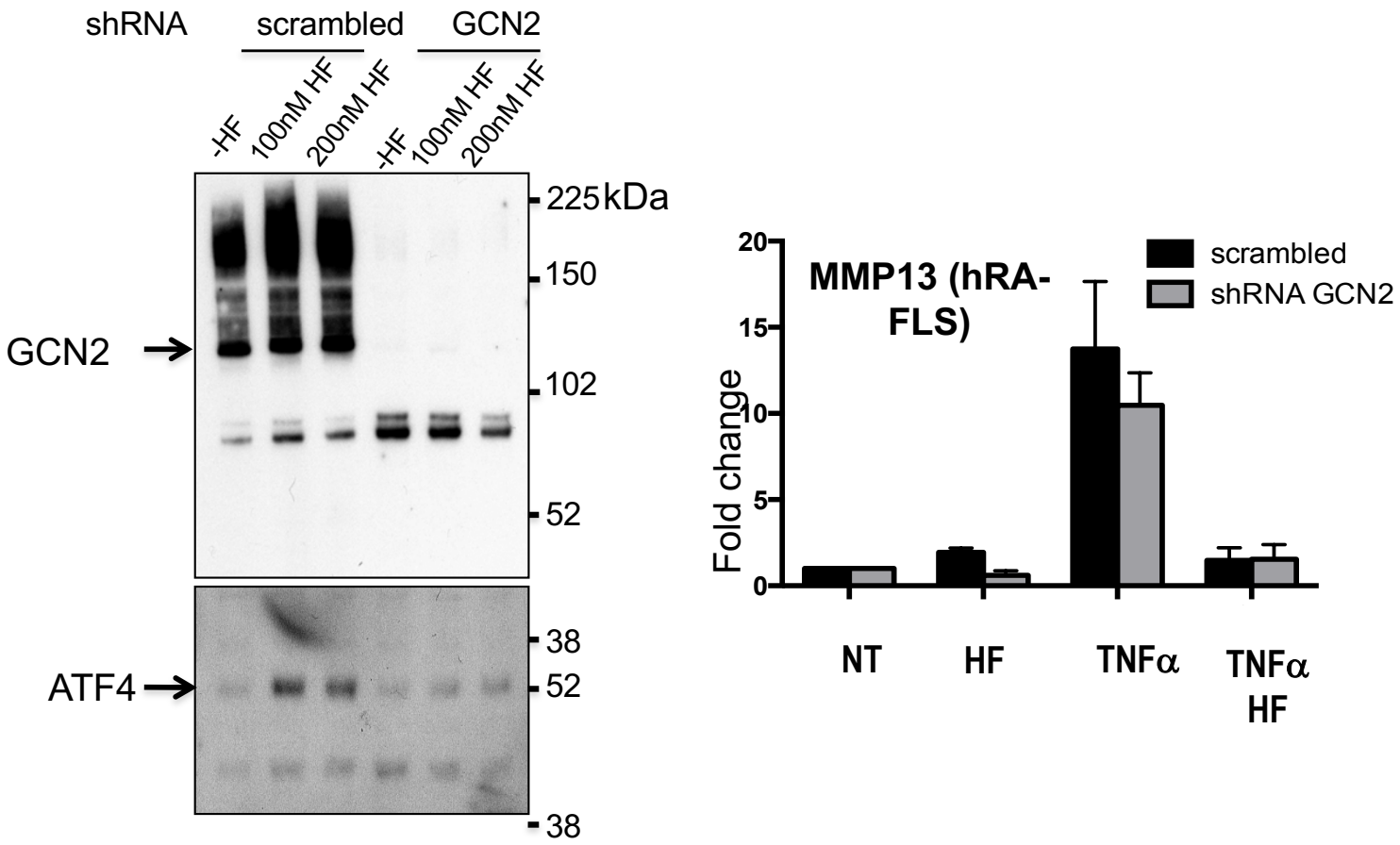

Fig. S8 (related to Fig.2). HF Inhibits TNFα induction of MMP13 in GCN2 depleted primary RA synoviocytes. A) HF does not activate the AAR pathway in GCN2-knock down RA synoviocytes**.** Human RA synoviocytes were transfected with a lentiviral vector carrying shRNA against GCN2 or scrambled. Following antibiotic selection, GCN2-knock down synoviocytes treated with HF (100-200nM) for 6 hours. Western blot analysis was performed as previously described. Results are representative of three independent experiments. **B)** GCN2 knockdown does not affect inhibition of TNFα induced MMP13 by HF. GCN2-knock down synoviocytes treated with HF (200 nM) for 16 hours, followed by TNFα for 6 hours. Transcript levels of target genes were quantified by qPCR and standardized to a housekeeping gene (PGK1) . Results are representative of three independent experiments.

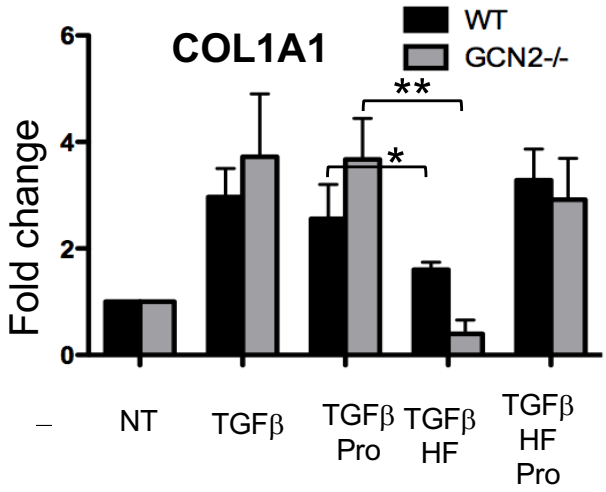

Fig.S9 (Related to Fig.2). HF inhibits TGFß effects in GCN2 null cells. . Mouse primary dermal fibroblasts from wild type (WT) and GCN2 knockout (GCN2-/-) were treated with HF and/or TGFb. Transcript levels of target genes were quantified by qPCR and normalized to a housekeeping gene control (GAPDH) . Results are representative of three independent experiments.

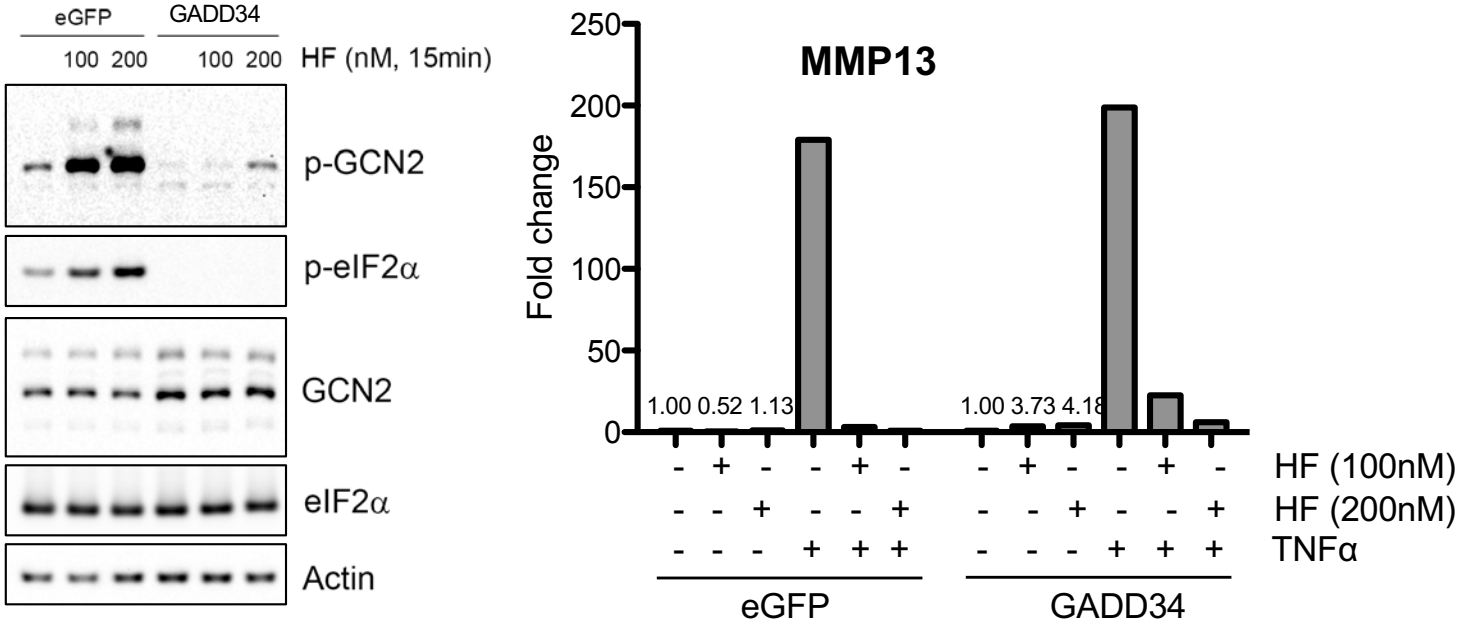

Fig.S10 (related to Fig.2).GCN2 independent effects of HF are not dependent on eIF2α phosphorylation . K4 were transfected with a retroviral vector carrying the C-terminal portion of the eIF2α phosphatase GADD34 (haA1) gene. eGFP gene was used for negative control. GADD34-overexpressed cells were serum starved (0.2% FBS) for 24 hours, treated with HF for 15 mins, and assayed by western blotting for phosphorylated-GCN2 and eIF2α. For transcript levels of MMP13 and CXCL10, cells were serum starved (0.2% FBS) for 24 hours, pretreated with HF, and treated with TNFα for 6 hours. Transcript levels were quantified by qPCR, and normalized to GAPDH.

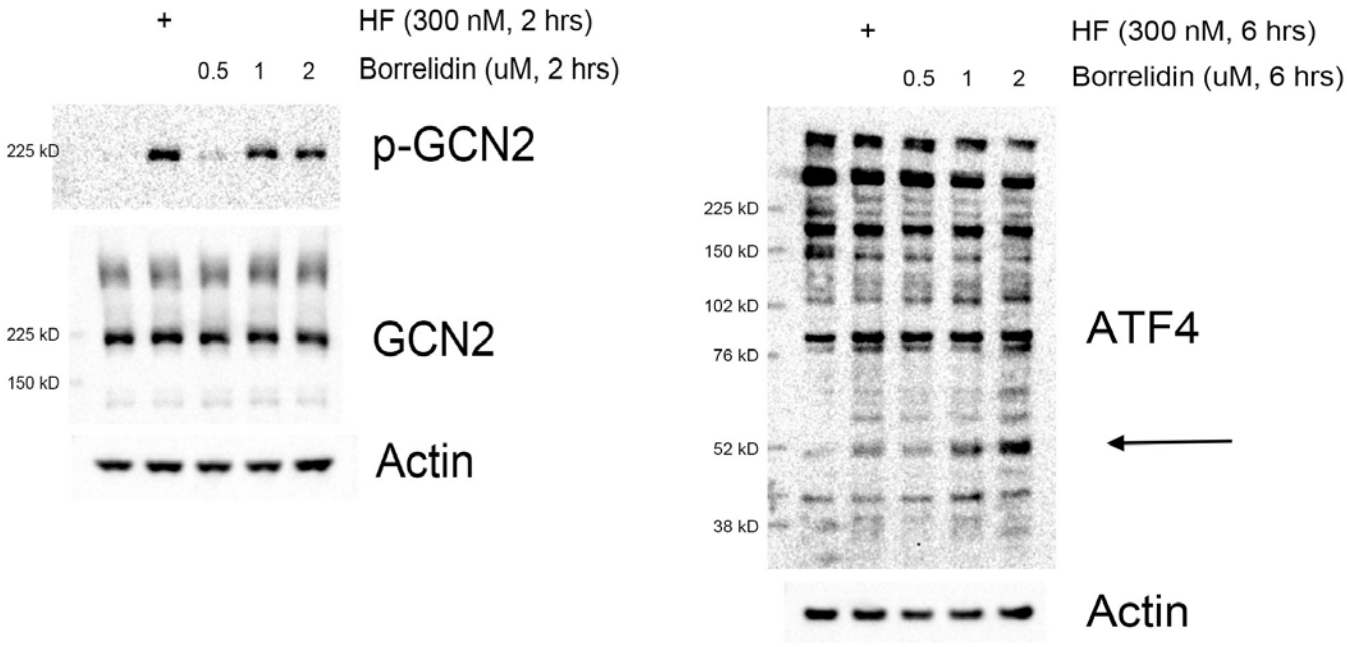

Fig. S11 (related to Fig.3). Matching of HF and Borrelidin effects on AAR markers Human RA-FLS were serum starved (0.2% FBS) for 24 hours, treated with 300 nM HF or Borrelidin for 2 or 6 h ours, and analyzed by western blotting for total GCN2, phosphorylated GCN2 (on Thr899), and AT F4. Cytoplasmic actin (Actin) was used as a loading control for Western blotting.

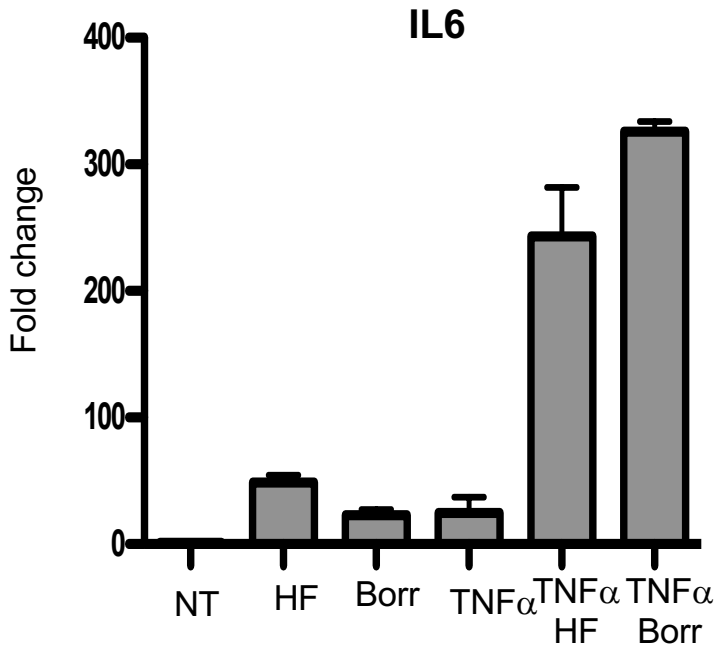

Fig. S12 (Related to Fig.3). **Borrelidin and HF enhance IL6 induction by TNFα.** Primary hu man RA-FLS were treated with 300 nM HF or 1μM of Borrelidin for 16 hours, treated with TNFα f or 4 hours, and analyzed by qRT-PCR. The transcript levels were normalized PGK1 levels. Resu lts are representative of three independent experiments.

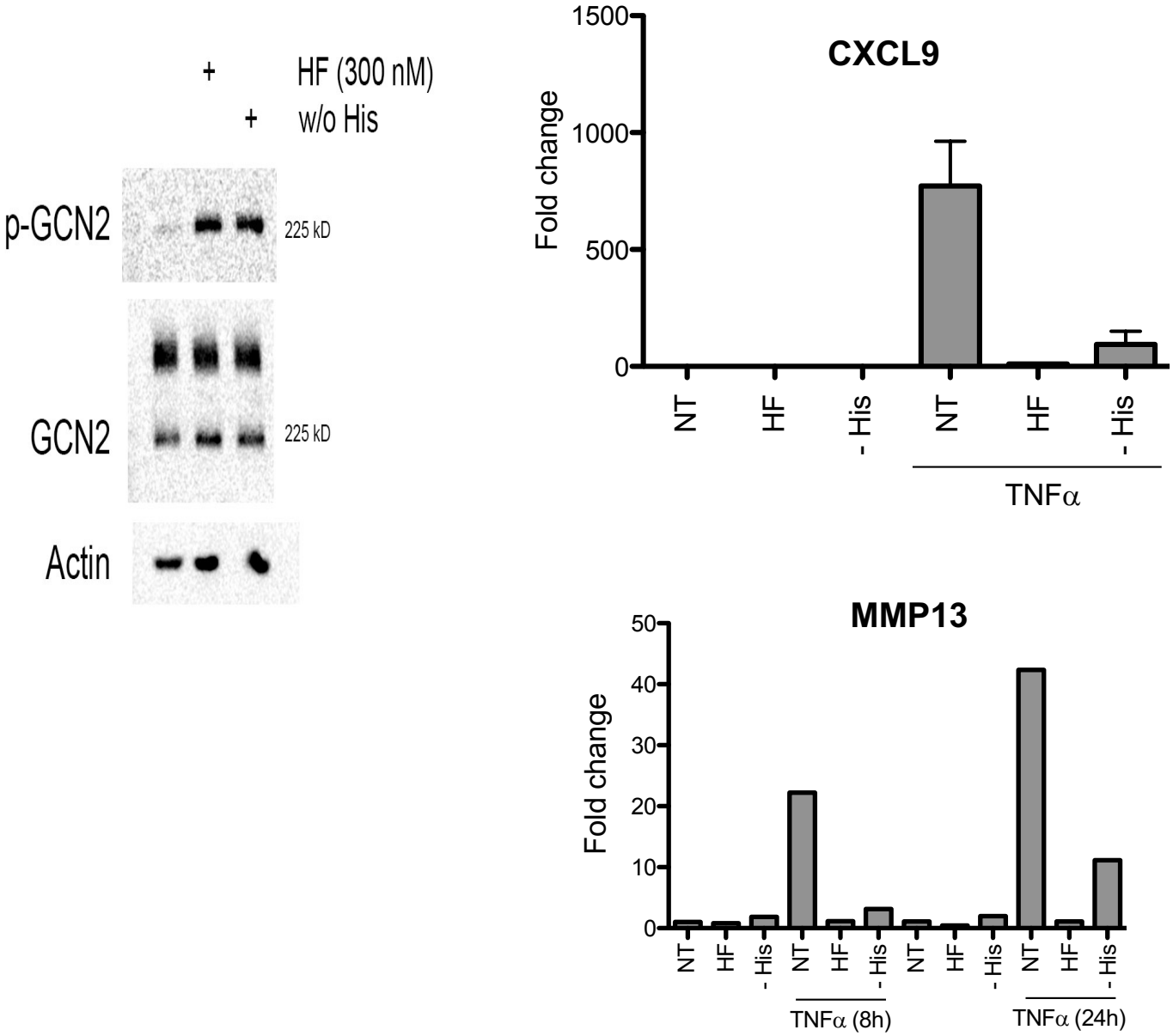

Fig. S13 (Related to Fig.3).Histidine deprivation activates the AAR and mimics effects of HF. To examine for induction of the AAR, human RA-FLS were serum starved (0.2% FBS) for 24 hours, treated with 300 nM HF or Histidine depletion (w/o His) for 2 hours, and analyzed by western blotting for total GCN2 and phosphorylated GCN2 (on Thr899). Cytoplasmic actin (Actin) was used as a loading control for Western blotting. For transcript levels, human RA-FLS were serum starved (0.2% FBS) for 24 hours, treated with 300 nM HF or Histidine depletion (w/o His) for 16 hours, treated with TNFα for 8 or 24 hours (8 hours for CXCL9), and analyzed by qRT-PCR. The transcript levels were normalized to PGK1.

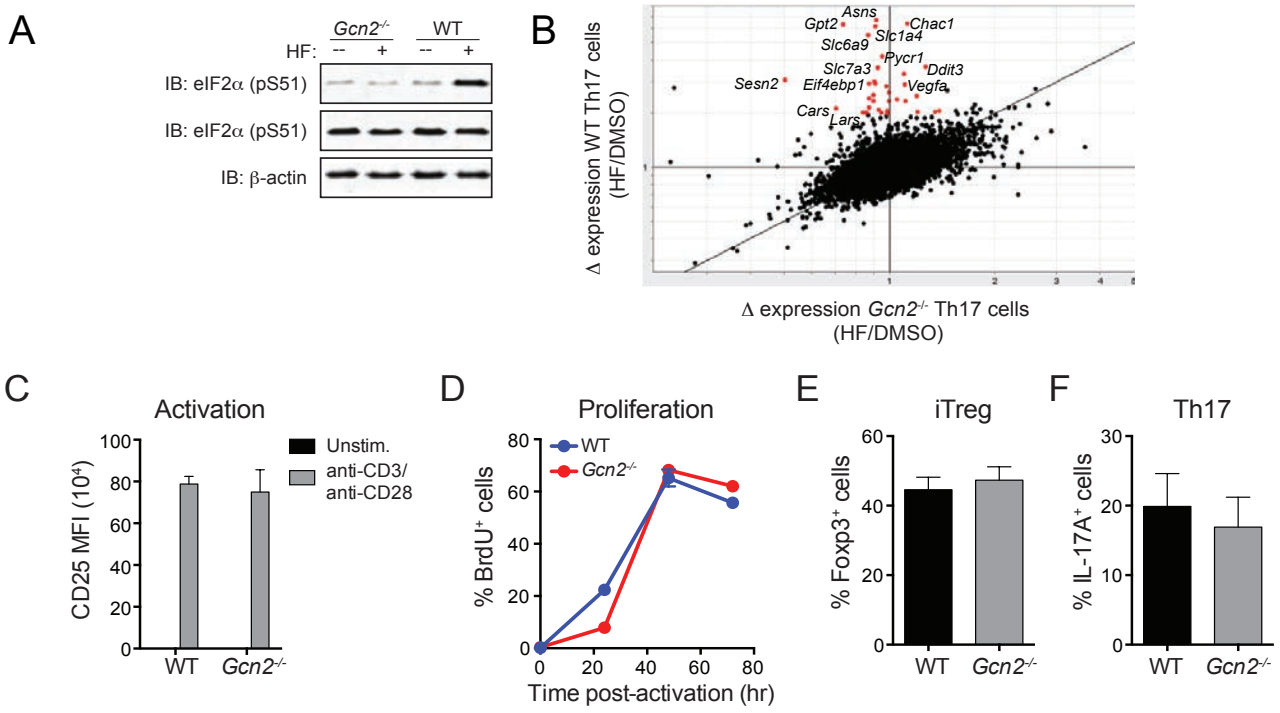

Figure S14 (Related to Fig.4). HF responses and function of Gcn2-deficient T cells. (A) eIF2α phosphorylation (serine 51) in wild type or Gcn2-deficient CD4+ T cells stimulated for 4 hr with anti-CD3/anti-CD28 antibodies +/- 10 nM HF was determined by western blot. (B) Differential gene expression, determined by microarray, in wild type or Gcn2-deficient CD4+ T cells stimulated for 4 hr in Th17-polarizing cytokine conditions (anti-CD3/anti-CD28 plus TGFβ and IL-6) in the absence or presence of 10 nM HF. Data are presented as fold-change, fold-change plot; gene expression in HF- vs. DMSO-treated wild type (WT, y-axis) and Gcn2-deficient (x-axis) T cells. Canonical Gcn2-dependent amino acid starvation response genes are highlighted in red and labeled. (C) CD25 expression (MFI, mean fluorescence intensity), determined by FACS analysis, in wild type or Gcn2-deficient CD4+ T cells stimulated for 24 hr with anti-CD3/anti-CD28 antibodies. (D) Anti-CD3/anti-CD28-induced proliferation in wild type or Gcn2-deficient CD4+ T cells determined by BrdU incorporation and FACS analysis. Efficiency of induced T regulatory (iTreg) cell (E) or Th17 (F) differentiation in wild type or Gcn2-deficient CD4+ T cells. iTreg and Th17 differentiation was assessed by FACS analysis of Foxp3+ or IL-17A+ cells, respectively. All data are representative of 2-3 independent experiments; microarray analysis incorporates data from biological duplicate samples. The number of genes affected by HF vs. DMSO treatment at each timepoint at least 2.5-fold are shown above the bar for each timepoint.